

Electronic Thesis and Dissertation Repository

11-26-2014 12:00 AM

Influence of Polycaprolactone and Basic Fibroblast Growth Factor on Gingival Fibroblasts

Sarah Michelsons

The University of Western Ontario

Supervisor

Dr. Douglas Hamilton

The University of Western Ontario

Graduate Program in Anatomy and Cell Biology

A thesis submitted in partial fulfillment of the requirements for the degree in Master of Science

© Sarah Michelsons 2014

Follow this and additional works at: <https://ir.lib.uwo.ca/etd>



Part of the [Medical Cell Biology Commons](#)

Recommended Citation

Michelsons, Sarah, "Influence of Polycaprolactone and Basic Fibroblast Growth Factor on Gingival Fibroblasts" (2014). *Electronic Thesis and Dissertation Repository*. 2607.

<https://ir.lib.uwo.ca/etd/2607>

This Dissertation/Thesis is brought to you for free and open access by Scholarship@Western. It has been accepted for inclusion in Electronic Thesis and Dissertation Repository by an authorized administrator of Scholarship@Western. For more information, please contact wlsadmin@uwo.ca.

INFLUENCE OF POLYCAPROLACTONE AND BASIC FIBROBLAST GROWTH
FACTOR ON GINGIVAL FIBROBLASTS

(Thesis format: Integrated Article)

by

Sarah Elizabeth Michelsons

Graduate Program in Anatomy & Cell Biology

A thesis submitted in partial fulfillment
of the requirements for the degree of
Master of Science

The School of Graduate and Postdoctoral Studies
The University of Western Ontario
London, Ontario, Canada

© Sarah Michelsons 2014

Abstract

Guided tissue regeneration (GTR) to regenerate periodontal tissue involves placement of a cell-occlusive barrier membrane functionally excluding the gingiva and associated oral epithelium from the periodontal defect. Gingival connective tissue contains a rich vascular plexus and is a source of progenitor cells which could contribute to periodontal regeneration. We have investigated the use of a novel bioresorbable and bioactive electrospun fibrous polycaprolactone (PCL) scaffold loaded with microspheres releasing basic fibroblast growth factor (bFGF) to promote gingival connective tissue growth while maintaining a barrier to the oral epithelium. Scaffolds supported an increase in human gingival fibroblast cell number and mesenchymal cell infiltration in a bFGF dose dependent manner while excluding oral epithelial cell penetration. Scaffold treatment during early healing of rat gingival wounds showed good biocompatibility. This study suggests that PCL electrospun scaffolds both with and without bFGF microspheres represent a promising alternative to the current generation of GTR barrier membranes.

Keywords

Gingival Fibroblasts, Oral Epithelium, Polycaprolactone, Electrospun Scaffold, Basic Fibroblast Growth Factor, Guided Tissue Regeneration.

Co-Authorship Statement

This thesis was written by S.E. Michelsons with input, suggestions, and revisions from Dr. D. W. Hamilton.

Experiments were designed by Dr. D. W. Hamilton. All studies were completed by S. E. Michelsons with the exception of: S. Kim (PhD candidate) performed all surgeries for the *in vivo* aspect of the project with technical assistance by S. E. Michelsons; X. Li (PhD candidate) fabricated the scaffolds used in this study under the supervision of Dr. J. Guan (The Ohio State University); K. Martin (Dentistry Summer Research Student) conducted qRT-PCR on hGFs on the scaffolds to assess decorin and versican mRNA expression levels (Appendix I).

Acknowledgments

I would first like to thank my supervisor, Dr. Hamilton. His guidance and mentorship during my graduate studies has been instrumental in helping me achieve my goals and better my research and critical thinking skills. I appreciate your encouragement and input in all of my scientific undertakings, from work in the lab to presentations and scholarship applications. You have taught me the value of attention to detail in all aspects of scientific work extending bench-top to communication. I appreciate the opportunity to have completed my graduate studies in your lab under your mentorship.

To the members of the Hamilton lab, past and present, thank you for your friendship over the past two years. The friendships I have made here made the lab quite the enjoyable place to have completed my graduate work. Competitions for who could come in first for the day; for that day's music selection or purely for bragging rights, proved to be both entertaining and motivating. Chris was a wealth of scientific knowledge and his guidance with scientific techniques was much appreciated, more so than his jokes. Shawna provided me with my knowledge in cell culture, microscopy and general scientific technique for which I am grateful. Shawna's commitment to research and her persistence, determination and overall hardworking attitude are to be admired. Her willingness to participate in scientific discussion and offering helpful advice whenever needed played a significant role in the completion of my studies. Kendal's undying need for organization has made my time in the lab much easier. Thank you for your helpful tips and troubleshooting discussions when problems arose. Kendal's culinary expertise in the form of delicious muffins, cookies and a gigantic birthday cake was much appreciated. JT's knowledge of scientific technique has encouraged and motivated me to think critically about the scientific techniques I choose and the work which I have done. JT's science puns, which seemed to go on for ages, and countless personal stories made the lab that much more enjoyable. Thank you to Hong for always showing an interest in my research.

To my friends Salman and Eliot at Western, thank you for always being there for me. Knowing that you were there if I needed you was reassuring during my graduate studies.

Thank you to my friend Ryan for always being one email away. Your willingness to edit anything I sent your way was truly appreciated.

To my family, I love you. My sister Susan has been my best friend throughout everything I have done in the past two years, both related to my graduate work and personal life. Thank you for making me laugh harder than anyone and making the rough times bearable. I appreciate all of your advice, even though I sometimes don't take it. Thank you to my brother Steven for always taking an interest in what I am up to in the lab and always asking how things are going. My parents, Barbara and Juris, have been my role models and heroes throughout my entire life and in particular the past two years. Thank you for setting a good example; I aspire to be like you when I am older. Thank you for pushing me when I needed to be pushed, supporting me the entire time and catching me when I fall. Without your guidance I would not be where I am today, and for that I will always be grateful.

Table of Contents

Abstract.....	ii
Co-Authorship Statement.....	iii
Acknowledgments.....	iv
List of Figures.....	x
List of Appendices.....	xii
List of Abbreviations.....	xiii
Chapter 1.....	1
1 Introduction.....	1
1.1 Chapter Summary.....	1
1.2 The Periodontium.....	3
1.2.1 Structure and Function.....	3
1.2.2 Periodontal Diseases.....	7
1.3 Gingival Wound Healing.....	9
1.3.1 Connective Tissue.....	9
1.3.2 Epithelial Component.....	10
1.4 Periodontal Disease Treatments.....	11
1.4.1 Periodontal Plastic Surgery.....	11
1.4.2 Guided Tissue Regeneration.....	12
1.4.3 Scaffold Membrane-Mediated Periodontal Regeneration.....	18
1.4.4 Biological Agents for Periodontal and Gingival Repair.....	22
1.5 Basic Fibroblast Growth Factor.....	23
1.5.1 General Structure and Function.....	23
1.5.2 Angiogenesis.....	25

1.5.3	Chemotaxis	25
1.5.4	Mitogenic Effects.....	25
1.5.5	Role of bFGF in Wound Healing.....	26
1.6	Hypothesis and Objectives.....	27
1.6.1	Rationale	27
1.6.2	Overall Hypothesis.....	27
1.6.3	Specific Hypothesis and Objectives.....	27
1.7	References.....	29
Chapter 2.....		42
2	Influence of Electrospun Polycaprolactone Fibrous Scaffolds Loaded with Basic Fibroblast Growth Factor Microspheres on Gingival Augmentation	42
2.1	Introduction.....	42
2.2	Materials and Methods.....	44
2.2.1	Cell Cultures and Tissue Explants	44
2.2.2	Electrospun Fibrous Polycaprolactone Scaffolds Loaded with bFGF.....	48
2.2.3	Human Gingival Fibroblast Attachment.....	49
2.2.4	Gingival Fibroblast Cell Number.....	49
2.2.5	<i>Ex-Vivo</i> Explant Cultures.....	50
2.2.6	Immunocytochemical Analysis.....	51
2.2.7	Human Gingival Fibroblast Extracellular Matrix Gene Expression.....	52
2.2.8	Rat Gingivectomy Model.....	53
2.2.9	Statistical Analysis.....	59
2.3	Results.....	60
2.3.1	Attachment and Morphology of hGFs on PCL Electrospun Scaffolds Loaded With bFGF	60
2.3.2	bFGF Loaded PCL Electrospun Scaffolds Increase hGF Cell Number ...	60

2.3.3	Interaction of Gingival Explant Tissue with PCL Electrospun Scaffolds Loaded with bFGF	66
2.3.4	hGF ECM Secretion is Modulated by bFGF on PCL Electrospun Scaffolds	74
2.3.5	Effect of PCL Electrospun Fibrous Scaffolds Loaded with bFGF Microspheres on Fibronectin and Biglycan mRNA.....	81
2.3.6	Localization of M2 Macrophages in Rat Gingival Wounds Treated with PCL Electrospun Scaffolds	81
2.3.7	Proliferating Cells in Rat Gingival Wounds Treated with PCL Electrospun Scaffolds	81
2.3.8	Myofibroblasts in Rat Gingival Wounds Treated with PCL Electrospun Scaffolds	91
2.3.9	Collagen Deposition in Rat Gingival Wounds Treated with PCL Electrospun Scaffolds	91
2.3.10	Connective Tissue Area in Rat Gingival Wounds Treated with PCL Electrospun Scaffolds	91
2.3.11	Epithelial Migration in Rat Gingival Wounds Treated with PCL Electrospun Scaffolds	103
2.3.12	Biologic Width of Rat Gingival Wounds Treated with PCL Electrospun Scaffolds	103
2.4	Discussion	108
2.5	Conclusion	116
2.6	Acknowledgements.....	116
2.7	References.....	117
Chapter 3	124
3	General Discussion.....	124
3.1	Summary and Conclusions	124
3.2	Contributions to the Current State of Knowledge.....	125
3.2.1	General Significance.....	125
3.2.2	Role of Scaffold Architecture in Determining Cellular Responses	126

3.2.3	Role of bFGF in Scaffold Bioactivity	127
3.2.4	PCL Electrospun Scaffolds Loaded with bFGF for Tissue Repair	128
3.3	Future Directions	129
3.3.1	Adhesion Dynamics of Cellular Interaction with PCL Electrospun Scaffolds	129
3.3.2	Effect of Lipopolysaccharide on hGF Interaction with PCL Electrospun Scaffolds	130
3.3.3	Analysis of PCL Electrospun Scaffolds on Initial and Late Wound Healing Response.....	131
3.3.4	Assessing Cell Recruitment During Healing – Lineage Tracing to Assess the Role of Pericytes	132
3.4	Limitations	133
3.5	Final Summary	134
3.6	References.....	135
	Appendix and Curriculum Vitae.....	139

List of Figures

Figure 1.1 - Anatomy of the periodontium.	4
Figure 1.2 - Guided tissue regeneration.	13
Figure 2.1 – Gingival tissue explant as an <i>ex vivo</i> experimental system.	46
Figure 2.2 - Gingivectomy in a rat model and scaffold placement.	54
Figure 2.3 - Biologic width.	57
Figure 2.4 - hGF attachment and morphology.	61
Figure 2.5 - hGF cell number.	64
Figure 2.6 - SEM of gingival tissue explants.	67
Figure 2.7 - Population of the PCL electrospun scaffolds by cells from gingival tissue explants.	69
Figure 2.8 - PCL electrospun scaffolds as a barrier to oral epithelial cells.	72
Figure 2.9 - Fibronectin immunoreactivity on the scaffold surface.	75
Figure 2.10 - Biglycan immunoreactivity on the scaffold surface.	77
Figure 2.11 - Decorin immunoreactivity on the scaffold surface.	79
Figure 2.12 - Influence of PCL electrospun scaffolds loaded with bFGF on fibronectin and biglycan mRNA levels.	82
Figure 2.13 - M2 macrophage localization following <i>in vivo</i> gingivectomy.	84
Figure 2.14 - Cell proliferation following <i>in vivo</i> gingivectomy.	87
Figure 2.15 - Myofibroblast populations following <i>in vivo</i> gingivectomy.	92

Figure 2.16 - Collagen deposition following <i>in vivo</i> gingivectomy.	96
Figure 2.17 - Connective tissue area following <i>in vivo</i> gingivectomy.	101
Figure 2.18 - Epithelium length following <i>in vivo</i> gingivectomy.....	104
Figure 2.19 - Biologic width measurement following <i>in vivo</i> gingivectomy.	106

List of Appendices

Appendix A: Animal protocol approval.	140
Appendix B: Human ethics approval.	141
Appendix C: Fibronectin immunoreactivity on the scaffold surface at low magnification.	142
Appendix D: No primary antibody negative control fibronectin immunofluorescence.	143
Appendix E: Biglycan immunoreactivity on the scaffold surface at low magnification.	145
Appendix F: No primary antibody negative control biglycan immunofluorescence.....	146
Appendix G: Decorin immunoreactivity on the scaffold surface at low magnification.	148
Appendix H: No primary antibody negative control decorin immunofluorescence.....	149
Appendix I: Influence of PCL electrospun scaffolds loaded with bFGF on decorin and versican mRNA levels.	151
Appendix J: Collagen deposition in uninjured rat gingiva and immediately following gingivectomy.....	153
Appendix K: Myofibroblast population following <i>in vivo</i> gingivectomy.	154
Appendix L: No primary antibody negative control immunohistochemistry.....	157

List of Abbreviations

α -SMA	Alpha smooth muscle actin
AA	Antibiotic-antimicotic
bFGF	Basic fibroblast growth factor
BMP-2	Bone morphogenetic protein-2
BSA	Bovine serum albumin
DAB	3, 3'-diaminobenzidine
DAPI	4', 6-diamidino-2-phenylindole
DMEM	Dulbecco's Modified Eagle Medium
ECM	Extracellular matrix
ePTFE	Expanded polytetrafluoroethylene
FBS	Fetal bovine serum
FGFR	Fibroblast growth factor receptor
FGFR1	Fibroblast growth factor receptor tyrosine kinase-1
GTE	Gingival tissue explant
GTR	Guided tissue regeneration
H&E	Hematoxylin and eosin
hGF	Human gingival fibroblast
HMDS	Hexamethyldisilazane
HMW	High molecular weight

LPS	Lipopolysaccharide
PBS	Phosphate buffered saline
PCL	Polycaprolactone
PDGF	Platelet derived growth factor
PDL	Periodontal ligament
PFA	Paraformaldehyde
PI3-Kinase	Phosphoinositide 3-kinase
PLGA	Poly (lactide- <i>co</i> -glycolide)
RT	Room temperature
RT-qPCR	Quantitative real-time reverse transcription polymerase chain reaction
SCTG	Subepithelial connective tissue graft
SD	Standard deviation
SEM	Scanning electron microscopy
SLRPG	Small leucine rich proteoglycans
TGF- β 1	Transforming growth factor- β 1
VEGF	Vascular endothelial growth factor

Chapter 1

1 Introduction

1.1 Chapter Summary

Periodontal diseases are pathologies which affect the tissues supporting teeth and are highly prevalent, affecting up to 90% of the world's population (Pihlstrom, Michalowicz et al. 2005). These supporting tissues are collectively termed the periodontium and function as a unit to securely anchor each tooth into the jaw. The periodontium is composed of four tissues; the gingiva, the periodontal ligament (PDL), cementum and the alveolar bone (AAP 2001). Periodontitis, often known as “gum” disease, is a severe, progressive inflammatory disease in which all of the tissues of the periodontium are negatively affected. This condition is characterized by plaque formation, a loss of connective tissue attachment to the tooth, formation of a periodontal pocket and degeneration of the PDL, cementum and alveolar bone which, if left untreated, can lead to tooth loss (AAP 2001, Pihlstrom, Michalowicz et al. 2005). Periodontitis is a significant healthcare burden as it is estimated that over 47% of the adult US population has periodontitis (Eke, Dye et al. 2012). Treatments aimed at removing the causative bacterial agents are successful at halting the progression of the disease, but due to the limited capacity of the periodontium for self-repair, usually result in minimal regeneration of the lost tissues and can leave the patient with severe gingival recession (Hughes, Ghuman et al. 2010). Therapeutic interventions such as guided tissue regeneration (GTR) have been devised to attempt to regenerate the lost periodontal structures.

GTR is a technique in which an occlusive barrier membrane is placed under the gingiva over the tooth root to functionally exclude the gingival connective tissue and epithelium from contacting the root thus providing the periodontal ligament and alveolar bone a space into which they can regenerate (Nyman, Gottlow et al. 1982). Occlusive membranes do not result in predictable or full regeneration of the lost periodontal structures, indicating that significant improvements can be made (Bartold, McCulloch et

al. 2000, Hughes, Ghuman et al. 2010). In addition, occlusive membranes exclude the gingival connective tissue from the defect site. This is problematic as the gingival connective tissue is a rich source of vasculature and contains progenitor cell populations which can contribute to periodontal regeneration (Schroeder and Listgarten 1997, Fournier, Larjava et al. 2013).

The overall focus of this work is the testing of a fibrous bioactive and bioresorbable scaffold to recruit cells from the gingival connective tissue while maintaining a barrier to oral epithelial cells. Electrospinning is a process that efficiently creates fibrous scaffolds which are ideal for use in tissue regenerative applications due to their high surface area to volume ratio and interconnected porosity allowing for cell infiltration and exchange of nutrients and waste products throughout the construct (Dong, Liau et al. 2009).

Polycaprolactone (PCL) is a bioresorbable aliphatic polyester which can be electrospun into a fibrous matrix and is advantageous for use due to its low cost, abundance, long degradation time and biocompatibility (Dong, Liau et al. 2009). To confer bioactivity to the scaffolds and promote *in situ* periodontal regeneration, basic fibroblast growth factor (bFGF) will be added to the scaffold during the electrospinning process by simultaneously electrospaying microspheres into the construct. The microspheres have a core-shell structure with bFGF stabilized by heparin as the core encapsulated by a poly (lactide-*co*-glycolide) (PLGA) shell allowing for sustained release of the growth factor (Guo, Elliott et al. 2012).

bFGF is capable of stimulating the proliferation of fibroblast cells in a dose-dependent manner, promoting angiogenesis, and accelerating oral wound healing (Gospodarowicz 1974, Murakami, Takayama et al. 2003, Oda, Kagami et al. 2004, Murakami and Simons 2008, Kitamura, Akamatsu et al. 2011). We hypothesize that scaffolds fabricated by electrospinning the biocompatible polyester PCL into a fibrous scaffold loaded with microspheres containing bFGF will promote gingival fibroblast proliferation while maintaining a barrier to oral epithelial cells and promote the healing of full-thickness gingival wounds in a rat model.

1.2 The Periodontium

1.2.1 Structure and Function

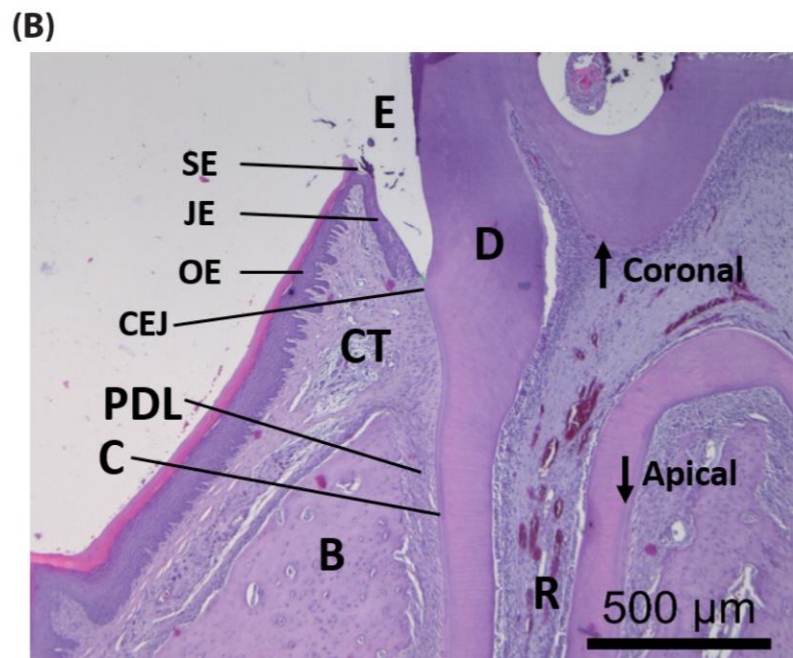
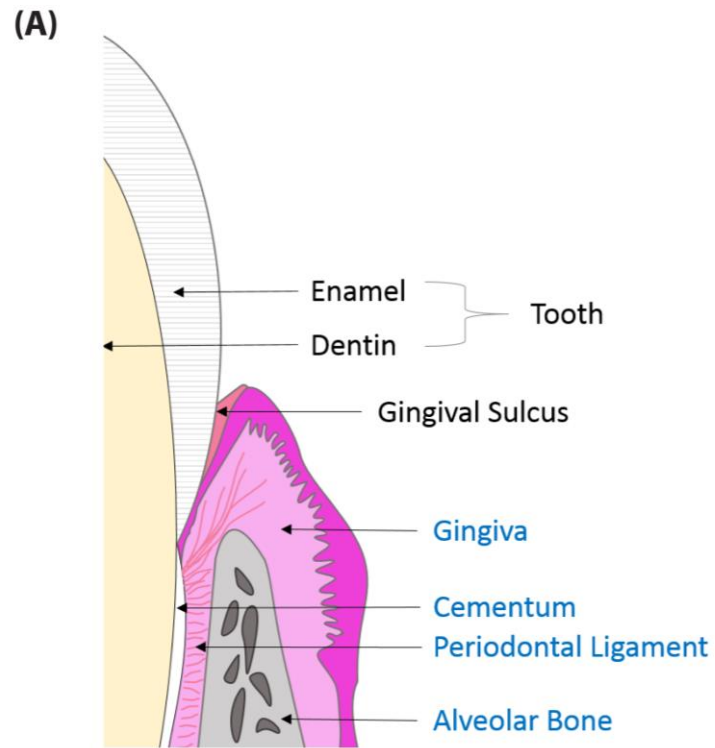
The periodontium encompasses all of the structures that anchor teeth into the jaw. The periodontium is comprised of both soft and hard connective tissues each of which plays a critical role in the structural and functional maintenance of tooth attachment and function. The periodontium is made up of four functional tissue components; the gingiva (commonly referred to as gums), the periodontal ligament (PDL), the alveolar bone and cementum (Bartold, Walsh et al. 2000) (Figure 1.1). Each of these tissues is unique in terms of extracellular matrix (ECM) and cellular composition.

The primary support for the tooth is provided by bone, with each tooth anchored into the jaw in a socket of mineralized alveolar bone through the PDL. The alveolar bone is made up of an outer compact bone layer with an interior cancellous bone portion (Hammarstrom and Lindskog 1985). The osteoblasts (bone forming cells) secrete the organic bone matrix, termed osteoid, which is primarily type I collagen (Piperni, Takamori et al. 2014). The secreted matrix is calcified and the resulting bone is 60% inorganic material by weight with crystalline hydroxyapatite being the most abundant inorganic constituent (Feng 2009). Bone remodeling occurs through the highly regulated and coordinated actions of the bone depositing osteoblasts and the bone resorbing osteoclasts (Charles and Aliprantis 2014).

The periodontal ligament is a dense connective tissue that forms the functional attachment between the mineralized tissues of the cementum and the alveolar bone. During mastication, the forces loaded on the teeth are dispersed through the PDL (Ho, Marshall et al. 2007). The principle cell type of the PDL is the fibroblast which is found in a matrix of principal fibers (large bundles of type I collagen that traverse the PDL and are embedded in the bone and cementum) (Cho and Garant 2000). In addition, the PDL matrix contains several small leucine rich proteoglycans (SLRPG) associated with the collagen fibril bundles, including lumican, fibromodulin, decorin, and biglycan (Matheson, Larjava et al. 2005).

Figure 1.1 - Anatomy of the periodontium.

Periodontium refers to the tissues which are critical in attaching teeth to the jaw. A) Schematic illustrating a cross sectional view of a tooth and surrounding tissue. Tissues of the periodontium are labelled in blue and are shown in reference to the tooth. B) Hematoxylin and eosin stained section of a rat molar and surrounding tissue. The tissues of the periodontium are labelled as periodontal ligament (PDL), cementum (C), alveolar bone (B) and the gingiva which is composed of connective tissue (CT) covered by oral epithelium (OE). The gingiva attaches to and forms a tight seal with the tooth through the junctional epithelium (JE) which merges with the sulcular epithelium (SE) in the gingival sulcus. The tooth is composed of dentin (D) with an enamel crown, shown as an enamel space (E) in histologic sections. The cementoenamel junction (CEJ) is a landmark feature where the cementum covering the tooth root (R) meets the enamel. Terminology regarding directionality associated with the tooth is such that coronal indicates towards the crown of the tooth and apical indicates towards the apex of the root.



Cementum is a thin layer of mineralized tissue found on the surface of the dentinal tooth root where the tooth root interfaces with the PDL (Foster 2012). Cementum functions to anchor the collagen fiber bundles of the PDL to the tooth root through structures termed Sharpey's fibers (Bosshardt and Selvi 1997). The organic component of cementum is mainly type I collagen (>90%) with approximately 5% type III collagen (Birkedal-Hansen, Butler et al. 1977) and is formed by cementoblasts which are derived from neural crest cells during development (ectomesenchymal origin) (Chai, Jiang et al. 2000).

The gingiva is composed of a type I collagen rich dense connective tissue with an overlying epithelium and forms a soft connective tissue covering over the PDL, alveolar bone, cementum, and tooth roots. Oral gingival epithelial cells (ectodermal origin) are the main cell type of the epithelium; however, other cells may be seen such as Langerhans cells, melanocytes and Merkel cells (Ramibri, Panzica et al. 1992, Barrett and Raja 1997, Bartold, Walsh et al. 2000). The epithelium of the gingiva is divided into three distinct anatomical regions which differ in their cellular organization, function and keratin composition (Mackenzie, Rittman et al. 1991). These regions are defined as the oral gingival, oral sulcular and junctional epithelia (Schroeder and Listgarten 1997). Overall, the epithelia functions to prevent bacterial infiltration into the underlying periodontium. The teeth present a unique challenge to this protective function in that the tooth is not an appendage of the mucosa, but rather perforates through it. Thus, a tight seal must be made between the hard tissue of the tooth and the epithelium of the gingiva. This occurs through the junctional epithelium which attaches to the tooth from the cemento-enamel junction to the bottom of the gingival sulcus (Bosshardt and Lang 2005). The junctional epithelium is a stratified, non-keratinizing epithelium which is bordered by two basal lamina; an external basal lamina found between the epithelium and the connective tissue and an internal basal lamina found between the epithelium and the surface of the tooth (Sawada and Inoue 1996, Bosshardt and Lang 2005). The connective tissue component of the gingiva is composed of gingival fibroblasts (mesenchymal origin) residing within an extracellular matrix of collagen, mainly type I, and proteoglycans including decorin, biglycan, versican, and CD44 (Bratt, Anderson et al. 1992, Larjava, Hakkinen et al. 1992, Hakkinen, Oksala et al. 1993). Collagen fibers of the matrix show considerable organization into thick bundles and form the gingival

supra-alveolar fiber apparatus which attaches to the tooth (Chavrier, Couble et al. 1984, Bartold, Walsh et al. 2000). Together, the connective tissue and epithelium maintain homeostasis of the periodontium by functionally excluding the oral environment from the underlying structures. The integrity of the barrier can however be compromised following injury, trauma or prolonged poor oral hygiene which then allows for invasion of the tissues by microbial organisms (Schroeder and Listgarten 1997).

1.2.2 Periodontal Diseases

Periodontal diseases are broadly defined as pathologies that affect the periodontium. These conditions can be inherited, but are usually acquired. Furthermore, periodontal diseases are influenced by genetic, traumatic, developmental or inflammatory factors (Pihlstrom, Michalowicz et al. 2005). However, the term periodontal disease is most commonly used to refer to the inflammatory conditions in which inflammation of the periodontium is caused by pathogenic bacteria in tooth plaque that accumulates on and around the tooth surfaces (Armitage 2004, Pihlstrom, Michalowicz et al. 2005).

Periodontal diseases range in severity with the mildest form being gingivitis. Gingivitis is mild inflammation that is confined to the gingiva and can be readily reversed by removing the causative bacterial agents through routine oral hygiene (Pihlstrom, Michalowicz et al. 2005). Although reversible, gingivitis is highly prevalent with more than 82% of adolescents and 50% of adults in the United States being affected (Albandar and Rams 2002). If gingivitis is allowed to persist, the condition progresses and can develop into the more serious periodontitis (Albandar and Rams 2002).

Periodontitis affects all of the structures of the periodontium and leads to destruction of the gingival connective tissue and the PDL, and resorption of the alveolar bone, which can lead to loosening of the tooth and eventual tooth loss (AAP 2001, Pihlstrom, Michalowicz et al. 2005). Periodontitis develops when bacterial components and their products which have accumulated around the teeth infiltrate the gingival epithelium into the connective tissue and cause a persistent host inflammatory response (Page, Offenbacher et al. 1997). The tight seal maintained by the junctional epithelium is compromised, exposing the underlying periodontium to the more than 500 bacterial species present in the oral cavity (Moore and Moore 1994, Bosshardt and Lang 2005).

The loss of connective tissue attachment results in the formation of a periodontal pocket which becomes lined with gingival epithelium and further accumulates bacteria and plaque (Page, Offenbacher et al. 1997). The pathogenesis is, in part, mediated through bacterial release of endotoxins and proteases which break down the tissues of the periodontium (Socransky and Haffajee 1994). Of even greater significance is that the persistence of bacteria activates the host immune inflammatory response, and if sustained, will result in release of proteolytic enzymes which further contribute to tissue breakdown (Pihlstrom, Michalowicz et al. 2005). During the inflammatory response, macrophages become activated and release several factors including interleukin 1 β , tumour necrosis factor α , matrix metalloproteinases, and prostaglandin E₂ (Page, Offenbacher et al. 1997). Gingival fibroblasts are activated to produce matrix metalloproteinases and prostaglandin E₂ in response to interleukin 1 β and tumour necrosis factor α (Page, Offenbacher et al. 1997). Matrix metalloproteinases mediate the destruction of the extracellular matrix components and prostaglandin E₂ mediates resorption of the alveolar bone (Page, Offenbacher et al. 1997).

Periodontitis has a high prevalence rate. Data from the 2009 and 2010 National Health and Nutrition Examination Survey estimated that 47% of the adult U.S. population is affected by periodontitis (Eke, Dye et al. 2012). Several factors predispose an individual to being affected by periodontal diseases including: poor oral hygiene, tobacco use, stress, diabetes, and age (Petersen and Ogawa 2005, Kinane, Bouchard et al. 2008). Periodontitis can also have interactions with other systemic conditions. Clinical studies suggest that periodontitis is more severe in patients with uncontrolled diabetes mellitus and can negatively impact cardiovascular events in susceptible individuals due to the high inflammatory burden associated with periodontitis (Kinane, Bouchard et al. 2008).

In addition to its high prevalence rate, the major concern with periodontitis is the limited ability of the periodontium to regenerate even after removal of the causative bacterial agents (Pihlstrom, Michalowicz et al. 2005, Hughes, Ghuman et al. 2010). Non-surgical treatment of periodontitis involves the removal of plaque and bacteria from around the tooth, however this only serves to stop the progression of the disease with little appreciable regeneration of the lost structures (Pihlstrom, Michalowicz et al. 2005,

Hughes, Ghuman et al. 2010). Following treatment, inflammation and swelling of the gingival tissue subsides, but apical migration of the epithelium and tissue shrinkage result in gingival recession (Tugnait and Clerehugh 2001).

When the gingival margin is located apical to the normal location at the cementoenamel junction, gingival recession is diagnosed (AAP 2001). In addition to being caused by periodontitis, gingival recession can be a result of trauma, poor tooth alignment, or thinning or reduction of the alveolar bone (Watson 1984, Chambrone and Chambrone 2003). Gingival recession can also affect individuals with good oral hygiene; a prevalence rate of 25% was evident in a sample population who had good oral hygiene and received regular dental care (Seritm, Wennstrom et al. 1994). The prevalence of gingival recession is high, with more than 50% of the population having at least one site of gingival recession (Kassab and Cohen 2003). Gingival recession may be present without being apparent to the patient, however other patients with recessions may experience pain and root hypersensitivity, fear over tooth loss, and esthetic concerns (Kassab and Cohen 2003). Exposure of the tooth root to the oral cavity due to gingival recession causes tooth sensitivity and may make the root more susceptible to abrasion and caries which is damaging to the health and survival of the tooth (Kassab and Cohen 2003). Gingival recession resultant from periodontitis indicates that the healing response is inadequate to restore the correct functional and anatomical structure of the periodontium.

1.3 Gingival Wound Healing

1.3.1 Connective Tissue

The basic stages of wound healing that take place during cutaneous wound repair also occur during healing of the oral mucosa. Three sequential, but overlapping, phases of wound healing are required: inflammatory phase, granulation tissue formation and matrix deposition and remodeling (Wikesjo and Selvi 1999). Immediately following connective tissue injury, plasma proteins from the blood, primarily fibrinogen, adhere to wound surfaces and the tooth root in preparation for the formation of a fibrin clot (Wikesjo and Selvi 1999, Polimeni, Xiropaidis et al. 2006). Within hours of injury, a pro-

inflammatory response is initiated, characterized by infiltration of neutrophils and monocytes to phagocytose cellular debris from the damaged and necrotic areas of the tissues (Polimeni, Xiropaidis et al. 2006). Up to three days following injury, inflammation persists with neutrophil infiltration gradually subsiding as macrophage influx becomes predominant. The phenotype of the macrophages switches to promote repair through the release of growth factors such as transforming growth factor- β 1 (TGF- β 1) which enables the transition to development of granulation tissue and the proliferative stage of repair (Leibovich and Ross 1975, Wikesjo and Selvi 1999). As granulation tissue forms up to day seven following injury, fibroblasts and endothelial cells migrate into the wound area and proliferate, a provisional matrix is deposited, and angiogenesis occurs (Wikesjo and Selvi 1999, Polimeni, Xiropaidis et al. 2006). Fibroblast migration into the granulation tissue requires downregulation of integrins for collagen attachment (α 2 β 1) and upregulation of integrins for interaction with components of the provisional matrix: fibrin (α V β 3), fibronectin (α 4 β 1) and vitronectin (α V β 5) (Aukhil 2000). Following the events in the initial seven days post-injury, the wound enters the matrix remodeling phase wherein the granulation tissue matrix is remodeled into a more collagen rich, mature and stable matrix followed by the appearance of myofibroblasts which contract the wound (Wikesjo and Selvi 1999, Polimeni, Xiropaidis et al. 2006). Although the initial steps of wound healing are essentially analogous to most soft tissue healing, proper periodontal healing requires the connective tissue to make adequate adhesion to the tooth root through anchorage of collagen fibers to the cementum (Wikesjo and Selvi 1999).

1.3.2 Epithelial Component

Within hours of a gingival wound forming, basal epithelial cells start to proliferate and migrate into the fibrin clot in the wound area (Polimeni, Xiropaidis et al. 2006). In uninjured tissue, basal epithelial cells are attached to the basal lamina through integrin α 6 β 4 attachment to laminin (Aukhil 2000). To initiate migration in response to injury the epithelial cells must first break hemidesmosome connections with the basal lamina and express integrins suitable for migration through the fibrin clot (Borradori and Sonnenberg 1999, Aukhil 2000). Migrating epithelial cells start to express integrins α 5 β 1

(fibronectin), $\alpha V\beta 6$ (tenascin), $\alpha V\beta 5$ (vitronectin) and reorganize their distribution of integrin $\alpha 2\beta 1$ (collagen) allowing for migration over wound debris and the provisional wound matrix (Aukhil 2000). Migrating epithelial cells also upregulate tissue-type plasminogen activator and urokinase-type plasminogen activator which activate the plasminogen in the fibrin clot to plasmin allowing for the breakdown of the clot, thus creating a path through which migration can occur (Martin 1997). Once the wound is re-epithelialized a new basal lamina forms and epithelial cells return to their original phenotype (Aukhil 2000). The epithelium must also reform the junctional and sulcular epithelium found adjacent to the tooth. The junctional epithelium appears to be regenerated from undifferentiated cells from the sulcular epithelium (Sabag, Mery et al. 1984). Formation of a long junctional epithelium can occur following gingival wounding where the epithelium is found migrating apically along the tooth root hindering the formation of connective tissue attachment to the tooth root. This occurs as a result of the epithelium migrating faster than the formation and attachment of new connective tissue to the tooth root (Bartold, Walsh et al. 2000). The formation of this periodontal pocket is one of the major problems in the regeneration of gingival connective tissue and must be prevented.

Although the gingiva possesses considerable healing capacity following injury, repair following the repeated inflammatory response associated with inflammatory periodontal diseases results in tissue shrinkage, fibrosis and gingival recession (Hughes, Ghuman et al. 2010). This in combination with the formation of a periodontal pocket prevents proper anatomical self-repair of the periodontium thus requiring periodontal therapeutic intervention (Pihlstrom, Michalowicz et al. 2005).

1.4 Periodontal Disease Treatments

1.4.1 Periodontal Plastic Surgery

Periodontal plastic surgery refers to surgical techniques and procedures used to treat and correct several types of periodontal defects, including surgeries to correct gingival recession (Miller 1988). There are several procedures which can be used to correct gingival recession defects, such as coronally advanced flaps, free gingival grafts, laterally

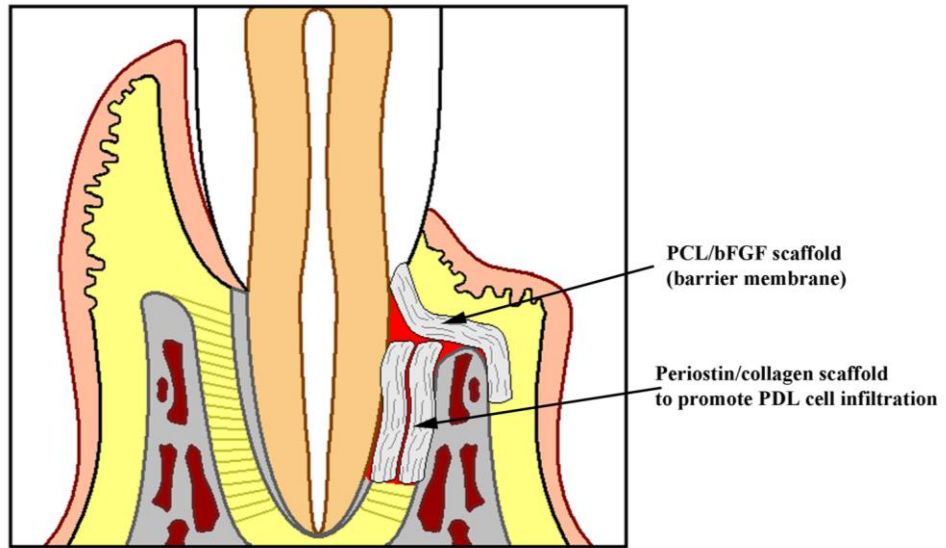
repositioned flaps and subepithelial connective tissue grafts (SCTGs) (Chambrone, Sukekava et al. 2010). SCTGs are considered the gold-standard for the treatment of gingival recession defects (Chambrone, Chambrone et al. 2008, Chambrone, Sukekava et al. 2010). In this procedure, a palatal donor site is raised and a connective tissue graft larger than the recession site is removed. The flap created at the donor site must then be sutured back into place. At the recipient site, a flap is raised with the harvested connective tissue graft placed over the exposed tooth root and sutured into place following cleaning of the root surface (Langer and Langer 1985, Raetzke 1985). Although considered the gold-standard, SCTG procedures are associated with several drawbacks mainly due to the need for a second surgical donor site. The donor site is associated with pain and discomfort, bleeding, morbidity, and the availability of donor tissue in the palate is extremely limited (Liu, Mao et al. 2011). In addition, as oral epithelial tissue proliferates faster than connective tissue or graft tissue, it commonly migrates down the tooth root forming a long junctional epithelium and impairing the ability of the connective tissue or graft to attach and provide root coverage (Bartold, McCulloch et al. 2000).

1.4.2 Guided Tissue Regeneration

Guided tissue regeneration (GTR) is a technique that involves the placement of a barrier membrane into the periodontal defect site immediately under the gingival tissue forming a physical gap or barrier to exclude epithelium from populating the damaged site; maintaining space for the PDL and alveolar bone to regenerate into (Fu, Su et al. 2012) (Figure 1.2). This technique was first introduced in 1982 when Nyman and colleagues (Nyman, Gottlow et al. 1982) used a Millipore filter as a membrane in a non-human primate model of periodontitis to regenerate periodontal structures and remains a routinely used surgery by periodontists. The use of barrier membranes for periodontal repair overcomes the drawbacks associated with SCTGs in that it does not rely on the availability of donor tissue.

Figure 1.2 - Guided tissue regeneration.

We propose the use of a PCL electrospun fibrous scaffold membrane as an alternative to the current cell-occlusive GTR membranes. Membranes are placed under the gingival connective tissue against the root of the tooth to prevent the apical migration of the oral epithelium. To promote PDL cell infiltration and bone regeneration a second scaffold or material can be placed into the periodontal defect.



GTR membranes must fulfill certain characteristic properties including biocompatibility and safety, space maintenance, ease of use, and cell exclusion (Aurer and Jorgic-Srdjak 2005). The concept of space maintenance and cell exclusion is such that the gingiva is excluded from the defect site providing the periodontal ligament cells with a space adjacent to the tooth into which they can selectively repopulate the defect (Gottlow, Nyman et al. 1986). As described below, several types of materials are used clinically as a barrier membrane. The types of membranes used can be classified into non-resorbable; those requiring surgical removal following periodontal regeneration, or resorbable; those which are degraded during the healing process. Resorbable membranes can be fabricated from natural or synthetic materials, as discussed in detail in the following sections.

1.4.2.1 Non-Resorbable Membranes - Gore-Tex[®]

Non-resorbable membranes maintain their structure and integrity throughout the healing process, with the most commonly used material being Gore-Tex[®]. Gore-Tex[®] expanded polytetrafluoroethylene (ePTFE) membranes were the first non-resorbable membranes approved for clinical use (Aurer and Jorgic-Srdjak 2005). ePTFE is manufactured from the inert and biocompatible fluorocarbon polymer polytetrafluoroethylene under tensile strength creating a porous and fibrous microstructured material (Aurer and Jorgic-Srdjak 2005). Although the use of these membranes show improvements in periodontal clinical parameters, complete regeneration remains a challenge (Gottlow, Nyman et al. 1986, Stahl, Froum et al. 1990, Kersten, Chamberlain et al. 1992, Wadhawan, Gowda et al. 2012). These occlusal membranes provide adequate space maintenance and cell exclusion in the defect site, but as they are non-resorbable, a second surgery is required to retrieve the membrane. This is not ideal as it increases surgical time for the patient, increases the cost of the GTR procedure and adds additional surgical trauma to any newly formed periodontal tissue (Gottlow 1993).

1.4.2.2 Biodegradable and Bioresorbable Membranes

To eliminate the need for a second surgery to remove membranes following healing, resorbable membranes for periodontal regeneration were developed. These membranes

act as a space making barrier during the healing period and following the establishment of new periodontal attachment the material degrades, ideally without affecting the regeneration of the periodontal tissues (Gottlow 1993). While natural materials have been investigated for use as membranes, their biomechanical properties are not optimal for an active biomechanical environment where aggressive oral epithelial migration occurs. The material must have resilience and strength which membranes made from natural material rarely possess (Aurer and Jorgic-Srdjak 2005). Several synthetic biomaterials have now been developed for use as barrier membranes. Synthetic polymers are an attractive option due to their low cost, abundance, ease of fabrication and large customization potential. Polylactic acid (PLA), polyglycolic acid (PGA), PCL and their copolymers have been widely investigated. These three polyesters have been approved by the U.S. Food and Drug Administration for use in medical applications such as bioabsorbable sutures and applications for drug delivery (Dong, Liau et al. 2009).

1.4.2.2.1 Collagen

Collagen membranes were developed for GTR applications due to their inherent biocompatibility and their chemotactic properties for fibroblasts (Postlethwaite, M. et al. 1978, Rothamel, Schwarz et al. 2004), examples of which include: BioMend® and Bio-Gide®. Collagen membranes were found to support connective tissue attachment and prevent epithelial migration along the tooth root in canine periodontal defects (Blumenthal 1988, Pitaru, Tal et al. 1989) and were found to be as effective as ePTFE membranes at restoring clinical periodontal attachment in clinical studies (Blumenthal 1988, Pitaru, Tal et al. 1989, Tatakis, Promsudthi et al. 1999). The degradation of collagen membranes occurs through the enzymatic activity of inflammatory cells and degrade within 4-8 weeks (Blumenthal 1988, Pitaru, Tal et al. 1989, Tatakis, Promsudthi et al. 1999). For effective space maintenance in the defect site the membrane must withstand the forces created by flap placement and associated with mastication (Tatakis, Promsudthi et al. 1999). The failure of collagen membranes to withstand such forces, along with their rapid degradation in particular when exposed to enzymes associated with saliva and the inflammatory response may contribute to their variability in regenerating

periodontal tissue and the inability to promote complete periodontal defect fill (Pitaru, Ta et al. 1987, Bunyaratavej and Wang 2001).

1.4.2.2.2 Polylactic Acid

PLA is a synthetic poly (α -hydroxy acid) which is manufactured by catalytic polymerization of lactic acid monomers (Tatakis, Promsudthi et al. 1999). In contrast to collagen which degrades by enzymatic activity, poly (α -hydroxy acids) are degraded by hydrolysis with the resulting degradation products being metabolized by the citric acid (Kreb) cycle to produce water and carbon dioxide (Tatakis, Promsudthi et al. 1999). PLA hydrolysis is relatively slow and produces monomers of lactic acid, linear dimers and other oligomers (Marcato, Paganetto et al. 1996) which can be cytotoxic in high concentrations, although the polymers themselves are biocompatible *in vitro* (Ignatius and Claes 1996). Although PLA is biocompatible *in vitro*, implantation into periodontal defects initiates an inflammatory response at 4 weeks (Wikesjö and Nilvéus 1990) and severe bone resorption was observed 4 months following implantation (Mau, Cheng et al. 2012). This suggests that PLA is not an ideal synthetic biomaterial for GTR membranes.

1.4.2.2.3 Polyglycolic Acid

PGA has a relatively fast degradation rate compared to other synthetic aliphatic polyesters (Dong, Liao et al. 2009). PGA is used clinically for pins, screws, rods and implants in orthopedic applications. PGA implants in bone are associated with localized inflammation which does not compromise repair, however this inflammatory response may be problematic when using PGA for soft tissue wound repair or regenerative applications where the tissue is already inflamed (Bostman, Hirvensalo et al. 1990, Ceonzo, Gaynor et al. 2006). Subcutaneous PGA polymer implants have been associated with an acute inflammatory response, the magnitude of which is proportional to the degradation time of the polymer, with faster degradation times inducing greater inflammatory responses (Burdick, Padera et al. 2002). As with PLA, high concentrations of the degradation products can be cytotoxic and damage surrounding tissue (Bostman, Hirvensalo et al. 1990, Ashammakhi and Rokkanen 1997, Ceonzo, Gaynor et al. 2006, Dong, Liao et al. 2009). The inflammatory response to PGA may affect matrix

production and ultimately the integrity of the healing tissue (Kojima, Bonassar et al. 2002). To prolong the degradation time and make PGA more suitable in terms of providing adequate support for regenerating periodontal tissue and reducing the inflammatory response for membranous tissue repair applications, PGA is often combined with PLA to form the copolymer poly (lactide-*co*-glycolide) (PLGA) which has an intermediate degradation time between the two polymers. Gingival fibroblasts cultured on PLGA membranes *in vitro* had decreased proliferation compared to gingival fibroblasts cultured on collagen membranes, indicating that collagen membranes may preferentially promote gingival tissue repair (Hakki, Korkusuz et al. 2013).

Barrier membranes currently used for GTR that are completely occlusal do not work well. As described above, the use of barrier membranes in periodontal procedures does not provide predictable or full regeneration of the damaged periodontium, making it clear that several improvements need to be made to the GTR technique (Kersten, Chamberlain et al. 1992, Greenstein and Caton 1993, Ivanovski 2009, Hughes, Ghuman et al. 2010). Space provision by GTR membranes appears to be a requirement for facilitating periodontal regeneration, whereas tissue occlusion does not appear to be a necessity (Wikesjo, Lim et al. 2003, Polimeni, Albandar et al. 2005). The use of an occlusive membrane which excludes gingival connective tissue from a regenerating periodontal defect is less than ideal as the gingiva contains a rich vascular plexus and is a potential source of progenitor cells (Schroeder and Listgarten 1997, Fournier, Larjava et al. 2013). A new generation of biomaterials needs to be developed and investigated for improved GTR. One potential improvement is developing a fibrous, selectively occlusive biomaterial scaffold membrane as an alternative to the current occlusal barrier membranes.

1.4.3 Scaffold Membrane-Mediated Periodontal Regeneration

Scaffold membrane-mediated tissue regeneration is a strategy that is focused on promoting regeneration of the normal tissue architecture to restore tissue function through the use of a specifically designed biomaterial scaffold. This technique uses biocompatible, resorbable biomaterial scaffold membranes fabricated to act as a supportive three dimensional matrix, as opposed to cell-occlusive barrier membranes

used currently for GTR. Ideally these scaffolds can mimic the natural fibrous structure of the ECM, facilitating cell attachment and subsequent infiltration to promote the formation of a functional cellular and vascular connective tissue attachment to the tooth root while acting as a barrier for unfavourable cells, specifically epithelial cells (Schroeder and Listgarten 1997, Sun, Qu et al. 2012). The scaffolds can also be engineered to incorporate growth factors that allow for their controlled and sustained release in the defect site (Kaigler, Cirelli et al. 2006, Barnes, Sell et al. 2007, Kao, Murakami et al. 2009).

Several scaffold materials have been tested for periodontal tissue healing applications (Nakahara, Nakamura et al. 2003, Mohammadi, Shokrgozar et al. 2007, Jansen, Kuijpers-Jagtman et al. 2008, Ayvazyan, Morimoto et al. 2011, Lotfi, Shokrgozar et al. 2011). Collagen scaffolds were shown to be biocompatible in palatal wound healing applications (Jansen, Kuijpers-Jagtman et al. 2008, Ayvazyan, Morimoto et al. 2011); however, due to the requirement for mechanical stability in periodontal defects collagen scaffolds are not ideal. Chitosan scaffolds, created by alkaline deacetylation of chitin (Akncbay, Senel et al. 2007), and collagen scaffolds seeded with gingival fibroblasts increased the width of keratinized gingival tissue in a canine model and in a clinical setting, respectively (Mohammadi, Shokrgozar et al. 2007, Lotfi, Shokrgozar et al. 2011). This method, however, requires a separate initial surgery for the harvesting of gingival fibroblasts and requires *ex vivo* culture of the cells thus increasing the time, cost, and complexity of such a procedure (Sun, Qu et al. 2012). Advances in the field of materials engineering make it possible to design biofunctional biomaterial scaffolds which can be used to recruit endogenous cells surrounding the defect site to promote *in situ* periodontal tissue regeneration (Sun, Qu et al. 2012), which is the focus of this thesis.

1.4.3.1 Scaffold Fabrication

Development of optimal scaffolds requires: 1) selection of the appropriate material, 2) fabrication of the appropriate structural architecture, and 3) addition of appropriate biological signals, such as growth factors. Synthetic polyesters have been widely studied for use in biomaterial scaffolds due to their availability and abundance, ease of fabrication, customizability in terms of strength and degradation rate, and their

biocompatibility and biodegradability characteristics. One particularly attractive property of synthetic polymers is that they can be electrospun to create structures similar in size to native ECM.

1.4.3.2 Electrospinning

Electrospinning is a process which can be used to fabricate fiber-based constructs from both natural and synthetic polymers. The polymer is dissolved in a solvent and the resulting solution is charged. A collection plate is oppositely charged and the polymer solution is drawn into fibers by static electricity. As the solvent evaporates, the solid polymer fibrous structure is left behind (Kumbar, James et al. 2008). This technique allows fabrication of scaffolds which closely mimic the fibrous nature of the ECM. The fibers produced by electrospinning are non-woven and have an interconnected porosity allowing for cells to interact with the fibers while permitting cell infiltration throughout the porous scaffold network and maintaining nutrient and waste exchange within the scaffold (Dong, Liao et al. 2009).

The process of electrospinning has several advantages over other methods for scaffold fabrication such as phase separation and self-assembly. Electrospinning is able to be carried out in the laboratory setting but is scalable and can be adapted to large scale processing, it is cost effective, convenient, and the diameter and alignment of the fibers is able to be manipulated (Murugan and Ramakrishna 2007). The electrospinning apparatus can also be set up to produce different nanofibrous structures such as aligned nanofibers, tubular structures, and core-shell structures (Dong, Liao et al. 2009).

Several natural and synthetic materials have been electrospun into fibrous scaffolds. Natural materials which have been electrospun include collagen, chitosan, agarose, and alginate (Matthews, Wnek et al. 2002, Bhattarai, Edmondson et al. 2005, Shu-Hua Teng, Peng Wang et al. 2009, Bonino, Krebs et al. 2011). Although these materials are capable of being electrospun into fibrous scaffold membranes, their weak mechanical properties and short degradation time limit their use for GTR membrane applications where they are required to withstand the tissue tension forces associated with flap placement following surgery and forces transmitted through the flaps from mastication (Tatakis, Promsudthi et

al. 1999, Li, Laurencin et al. 2002, Teo, He et al. 2006). Synthetic polymers offer greater mechanical stability compared to natural polymers. Synthetic polymers which have been electrospun include PLA, PGA, and PCL and their copolymers (Huang, Zhang et al. 2003).

1.4.3.3 Polycaprolactone

PCL is a bioresorbable, aliphatic polyester with a molecular weight of 80,000 and a relatively long degradation time compared to other synthetic polyesters, making it suitable for space provision in GTR applications (Lam, Hutmacher et al. 2009). PCL is quite stable during *in vitro* hydrolysis testing however shows a faster degradation rate by microorganisms and enzymes (Zeng, Chen et al. 2004, Dong, Liao et al. 2009). The degradation of PCL occurs in two stages. The first is non-enzymatic bulk hydrolysis in which the carboxylic acid end groups autocatalyze the hydrolysis of the ester linkages decreasing the molecular weight of the polymer without a decrease in weight (Woodward, Brewer et al. 1985). Once the molecular weight of the polymer decreases to 5,000 weight loss occurs as the oligomeric species produced become small enough to diffuse away from the bulk polymer (Woodward, Brewer et al. 1985). In the second stage, low molecular weight PCL particles are ingested by neutrophils, macrophages, giant cells and to a lesser extent, fibroblasts *in vivo* (Woodward, Brewer et al. 1985). PCL fibrous scaffolds were found to have a faster degradation rate *in vivo* compared to *in vitro* with smaller diameter fibers degrading faster than larger diameter fibers (Bölgen, Menceloglu et al. 2005). Implantation of PCL scaffold matrices in both intramuscular and subcutaneous sites were found to be biocompatible and did not elicit a negative host response at 3 and 6 months post implantation (Lam, Hutmacher et al. 2009). This is in contrast to the inflammatory response observed with PLA and PGA membranes, as mentioned previously. Due to its long degradation time and biocompatibility, we hypothesize that PCL is an appropriate material for fabrication of electrospun fibrous scaffolds for periodontal regenerative applications. While fibrous PCL scaffolds can be made to mimic the structural architecture of the ECM, this polymer lacks bioactivity, which can impair tissue response.

1.4.3.4 Enhancing Scaffold Bioactivity

Growth factors play important roles in the wound healing process, including the induction of cell migration, proliferation and differentiation. Several studies have found the delivery of growth factors to periodontal defect sites to be advantageous and promote regeneration (Howell, Fiorellini et al. 1997, Oda, Kagami et al. 2004, Nemcovsky, Zahavi et al. 2006, Fu, Su et al. 2012). The application of growth factors has had limited clinical success, due to the rapid diffusion and degradation of topically applied growth factors, their short half-lives, and the need to be administered in large doses (Kaigler, Cirelli et al. 2006, Hughes, Ghuman et al. 2010). There is a clear need for a more sustained method of delivery. Our aim is to create a bioactive PCL electrospun fibrous scaffold that can be used for applications in periodontal regeneration.

1.4.3.4.1 Electro spraying Core-Shell Microspheres

To confer bioactivity to the PCL electrospun fibrous scaffolds growth factors will be delivered in the form of core-shell structured microspheres loaded into the fibrous structure of the scaffold. Incorporation of growth factors into the scaffolds using this method will allow for controlled and temporally sustained release of the growth factor. Core-shell structures are produced by a coaxial electro spraying process wherein two streams of materials are combined; an inner nozzle, containing the core material solution, and an outer nozzle containing the shell material solution (Hwang, Jeong et al. 2008). Coaxial electro spraying can create uniform sized microspheres with an outer polymer shell and inner colloid core (Hwang, Jeong et al. 2008). As the outer shell material degrades the inner core material is released in a controlled and sustained manner (Wu, Liao et al. 2010). By combining the electro spraying and electro spinning processes, the microspheres can be uniformly distributed within the scaffold (Guo, Elliott et al. 2012). Due to its relatively fast degradation rate and biocompatibility when used in moderation, PLGA was chosen as the material for the shell structure.

1.4.4 Biological Agents for Periodontal and Gingival Repair

Several growth factors have been investigated for use in periodontal tissue repair, including platelet derived growth factor (PDGF), transforming growth factor- β 1 (TGF-

β 1) and bone morphogenetic protein-2 (BMP-2). While PDGF and TGF- β 1 do stimulate the proliferation of gingival fibroblasts (Dennison, Vallone et al. 1994), the effect of TGF- β 1 in particular on gingival tissue may promote fibrosis and scar formation (Raja, Byakod et al. 2009, Thompson, Hamilton et al. 2010). BMP-2 is strongly osteogenic, however it is less than ideal for use due to its high cost, potential to cause root resorption and ankyloses and its cytotoxic effects on PDL cells (Wikesjo, Guglielmoni et al. 1999, Ryoo, Lee et al. 2006, Muthukuru 2013). For these reasons and those listed below, we have focused our research program on bFGF. Murakami and colleagues (Murakami, Takayama et al. 1999, Murakami, Takayama et al. 2003) were able to regenerate periodontal structures in beagle dogs with experimentally induced periodontitis following topical application of recombinant bFGF. Topical application of bFGF was assessed in a large phase II clinical trial and found to be effective at regenerating the alveolar bone of patients with periodontitis, however did not result in gain of clinical attachment compared to vehicle alone (Kitamura, Akamatsu et al. 2011). Since bFGF is a potent mitogen of mesenchymal cells and promotes wound healing, as described below, we hypothesize that the sustained release of bFGF from PCL electrospun GTR scaffolds will be effective at promoting the regeneration of clinical attachment.

1.5 Basic Fibroblast Growth Factor

1.5.1 General Structure and Function

Basic fibroblast growth factor was first identified in brain and pituitary extracts based on its effects on the proliferation of 3T3 fibroblast cells (Gospodarowicz 1974). Human bFGF was initially thought to be synthesized as a 155 amino acid protein which shares a high degree of sequence homology (98.7%) with bovine bFGF indicating that it is highly conserved across species (Abraham, Whang et al. 1986). Human bFGF is encoded by one gene (*FGFB*) mapped to chromosome 4 (Abraham, Whang et al. 1986, Mergia, Eddy et al. 1986). bFGF has since been identified as an 18 kDa protein with several high molecular weight (HMW) (22-24 kDa) translational variants (Moscatelli, Joseph-Silverstein et al. 1987, Florkiewicz and Sommer 1989). Crystallographic analysis of the bFGF protein revealed that the structure is entirely composed of β -sheets (Zhang, Cousens et al. 1991). The tertiary structure of bFGF is composed of three 4-stranded β -

meander motifs to create a barrel which is closed at the amino- and carboxy-terminus (Zhang, Cousens et al. 1991). 18 kDa bFGF is primarily found in the cytosol and increases cell growth and migration, whereas HMW bFGF is primarily localized to the nucleus and increases cell growth but not migration and is required for cell growth in low serum conditions (Renko, Quarto et al. 1990, Bikfalvi, Klein et al. 1995).

In physiological systems, heparin or heparan sulfate proteoglycans protect bFGF from denaturation by binding to basic residues in the tenth and eleventh β strand of bFGF and are required for bFGF to activate fibroblast growth factor receptor (FGFR) tyrosine kinases (Rapraeger, Krufka et al. 1991, Kan, Wang et al. 1993, Nissen, Shankar et al. 1999, Faham, Linhardt et al. 1998). Five FGFRs (FGFR 1-5) have been identified with bFGF binding with highest affinity to FGFR1 and FGFR2 (Mansukhani, Moscatelli et al. 1990, Mansukhani, Dell'Era et al. 1992, Ornitz, Xu et al. 1996, Laestander and Engstrom 2014). Upon activation, FGFR tyrosine kinases dimerize and become autophosphorylated (Bellot, Crumley et al. 1991). Several autophosphorylation sites in FGF receptor tyrosine kinase 1 (FGFR1) have been identified including Tyr-463, Tyr-583, Tyr-585, Tyr-653, Tyr-654, Tyr 730 and Tyr-766 (Mohammadi, Dikic et al. 1996). Autophosphorylation of Tyr-766 causes association with phospholipase C_{γ} which catalyses the hydrolysis of phosphatidylinositol into diacylglycerol and free inositol phosphate which in turn activates protein kinase C to increase intracellular calcium, affecting cytoskeletal organization (Peters, Marie et al. 1992, Laestander and Engstrom 2014). Autophosphorylation on Tyr-653 and Tyr-654 is required for the biological activity of the receptor and may activate the Ras signaling pathway through phosphorylation of Shc or a 90 kDa protein (pp90) (Mohammadi, Dikic et al. 1996). Activated FGFR activates the docking protein FGFR substrate 2 α which complexes with the adaptor protein Grb2, tyrosine phosphatase Shp2 and docking protein GAB1 (Laestander and Engstrom 2014). Guanine nucleotide exchange factor SOS binds to Grb2 and subsequently activates Ras-Mitogen activated protein kinase which through interaction with intracellular kinases and transcription factors ultimately results in regulation of gene expression, mainly with mitogenic effects (Laestander and Engstrom 2014).

1.5.2 Angiogenesis

bFGF is a potent modulator of angiogenesis. Angiogenesis requires the migration of endothelial cells and bFGF is one of the regulators of the migration of several types of endothelial cells. Endothelial cells synthesize bFGF and upregulate the synthesis and cytoplasmic stores during migration (Biro, Yu et al. 1994). Prior to DNA synthesis, bFGF accumulates in the nucleus of endothelial cells (Biro, Yu et al. 1994). Exogenous bFGF also plays a role in endothelial cell migration with the addition of bFGF to *in vitro* cultures enhancing migration and the addition of antibodies to bFGF inhibiting migration (Biro, Yu et al. 1994). bFGF induces the expression of another potent angiogenic factor, vascular endothelial growth factor (VEGF), in endothelial cells through both autocrine and paracrine mechanisms (Seghezzi, Patel et al. 1998). The angiogenic effects of bFGF *in vivo* are modulated through VEGF suggesting that bFGF acts upstream of VEGF in the process of angiogenesis (Seghezzi, Patel et al. 1998, Murakami and Simons 2008).

1.5.3 Chemotaxis

The formation of granulation tissue at a wound site requires the migration of fibroblasts from the surrounding tissue into the provisional matrix. bFGF stimulates the chemotaxis of skin fibroblasts and granulation tissue fibroblasts *in vitro* (Buckley-Sturrock, Woodward et al. 1989). bFGF has been shown to promote the migration of fibroblasts through the phosphoinositide 3-kinase (PI3-Kinase)-Rac1-JNK pathway (Kanazawa, Fujiwara et al. 2010). Transfection of NIH 3T3 fibroblasts with bFGF cDNA increased migration and the addition of antibodies to bFGF inhibited migration, indicating that bFGF plays a role in fibroblast migration and the effect is mediated in part through autocrine bFGF secreted into the extracellular space (Mignatti, Morimoto et al. 1991, Mignatti, Morimoto et al. 1992).

1.5.4 Mitogenic Effects

Fibroblast proliferation is essential during wound healing. Expression of bFGF cDNA in mouse BALB/c 3T3 fibroblast mouse cells induced the growth of these cells compared to non-transfected parental cells (Sasada, Kurokawa et al. 1988). bFGF is mitogenic for skin fibroblasts and granulation tissue fibroblasts (Buckley-Sturrock, Woodward et al.

1989). In addition, during periodontal wound healing a new functional epithelial seal must form, and bFGF has been shown to stimulate the proliferation of gingival epithelial cells, with the effect being moderately attenuated in the presence of serum (Takayama, Yoshida et al. 2002).

1.5.5 Role of bFGF in Wound Healing

The importance of bFGF in wound healing is evident from studies using bFGF knockout mice. Although the mice are viable, survive to adulthood and have no visible abnormalities, when injured, these mice show a significant decrease in the rate of skin healing (Ortega, Ittmann et al. 1998). Furthermore, the addition of bFGF to wounds accelerates the rate of wound healing (Ribatti, Nico et al. 1999, Akita, Akino et al. 2008, Tan, Xiao et al. 2008). Topical application of bFGF to experimentally created rat palatal wounds was found to accelerate the formation of granulation tissue and reepithelialization of the wound with an observed increase in basal epithelial cell proliferation (Oda, Kagami et al. 2004).

bFGF is known to have effects at several different stages of wound healing. During the inflammatory phase of wound healing, monocytes secrete growth factors to resolve the wound and stimulate the formation of granulation tissue (Wahl, Wong et al. 1989). Monocytes in the wound area are converted to macrophages and secrete several growth factors including platelet derived growth factor, interleukin-1, tumour necrosis factor and bFGF which act upon fibroblasts in the healing wound (Mahdavian Delavary, van der Veer et al. 2011). Angiogenesis is a key event in wound repair and involves the migration of endothelial cells from existing vasculature into the wound space. bFGF primes endothelial cells for angiogenesis and alters the expression of integrins allowing for migration into the wound bed (Klein, Giancotti et al. 1993). The final stage of wound repair is characterized by remodeling of the collagen matrix to produce a functional connective tissue. Apoptosis of myofibroblasts is required for wound resolution and bFGF has been shown to play a role in the apoptosis of myofibroblasts *in vitro* (Funato, Moriyama et al. 1997) and *in vivo* during palatal wound healing (Funato, Moriyama et al. 1999). bFGF downregulates collagen synthesis in normal skin fibroblasts and stimulates the production of the collagen digesting enzyme, collagenase,

in normal skin fibroblasts and granulation tissue fibroblasts (Buckley-Sturrock, Woodward et al. 1989, Tan, Rouda et al. 1993).

1.6 Hypothesis and Objectives

1.6.1 Rationale

Biomaterial scaffold membranes hold great promise for use in GTR applications in that they can be fabricated to mimic the fibrous ECM architecture of the connective tissue and can be used to deliver growth factors, thus acting as a mechanically stable substitute ECM during tissue repair. Electrospun PCL scaffolds loaded with bFGF microspheres have been shown to enhance dermal fibroblast infiltration *in vitro* and enhance angiogenesis in cutaneous wounds *in vivo* (Guo, Elliott et al. 2012). Since dermal fibroblasts differ from gingival fibroblasts (Palaiologou, Yukna et al. 2001) and the periodontium represents a unique wound healing environment, it is of significance to study the response of gingival fibroblasts to bFGF loaded electrospun PCL scaffolds and subsequently assess the ability of the scaffolds to promote gingival wound healing.

1.6.2 Overall Hypothesis

We hypothesize that the sustained release of bFGF from PLGA microspheres loaded on an electrospun PCL scaffold with a pore diameter of $17.1 \pm 8.3 \mu\text{m}$ will serve as a matrix for gingival fibroblast ingrowth and promote gingival wound healing.

1.6.3 Specific Hypothesis and Objectives

Release of bFGF from PCL electrospun scaffolds will increase the proliferation, matrix deposition and infiltration of gingival fibroblasts while maintaining a barrier to oral epithelial cells. bFGF release from PCL electrospun scaffolds will accelerate gingival wound healing. To test this hypothesis the following objectives were formulated:

1. To characterize the influence of PCL electrospun fibrous scaffolds loaded with bFGF microspheres on human gingival fibroblasts *in vitro* and gingival tissue *ex vivo*.

- a. Assess human gingival fibroblast attachment, proliferation and matrix synthesis and deposition.
 - b. Assess cell infiltration from gingival tissue explants.
2. To assess the influence of PCL electrospun fibrous scaffolds loaded with bFGF microspheres on the rate of wound healing following gingivectomy in a rat model.

1.7 References

AAP (2001). Glossary of Periodontal Terms. Chicago, IL, The American Academy of Periodontology.

Abraham, J. A., J. L. Whang, A. Tumolo, A. Mergia, J. Friedman, D. Gospodarowicz and J. C. Fiddes (1986). "Human basic fibroblast growth factor: nucleotide sequence and genomic organization." EMBO **5**(10): 2523-2528.

Akita, S., K. Akino, T. Imaizumi and A. Hirano (2008). "Basic fibroblast growth factor accelerates and improves second-degree burn wound healing." Wound Repair Regen **16**(5): 635-641.

Akncbay, H., S. Senel and Z. Y. Ay (2007). "Application of chitosan gel in the treatment of chronic periodontitis." J Biomed Mater Res B Appl Biomater **80**(2): 290-296.

Albandar, J. M. and T. E. Rams (2002). "Global epidemiology of periodontal diseases: An overview." Periodontology 2000 **29**: 7-10.

Armitage, G. C. (2004). "Periodontal diagnoses and classification of periodontal diseases." Periodontology 2000 **34**: 9-21.

Ashammakhi, N. and P. Rokkanen (1997). "Absorbable polyglycolide devices in trauma and bone surgery." Biomaterials **18**.

Aukhil, I. (2000). "Biology of wound healing." Periodontology 2000 **22**: 44-50.

Aurer, A. and K. Jorgic-Srdjak (2005). "Membranes for periodontal regeneration." Acta Stomat Croat **39**: 107-112.

Ayvazyan, A., N. Morimoto, N. Kanda, S. Takemoto, K. Kawai, Y. Sakamoto, T. Taira and S. Suzuki (2011). "Collagen-gelatin scaffold impregnated with bFGF accelerates palatal wound healing of palatal mucosa in dogs." J Surg Res **171**(2): e247-257.

Barnes, C. P., S. A. Sell, E. D. Boland, D. G. Simpson and G. L. Bowlin (2007). "Nanofiber technology: designing the next generation of tissue engineering scaffolds." Adv Drug Deliv Rev **59**(14): 1413-1433.

Barrett, A. W. and A. M. H. Raja (1997). "The immunohistochemical identification of human oral mucosal melanocytes." Archs oral Biol **42**: 77-81.

Bartold, P. M., C. A. G. McCulloch, A. S. Narayanan and S. Pitaru (2000). "Tissue engineering: A new paradigm for periodontal regeneration based on molecular and cell biology." Periodontology 2000 **24**: 253-269.

Bartold, P. M., L. J. Walsh and A. S. Narayanan (2000). "Molecular and cell biology of the gingiva." Periodontology 2000 **24**: 28-55.

Bellot, F., G. Crumley, J. M. Kaplow, J. Schlessinger, M. Jaye and C. A. Dionne (1991). "Ligand-induced transphosphorylation between different FGF receptors." EMBO **10**(10): 2849-2854.

Bhattacharai, N., D. Edmondson, O. Veis, F. A. Matsen and M. Zhang (2005). "Electrospun chitosan-based nanofibers and their cellular compatibility." Biomaterials **26**(31): 6176-6184.

Bikfalvi, A., S. Klein, G. Pintucci, N. Quarto, P. Mignatti and D. B. Rifkin (1995). "Differential modulation of cell phenotype by different molecular weight forms of basic fibroblast growth factor: Possible intracellular signaling by the high molecular weight forms." J Cell Biol **129**(1): 233-243.

Birkedal-Hansen, H., W. T. Butler and R. E. Taylor (1977). "Proteins of the periodontium." Calc Tiss Res **23**: 39-44.

Biro, S., Z. X. Yu, Y. M. Fu, G. Smale, J. Sasse, J. Sanchez, V. J. Ferrans and W. Casscells (1994). "Expression and subcellular distribution of basic fibroblast growth factor are regulated during migration of endothelial cells." Circ Res **74**(3): 485-494.

Blumenthal, N. M. (1988). "The use of collagen membranes to guide regeneration of new connective tissue attachment in dogs." J Periodontol **59**(12): 830-836.

Bölgen, N., Y. Z. Menciloglu, K. Acataş, I. Vargel and E. Piskin (2005). "In vitro and in vivo degradation of non-woven materials made of poly(ϵ -caprolactone) nanofibers prepared by electrospinning under different conditions." J Biomater Sci Polym Ed **16**(12): 1537-1555.

Bonino, C. A., M. D. Krebs, C. D. Saquing, S. I. Jeong, K. L. Shearer, E. Alsberg and S. A. Khaa (2011). "Electrospinning alginate-based nanofibers: From blends to crosslinked low molecular weight alginate-only systems." Carbohydr Polym **85**: 111-119.

Borradori, L. and A. Sonnenberg (1999). "Structure and function of hemidesmosomes: More than simple adhesion complexes." J Invest Dermatol **112**: 411-418.

Bosshardt, D. D. and N. P. Lang (2005). "The junctional epithelium: From health to disease." J Dent Res **84**(1): 9-20.

Bosshardt, D. D. and K. A. Selvi (1997). "Dental cementum: The dynamic tissue covering of the root." Periodontology 2000 **13**: 41-75.

Bostman, O., E. Hirvensalo, J. Makinen and P. Rokkanen (1990). "Foreign-body reactions to fracture fixation implants of biodegradable synthetic polymers." J Bone Joint Surg Br **72**(4): 592-596.

Bratt, P., M. M. Anderson, B. Mansson-Rahemtulla, J. W. Stevens, C. Znou and F. Rahemtulla (1992). "Isolation and characterization of bovine gingival proteoglycans versican and decorin." Int J Biochem **24**(10): 1573-1583.

Buckley-Sturrock, A., S. C. Woodward, R. M. Senior, G. L. Griffin, M. Klagsbrun and J. M. Davidson (1989). "Differential stimulation of collagenase and chemotactic activity in fibroblasts derived from rat wound repair tissue and human skin by growth factors." J Cell Physiol **138**: 70-78.

Bunyaratavej, P. and H.-L. Wang (2001). "Collagen Membranes: A Review." J Periodontol **72**: 215-229.

Burdick, J. A., R. F. Padera, J. V. Huang and K. S. Anseth (2002). "An investigation of the cytotoxicity and histocompatibility of in situ forming lactic acid based orthopedic biomaterials." J Biomed Mater Res **63**(5): 484-491.

Ceozzo, K., A. Gaynor, L. Shaffer, K. Kojima, C. A. Vacanti and G. L. Stahl (2006). "Polyglycolic acid induced inflammation: Role of hydrolysis and resulting complement activation1." Tissue Eng **12**(2).

Chai, Y., X. Jiang, Y. Ito, J. Bringas, P. , J. Han, D. H. Rowitch, P. Soriano, A. P. McMahon and H. M. Sucov (2000). "Fate of the mammalian cranial neural crest during tooth and mandibular morphogenesis." Development **127**: 1671-1679.

Chambrone, L., D. Chambrone, F. E. Pustiglioni, L. A. Chambrone and L. A. Lima (2008). "Can subepithelial connective tissue grafts be considered the gold standard procedure in the treatment of Miller Class I and II recession-type defects?" J Dent **36**(9): 659-671.

Chambrone, L. and L. A. Chambrone (2003). "Gingival recessions caused by lip piercing: Case report." J Can Dent Assoc **69**(8): 505-508.

Chambrone, L., F. Sukekava, M. G. Araujo, F. E. Pustiglioni, L. A. Chambrone and L. A. Lima (2010). "Root-coverage procedures for the treatment of localized recession-type defects: a Cochrane systematic review." J Periodontol **81**(4): 452-478.

Charles, J. F. and A. O. Aliprantis (2014). "Osteoclasts: more than 'bone eaters'." Trends Mol Med.

Chavrier, C., M. L. Couble, H. Magloire and J. A. Grimaud (1984). "Connective tissue organization of healthy human gingiva." J Periodontal Res **9**: 221-229.

Cho, M. I. and P. R. Garant (2000). "Development and general structure of the periodontium." Periodontology 2000 **24**: 9-27.

Dennison, D. K., D. R. Vallone, G. J. Pinero, B. Rittman and R. G. Caffesse (1994). "Differential effect of TGF-B1 and PDGF on proliferation of periodontal ligament cells and gingival fibroblasts." J Periodontol **65**: 641-648.

Dong, Y., S. Liau, M. Ngiam, C. K. Chan and S. Ramakrishna (2009). "Degradation behaviors of electrospun resorbable polyester nanofibers." Tissue Eng Part B Rev **15**(3): 333-351.

Eke, P. I., B. A. Dye, L. Wei, G. O. Thornton-Evans and R. J. Genco (2012). "Prevalence of periodontitis in adults in the United States: 2009 and 2010." J Dent Res **91**(10): 914-920.

Faham, S., R. J. Linhardt and D. C. Rees. "Diversity does make a difference: Fibroblast growth factor-heparin interactions." Curr Opin Struct Biol **8**: 578-586.

Feng, X. (2009). "Chemical and biochemical basis of cell-bone matrix interaction in health and disease." Curr Chem Biol **3**(2): 189-196.

Florkiewicz, R. Z. and A. Sommer (1989). "Human basic fibroblast growth factor gene encodes four polypeptides: Three initiate translation from non-AUG codons." Proc Natl Acad Sci U S A **86**: 3978-3981.

Foster, B. L. (2012). "Methods for studying tooth root cementum by light microscopy." Int J Oral Sci **4**: 119-128.

Fournier, B. P., H. Larjava and L. Hakkinen (2013). "Gingiva as a source of stem cells with therapeutic potential." Stem Cells Dev **22**(24): 3157-3177.

Fu, J.-H., C.-Y. Su and H.-L. Wang (2012). "Esthetic soft tissue management for teeth and implants." J Evid Based Dent Pract **12**(3): 129-142.

Funato, N., K. Moriyama, Y. Baba and T. Kuroda (1999). "Evidence for apoptosis induction in myofibroblasts during palatal mucoperiosteal repair." J Dent Res **78**(9): 1511-1517.

Funato, N., K. Moriyama, H. Shimokawa and T. Kuroda (1997). "Basic fibroblast growth factor induces apoptosis in myofibroblastic cells isolated from rat palatal mucosa." Biochem Biophys Res Commun **240**: 21-26.

Gospodarowicz, D. (1974). "Localisation of a fibroblast growth factor and its effect alone and with hydrocortisone on 3T3 cell growth." Nature **249**: 123-127.

Gottlow, J. (1993). "Guided tissue regeneration using bioresorbable and non-resorbable devices: Initial healing and long-term results." J Periodontol **64**: 1157-1165.

Gottlow, J., S. Nyman, J. Lindhe, T. Karring and J. Wennstrom (1986). "New attachment formation in the human periodontium by guided tissue regeneration." J Clin Periodontol **13**: 604-616.

Greenstein, G. and J. G. Caton (1993). "Biodegradable barriers and guided tissue regeneration." Periodontology 2000 **1**: 36-45.

Guo, X., C. G. Elliott, Z. Li, Y. Xu, D. W. Hamilton and J. Guan (2012). "Creating 3D angiogenic growth factor gradients in fibrous constructs to guide fast angiogenesis." Biomacromolecules **13**(10): 3262-3271.

- Hakki, S. S., P. Korkusuz, N. Purali, B. Bozkurt, M. Kus and I. Duran (2013). "Attachment, proliferation and collagen type I mRNA expression of human gingival fibroblasts on different biodegradable membranes." Connect Tissue Res **54**(4-5): 260-266.
- Hakkinen, L., O. Oksala, T. Salo, F. Rahemtulla and H. Larjava (1993). "Immunohistochemical localization of proteoglycans in human periodontium." J Histochem Cytochem **41**(11): 1689-1699.
- Hammarstrom, L. and S. Lindskog (1985). "General morphological aspects of resorption of teeth and alveolar bone." Int Endod J **18**: 93-108.
- Ho, S. P., S. J. Marshall, M. I. Ryder and G. W. Marshall (2007). "The tooth attachment mechanism defined by structure, chemical composition and mechanical properties of collagen fibers in the periodontium." Biomaterials **28**(35): 5238-5245.
- Howell, T. H., J. P. Fiorellini, D. W. Paquette, S. Offenbacher, W. V. Giannobile and S. E. Lynch (1997). "A phase I/II clinical trial to evaluate a combination of recombinant human platelet-derived growth factor-BB and recombinant human insulin-like growth factor-I in patients with periodontal disease." J Periodontol **68**: 1186-1193.
- Huang, Z.-M., Y.-Z. Zhang, M. Kotakic and S. Ramakrishna (2003). "A review on polymer nanofibers by electrospinning and their applications in nanocomposites." Compos Sci Technol **63**: 2223-2253.
- Hughes, F. J., M. Ghuman and A. Talal (2010). "Periodontal regeneration: a challenge for the tissue engineer?" Proc Inst Mech Eng H **224**(12): 1345-1358.
- Hwang, Y. K., U. Jeong and E. C. Cho (2008). "Production of uniform-sized polymer core-shell microcapsules by coaxial electrospinning." Langmuir **24**: 2446-2451.
- Ignatius, A. A. and L. E. Claes (1996). "In vitro biocompatibility of bioresorbable polymers: poly(L, DL-lactide) and poly(L-lactide-co-glycolide)." Biomaterials **17**: 831-839.
- Ivanovski, S. (2009). "Periodontal regeneration." Aust Dent J **54 Suppl 1**: S118-128.
- Jansen, R. G., A. M. Kuijpers-Jagtman, T. H. van Kuppevelt and J. W. Von den Hoff (2008). "Collagen Scaffolds Implanted in the Palatal Mucosa." J Craniofac Surg **19**(3): 599-608.
- Kaigler, D., J. A. Cirelli and W. V. Giannobile (2006). "Growth factor delivery for oral and periodontal tissue engineering." Expert Opin Drug Deliv **3**(5): 647-662.
- Kan, M., F. Wang, J. Xu, J. W. Crabb, J. Hou and W. L. McKeehan (1993). "An essential heparin-binding domain in the fibroblast growth factor receptor kinase." Science **259**: 1918-1921.

- Kanazawa, S., T. Fujiwara, S. Matsuzaki, K. Shingaki, M. Taniguchi, S. Miyata, M. Tohyama, Y. Sakai, K. Yano, K. Hosokawa and T. Kubo (2010). "bFGF regulates PI3-Kinase-Rac1-JNK pathway and promotes fibroblast migration in wound healing." PLoS One **5**(8): e12228.
- Kao, R. T., S. Murakami and O. R. Beirne (2009). "The use of biologic mediators and tissue engineering in dentistry." Periodontology 2000 **50**: 127-153.
- Kassab, M. M. and R. E. Cohen (2003). "The etiology and prevalence of gingival recession." J Am Dent Assoc **134**(2): 220-225.
- Kersten, B. G., A. D. H. Chamberlain, S. Khorsandi, U. E. Wikesjö, K. A. Selvig and R. E. Nilvéus (1992). "Healing of the intrabony periodontal lesion following root conditioning with citric acid and wound closure including an expanded PTFE membrane." J Periodontol **63**: 876-882.
- Kinane, D., P. Bouchard and E. o. E. W. o. P. Group (2008). "Periodontal diseases and health: Consensus report of the sixth European workshop on periodontology." J Clin Periodontol **35**(8 Suppl): 333-337.
- Kitamura, M., M. Akamatsu, M. Machigashira, Y. Hara, R. Sakagami, T. Hirofuji, T. Hamachi, K. Maeda, M. Yokota, J. Kido, T. Nagata, H. Kurihara, S. Takashiba, T. Sibutani, M. Fukuda, T. Noguchi, K. Yamazaki, H. Yoshie, K. Ioroi, T. Arai, T. Nakagawa, K. Ito, S. Oda, Y. Izumi, Y. Ogata, S. Yamada, H. Shimauchi, K. Kunimatsu, M. Kawanami, T. Fujii, Y. Furuichi, T. Furuuchi, T. Sasano, E. Imai, M. Omae, S. Yamada, M. Watanuki and S. Murakami (2011). "FGF-2 stimulates periodontal regeneration: results of a multi-center randomized clinical trial." J Dent Res **90**(1): 35-40.
- Klein, S., F. G. Giancotti, M. Presta, S. M. Albelda, C. A. Buck and D. B. Rifkin (1993). "Basic fibroblast growth factor modulates integrin expression in microvascular endothelial cells." Mol Biol Cell **4**: 973-982.
- Kojima, K., L. J. Bonassar, A. K. Roy, C. A. Vacanti and J. Cortiella (2002). "Autologous tissue-engineered trachea with sheep nasal chondrocytes." J Thorac Cardiovasc Surg **123**: 1177-1184.
- Kumbar, S. G., R. James, S. P. Nukavarapu and C. T. Laurencin (2008). "Electrospun nanofiber scaffolds: engineering soft tissues." Biomed Mater **3**(3): 034002.
- Laestander, C. and W. Engstrom (2014). "Role of fibroblast growth factors in elicitation of cell responses." Cell Prolif **47**(1): 3-11.
- Lam, C. X., D. W. Hutmacher, J. T. Schantz, M. A. Woodruff and S. H. Teoh (2009). "Evaluation of polycaprolactone scaffold degradation for 6 months in vitro and in vivo." J Biomed Mater Res A **90**(3): 906-919.
- Langer, B. and L. Langer (1985). "Subepithelial connective tissue graft technique for root coverage." J Periodontol **56**(12): 715-720.

- Larjava, H., L. Hakkinen and F. Rahemtulla (1992). "A biochemical analysis of human periodontal tissue proteoglycans." Biochem. J. **284**: 267-274.
- Leibovich, S. J. and R. Ross (1975). "The role of the macrophage in wound repair." Am J Pathol **78**: 71-100.
- Li, W. J., C. T. Laurencin, E. J. Caterson, R. S. Tuan and F. K. Ko (2002). "Electrospun nanofibrous structure: A novel scaffold for tissue engineering." J Biomed Mater Res **60**: 613-621.
- Liu, J., J. J. Mao and L. Chen (2011). "Epithelial-mesenchymal interactions as a working concept for oral mucosa regeneration." Tissue Eng Part B Rev **17**(1): 25-31.
- Lotfi, G., M. A. Shokrgozar, R. Mofid, F. M. Abbas, F. Ghanavati, A. A. Bagheban and R. P. Shariati (2011). "A clinical and histologic evaluation of gingival fibroblasts seeding on a chitosan-based scaffold and its effect on the width of keratinized gingiva in dogs." J Periodontol **82**(9): 1367-1375.
- Mackenzie, I. C., G. Rittman, Z. Gao, I. Leigh and E. B. Lane (1991). "Patterns of cytokeratin expression in human gingival epithelia." J Periodont Res **26**: 468-478.
- Mahdavian Delavary, B., W. M. van der Veer, M. van Egmond, F. B. Niessen and R. H. Beelen (2011). "Macrophages in skin injury and repair." Immunobiology **216**(7): 753-762.
- Mansukhani, A., P. Dell'Era, D. Moscatelli, S. Kornbluth, H. Hanafusa and C. Basilico (1992). "Characterization of the murine BEK fibroblast growth factor (FGF) receptor: Activation by three members of the FGF family and requirement for heparin." Proc Natl Acad Sci U S A **89**: 3305-3309.
- Mansukhani, A., D. Moscatelli, D. Talarico, V. Levytska and C. Basilico (1990). "A murine fibroblast growth factor (FGF) receptor expressed in CHO cells is activated by basic FGF and Kaposi FGF." Proc Natl Acad Sci U S A **87**: 4378-4382.
- Marcato, B., G. Paganetto, G. Ferrara and G. Cecchin (1996). "High-performance liquid chromatographic determination of some of the hydrolytic decomposition products of poly(α -hydroxyacid)s." J Chromatogr B Biomed Appl **682**: 147-156.
- Martin, P. (1997). "Wound healing--aiming for perfect skin regeneration." Science **276**(5309): 75-81.
- Matheson, S., H. Larjava and L. Hakkinen (2005). "Distinctive localization and function for lumican, fibromodulin and decorin to regulate collagen fibril organization in periodontal tissues." J Periodontal Res **40**(4): 312-324.
- Matthews, J. A., G. E. Wnek, D. G. Simpson and G. L. Bowlin (2002). "Electrospinning of Collagen Nanofibers." Biomacromolecules **3**: 232-238.

- Mau, L. P., C. W. Cheng, P. Y. Hsieh and A. A. Jones (2012). "Biological complication in guided bone regeneration with a polylactic acid membrane: a case report." Implant Dent **21**(3): 171-174.
- Mergia, A., R. Eddy, J. A. Abraham and J. C. S. Fiddes, T. B. (1986). "The genes for basic and acidic fibroblast growth factors are on different human chromosomes." Biochem Biophys Res Commun **138**(2): 644-651.
- Mignatti, P., T. Morimoto and D. B. Rifkin (1991). "Basic fibroblast growth factor released by single, isolated cells stimulates their migration in an autocrine manner." Proc Natl Acad Sci U S A **88**: 11007-11011.
- Mignatti, P., T. Morimoto and D. B. Rifkin (1992). "Basic fibroblast growth factor, a protein devoid of secretory signal sequence, is released by cells via a pathway independent of the endoplasmic reticulum-Golgi complex." Journal of Cellular Physiology **151**: 81-93.
- Miller, P. D., Jr. (1988). "Regenerative and reconstructive periodontal plastic surgery. Mucogingival surgery." Dent Clin North Am **32**(2): 287-306.
- Mohammadi, M., I. Dikic, A. Sorokin, W. H. Burgess, M. Jaye and J. Schlessinger (1996). "Identification of Six Novel Autophosphorylation Sites on Fibroblast Growth Factor Receptor 1 and Elucidation of Their Importance in Receptor Activation and Signal Transduction." Mol Cell Biol **16**(3): 977-989.
- Mohammadi, M., M. A. Shokrgozar and R. Mofid (2007). "Culture of human gingival fibroblasts on a biodegradable scaffold and evaluation of its effect on attached gingiva: a randomized, controlled pilot study." J Periodontol **78**(10): 1897-1903.
- Moore, W. E. C. and L. H. Moore (1994). "The bacteria of periodontal diseases." Periodontology 2000 **5**: 66-77.
- Moscatelli, D., J. Joseph-Silverstein, R. Manejias and D. B. Rifkin (1987). "Mr 25,000 heparin-binding protein from guinea pig brain is a high molecular weight form of basic fibroblast growth factor." Proc Natl Acad Sci U S A **84**: 5778-5782.
- Murakami, M. and M. Simons (2008). "Fibroblast growth factor regulation of neovascularization." Curr Opin Hematol **15**(3): 215-220.
- Murakami, S., S. Takayama, K. Ikezawa, Y. Shimabukuro, M. Kitamura, T. Nozaki, A. Terashima, T. Asano and H. Okada (1999). "Regeneration of periodontal tissues by basic fibroblast growth factor." J Periodont Res **34**: 425-430.
- Murakami, S., S. Takayama, M. Kitamura, Y. Shimabukuro, K. Yanagi, K. Ikezawa, T. Saho, T. Nozaki and H. Okada (2003). "Recombinant human basic fibroblast growth factor (bFGF) stimulates periodontal regeneration in class II furcation defects created in beagle dogs." J Periodont Res **38**: 97-103.

- Murugan, R. and S. Ramakrishna (2007). "Design strategies of tissue engineering scaffolds with controlled fiber orientation." Tissue Eng **13**(8): 1845-1866.
- Muthukuru, M. (2013). "Bone morphogenic protein-2 induces apoptosis and cytotoxicity in periodontal ligament cells." J Periodontol **84**(6): 829-838.
- Nakahara, T., T. Nakamura, E. Kobayashi, M. Inoue, K. Shigeno, Y. Tabata, K. Eto and Y. Shimizu (2003). "Novel approach to regeneration of periodontal tissues based on in situ tissue engineering: Effects of controlled release of basic fibroblast growth factor from a sandwich membrane." Tissue Engineering **9**(1): 153-162.
- Nemcovsky, C. E., S. Zahavi, O. Moses, E. Kebudi, Z. Artzi, L. Beny and M. Weinreb (2006). "Effect of enamel matrix protein derivative on healing of surgical supra-infrabony periodontal defects in the rat molar: a histomorphometric study." J Periodontol **77**(6): 996-1002.
- Nissen, N. N., R. Shankar, R. L. Gamelli, A. Singh and L. A. Dipietro (1999). "Heparin and heparan sulphate protect basic fibroblast growth factor from non-enzymic glycosylation." J Biochem **338**: 637-642.
- Nyman, S., J. Gottlow, T. Karring and J. Lindhe (1982). "The regenerative potential of the periodontal ligament An experimental study in the monkey." J Clin Periodontol **9**: 257-265.
- Oda, Y., H. Kagami and M. Ueda (2004). "Accelerating effects of basic fibroblast growth factor on wound healing of rat palatal mucosa." J Oral Maxofac Surg **62**: 73-80.
- Ornitz, D. M., J. Xu, J. S. Colvin, D. G. McEwen, C. A. MacArthur, F. Coulier, G. Gao and M. Goldfarb (1996). "Receptor specificity of the fibroblast growth factor family." J Biol Chem **271**(25): 15292-15297.
- Ortega, S., M. Ittmann, S. H. Tsang, M. Ehrlich and C. Basilico (1998). "Neuronal defects and delayed wound healing in mice lacking fibroblast growth factor 2." Proc Natl Acad Sci U S A **95**: 5672-5677.
- Page, R. C., S. Offenbacher, H. E. Shroeder, G. J. Seymour and K. S. Kornman (1997). "Advances in the pathogenesis of periodontitis: summary of developments, clinical implications and future directions." Periodontology 2000 **14**: 216-248.
- Palaiologou, A. A., R. A. Yukna, R. Moses and T. E. Lallier (2001). "Gingival, Dermal, and Periodontal Ligament Fibroblasts Express Different Extracellular Matrix Receptors." J Periodontol **72**: 798-807.
- Peters, K. G., J. Marie, E. Wilson, H. E. Ives, J. Escobedo, M. Del Rosario, D. Mirda and L. T. Williams (1992). "Point mutation of an FGF receptor abolishes phosphatidylinositol turnover and Ca²⁺ flux but not mitogenesis." Nature **358**: 678-681.

- Petersen, P. E. and H. Ogawa (2005). "Strengthening the Prevention of Periodontal Disease: The WHO Approach." J Periodontol **76**: 2187-2193.
- Pihlstrom, B. L., B. S. Michalowicz and N. W. Johnson (2005). "Periodontal diseases." The Lancet **366**(9499): 1809-1820.
- Piperni, S. G., E. R. Takamori, S. Sartoretto, K. B. Paiva, J. M. Granjeiro, R. C. de Oliveira and W. F. Zambuzzi (2014). "Cellular behavior as a dynamic field for exploring bone bioengineering: A closer look at cell-biomaterial interface." Arch Biochem Biophys.
- Pitaru, S., H. Ta, M. Soldinger, A. Grosskopf and M. Noff (1987). "Partial regeneration of periodontal tissues using collagen barriers initial observations in the canine." J Periodontol **59**(6): 380-386.
- Pitaru, S., H. Tal, M. Soldinger and M. Noff (1989). "Collagen membranes prevent apical migration of epithelium and support new connective tissue attachment during periodontal wound healing in dogs." J Periodont Res **24**: 247-253.
- Polimeni, G., J. M. Albandar and U. M. Wikesjo (2005). "Prognostic factors for alveolar regeneration: effect of space provision." J Clin Periodontol **32**(9): 951-954.
- Polimeni, G., A. V. Xiropaidis and U. M. E. Wikesjo (2006). "Biology and principles of periodontal wound healing/regeneration." Periodontology 2000 **41**: 30-47.
- Postlethwaite, A. E., J. M. and A. H. Kang (1978). "Chemotactic attraction of human fibroblasts to type I, II, and III collagens and collagen-derived peptides." Proc Natl Acad Sci U S A **75**(2).
- Raetzke, P. B. (1985). "Covering localized areas of root exposure employing the "envelope" technique." J Periodontol **56**(7): 397-402.
- Raja, S., G. Byakod and P. Pudukalkatti (2009). "Growth factors in periodontal regeneration." Int J Dent Hyg **7**(2): 82-89.
- Ramibri, G., G. C. Panzica, C. Viglietti-Panzica, R. Modica, D. R. Springall and P. J. M. (1992). "Non-innervated merkel cells and merkel-neurite complexes in human oral mucosa revealed using antiserum to protein gene product 9.5." Archs oral Biol **37**(4): 263-269.
- Rapraeger, A. C., A. Krufka and B. B. Olwin (1991). "Requirement of heparan sulfate for bFGF-mediated fibroblast growth and myoblast differentiation." Science **252**: 1705-1708.
- Renko, M., N. Quarto, T. Morimoto and D. B. Rifkin (1990). "Nuclear and cytoplasmic localization of different basic fibroblast growth factor species." J Cell Physiol **144**: 108-114.

- Ribatti, D., B. Nico, A. Vacca, L. Roncali and M. Presta (1999). "Endogenous and exogenous fibroblast growth factor-2 modulate wound healing in the chick embryo chorioallantoic membrane." Angiogenesis **3**: 89-95.
- Rothamel, D., F. Schwarz, A. Sculean, M. Hertel, W. Scherbaum and J. Becker (2004). "Biocompatibility of various collagen membranes in cultures of human PDL fibroblasts and human osteoblast-like cells." Clin Oral Implants Res **15**(4): 443-449.
- Ryoo, H. M., M. H. Lee and Y. J. Kim (2006). "Critical molecular switches involved in BMP-2-induced osteogenic differentiation of mesenchymal cells." Gene **366**(1): 51-57.
- Sabag, N., C. Mery, M. Garcia, V. Vasquez and V. Cueto (1984). "Epithelial Reattachment After Gingivectomy in the Rat." J Periodontol **55**(3): 135-141.
- Sasada, R., T. Kurokawa, M. Iwane and K. Igarashi (1988). "Transformation of mouse BALB/C 3T3 cells with human basic fibroblast growth factor cDNA." Mol Cell Biol **8**(2): 588-594.
- Sawada, T. and S. Inoue (1996). "Ultrastructural characterization of internal basement membrane of junctional epithelium at dentogingival border." Anat Rec **246**: 317-324.
- Schroeder, H. E. and M. A. Listgarten (1997). "The gingival tissues: the architecture of periodontal protection." Periodontology 2000 **13**: 91-120.
- Seghezzi, G., S. Patel, C. J. Ren, A. Gualandris, G. Pintucci, E. S. Robbins, R. L. Shapiro, A. C. Galloway, D. B. Rifkin and P. Mignatti (1998). "Fibroblast growth factor-2 (FGF-2) induces vascular endothelial growth factor (VEGF) expression in the endothelial cells of forming capillaries: An autocrine mechanism contributing to angiogenesis." The Journal of Cell Biology **141**(7): 1659-1673.
- Serim, G., J. Wennstrom, J. Lindhe and L. Eneroth (1994). "The prevalence and distribution of gingival recession in subjects with a high standard of oral hygiene." J Clin Periodontol **21**: 57-63.
- Shu-Hua Teng, S.-H., P. Peng Wang and H.-E. Kim (2009). "Blend fibers of chitosan-agarose by electrospinning." Materials Letters **63**: 2510-2512.
- Socransky, S. S. and A. D. Haffajee (1994). "Evidence of bacterial etiology: a historical perspective." Periodontology 2000 **5**: 7-25.
- Stahl, S. S., S. Froum and D. Tarnow (1990). "Human histologic responses to guided tissue regenerative techniques in intrabony lesions Case reports on 9 sites." J Clin Periodontol **17**: 191-198.
- Sun, H. H., T. J. Qu, X. H. Zhang, Q. Yu and F. M. Chen (2012). "Designing biomaterials for in situ periodontal tissue regeneration." Biotechnol Prog **28**(1): 3-20.

- Takayama, S., J. Yoshida, H. Hirano, H. Okada and S. Murakami (2002). "Effects of basic fibroblast growth factor on human gingival epithelial cells." J Periodontol **73**: 1467-1473.
- Tan, E. M. L., S. Rouda, S. S. Greenbaum, J. Moore, J. H., J. W. Fox IV and S. Sollberg (1993). "Acidic and basic fibroblast growth factors down-regulate collagen gene expression in keloid fibroblasts." Am J Pathol **142**(2): 463-470.
- Tan, Y., J. Xiao, Z. Huang, Y. Xiao, S. Lin, L. Jin, W. Feng, L. Cai and X. Li (2008). "Comparison of the therapeutic effects recombinant human acidic and basic fibroblast growth factors in wound healing in diabetic patients." Journal of Health Science **54**(4): 432-440.
- Tatakis, D. N., A. Promsudthi and U. E. Wikesjö (1999). "Devices for periodontal regeneration." Periodontology 2000 **19**: 59-73.
- Teo, W. E., W. He and S. Ramakrishna (2006). "Electrospun scaffold tailored for tissue-specific extracellular matrix." Biotechnol J **1**(9): 918-929.
- Thompson, K., D. W. Hamilton and A. Leask (2010). "ALK5 inhibition blocks TGF β s-induced CCN2 expression in gingival fibroblasts." J Dent Res **89**(12): 1450-1454.
- Tugnait, A. and V. Clerehugh (2001). "Gingival recession - its significance and management." J Dent **29**: 381-394.
- Wadhawan, A., T. M. Gowda and D. S. Mehta (2012). "Gore-tex((R)) versus resolut adapt((R)) GTR membranes with perioglas((R)) in periodontal regeneration." Contemp Clin Dent **3**(4): 406-411.
- Wahl, S. M., H. Wong and N. McCartney-Francis (1989). "Role of growth factors in inflammation and repair." J Cell Biochem **40**: 193-199.
- Watson, P. J. C. (1984). "Gingival recession." Journal of Dentistry **12**(1): 29-35.
- Wikesjö, U. E. and R. Nilvéus (1990). "Periodontal Repair in Dogs: Effect of Wound Stabilization on Healing." J Periodontol **61**: 719-724.
- Wikesjo, U. M. E., P. Guglielmoni, A. Promsudthi, K.-S. Cho, L. Trombelli, K. A. Selvig, L. Jin and J. M. Wozney (1999). "Periodontal repair in dogs: effect of rhBMP-2 concentration on regeneration of alveolar bone and periodontal attachment." J Clin Periodontol **26**: 392-400.
- Wikesjo, U. M. E., W. H. Lim, R. C. Thomson and W. R. Hardwick (2003). "Periodontal repair in dogs: gingival tissue occlusion, a critical requirement for GTR?" J Clin Periodontol **30**: 655-664.
- Wikesjo, U. M. E. and K. A. Selvi (1999). "Periodontal wound healing and regeneration." Periodontology 2000 **19**: 21-39.

Woodward, S. C., P. S. Brewer and F. Moatamed (1985). "The intracellular degradation of poly(E-caprolactone)." J Biomed Mater Res **19**: 437-444.

Wu, Y., I. C. Liao, S. J. Kennedy, J. Du, J. Wang, K. W. Leong and R. L. Clark (2010). "Electrosprayed core-shell microspheres for protein delivery." Chem Commun (Camb) **46**(26): 4743-4745.

Zeng, J., X. Chen, Q. Liang, X. Xu and X. Jing (2004). "Enzymatic degradation of poly(L-lactide) and poly(epsilon-caprolactone) electrospun fibers." Macromol Biosci **4**(12): 1118-1125.

Zhang, J., L. S. Cousens, P. J. Barr and S. R. Sprang (1991). "Three-dimensional structure of human basic fibroblast growth factor, a structural homolog of interleukin 1B." Proc Natl Acad Sci U S A **88**: 3446-3450.

Chapter 2

2 Influence of Electrospun Polycaprolactone Fibrous Scaffolds Loaded with Basic Fibroblast Growth Factor Microspheres on Gingival Augmentation

2.1 Introduction

Periodontal disease affect the tissues that support the teeth (AAP 2001). Collectively referred to as the periodontium, these tissues are comprised of the alveolar bone, cementum, periodontal ligament (PDL) and the gingiva. Periodontal disease ranges in severity from mild inflammation of the gingiva, termed gingivitis, to more aggressive bacterial-induced inflammatory conditions. Periodontitis is the more severe periodontal pathology in which the chronic presence of bacteria induces a host immune response resulting in the loss of connective tissue attachment to the tooth; destruction of the gingiva, PDL, and cementum followed by resorption of the alveolar bone which can result in tooth mobility and loss (Pihlstrom, Michalowicz et al. 2005). Periodontitis is one of the most common connective tissue disorders worldwide and affects 47% of the U.S. adult population (Eke, Dye et al. 2012). In addition to its high prevalence, the main concern with periodontitis is the limited capacity for repair of the periodontium, and without surgical intervention, the disease is irreversible (Bartold, McCulloch et al. 2000).

Conventional interventions remove the causative bacterial agents and serve to slow the progression of periodontitis, but do not facilitate appreciable or predictable regeneration of the lost periodontal structures. Such interventions often result in tissue shrinkage and fibrosis leaving the patient with gingival recession (Wikesjo and Selvi 1999, Hughes, Ghuman et al. 2010). Guided tissue regeneration is a surgical intervention for periodontitis wherein a barrier membrane is placed under the gingival connective tissue and against the tooth to function as a space making barrier excluding the gingival tissue from the regenerating periodontal defect, thus creating a compartment into which the PDL and alveolar bone can repopulate (Aurer and Jorgic-Srdjak 2005). Resorbable membranes for GTR have been developed as they eliminate the need for a second surgery for membrane removal. However, the membranes employed are not optimal exhibiting

variable clinical improvement, therefore significant improvements can be made to their design (Bartold, McCulloch et al. 2000). As current membranes are cell occlusive, gingival connective tissue is isolated from the periodontal pocket cutting off a potential supply of stem and progenitor cells from the healing defect along with the rich vascular supply (Schroeder and Listgarten 1997, Fournier, Larjava et al. 2013).

With increasing knowledge of wound healing and advances in technology in the field of materials science, biomaterial scaffold-membranes can be fabricated which play a more active role in periodontal wound healing. PCL is a bioresorbable, aliphatic polyester (M_w 80 000) with a relatively long degradation time (Dong, Liao et al. 2009). PCL is an ideal biomaterial for use in scaffold membrane applications due to its low cost, ease of fabrication, biocompatibility, and has been approved by the U.S. Food and Drug Administration for medical applications (Dong, Liao et al. 2009). Several techniques exist for fabrication of fibrous biomaterial scaffolds including phase separation (Nam and Park 1999), self-assembly (Zhang 2003) and electrospinning (Pham, Sharma et al. 2006). Electrospinning is advantageous in that the set-up is convenient and cost effective, and unlike the other methods, is easily scalable (Dong, Liao et al. 2009). Electrospinning produces scaffolds which are ideal for tissue regeneration applications due to the ability to customize fiber diameter and orientation, the high surface area to volume ratio, interconnected porosity, and the ability to incorporate growth factors, thus closely mimicking the structure of the natural ECM. Moreover, by tailoring the pore size between the fibers in the scaffold, cell migration into and through the scaffold can be facilitated (Lowery, Datta et al. 2010).

In addition to alterations in the structure of the scaffold, incorporation of growth factors into the scaffold increases their biocompatibility and functionality. The heparin-binding protein bFGF is a potent mitogen capable of stimulating fibroblast proliferation in a dose-dependent manner (Gospodarowicz 1974, Nugent and Iozzo 2000). bFGF is also a potent stimulator of angiogenesis *in vivo* and stimulates the migration and proliferation of endothelial cells *in vitro* (Gospodarowicz, Ferrara et al. 1987, Murakami and Simons 2008). bFGF accelerates the healing of oral wounds and stimulates periodontal regeneration in animal models (Murakami, Takayama et al. 1999, Murakami, Takayama

et al. 2003, Oda, Kagami et al. 2004, Ayvazyan, Morimoto et al. 2011). These observations were further investigated in clinical trials that found that topical applications of bFGF were able to regenerate periodontal tissue in patients with periodontitis (Kitamura, Nakashima et al. 2008, Kitamura, Akamatsu et al. 2011). While bFGF has shown promise clinically, topical application is not an optimal method of delivery due to the requirement for a large dose to be administered in an effort to compensate for the rapid degradation and inactivation of growth factors delivered this way. Attempts at sustained release of bFGF from scaffolds has been investigated using chitosan/hydroxyapatite freeze dried scaffolds and collagen/gelatin scaffolds (Tigli, Akman et al. 2009, Akman, Tigli et al. 2010). However these scaffolds either have a fairly rapid release of bFGF or rapid degradation of the scaffold itself. We have previously developed a PCL electrospun scaffold loaded with microspheres of poly (lactide-*co*-glycolide) containing a core of bFGF stabilized with heparin, which supported the migration of dermal fibroblasts into the scaffold *in vitro* and promoted angiogenesis following subcutaneous implantation (Guo, Elliott et al. 2012).

The aim of this study was to investigate the *in vitro* biocompatibility of human gingival fibroblasts on PCL electrospun scaffolds loaded with bFGF microspheres and the efficacy of the scaffolds in the early stages of gingival wound healing *in vivo*. The attachment, proliferation, infiltration/migration, and matrix synthesis of human gingival fibroblasts on scaffolds loaded with bFGF microspheres was evaluated and compared to scaffolds without bFGF. We then assessed the influence of PCL scaffolds loaded with bFGF microspheres on reepithelialization and connective tissue formation following gingivectomy in a rat model.

2.2 Materials and Methods

2.2.1 Cell Cultures and Tissue Explants

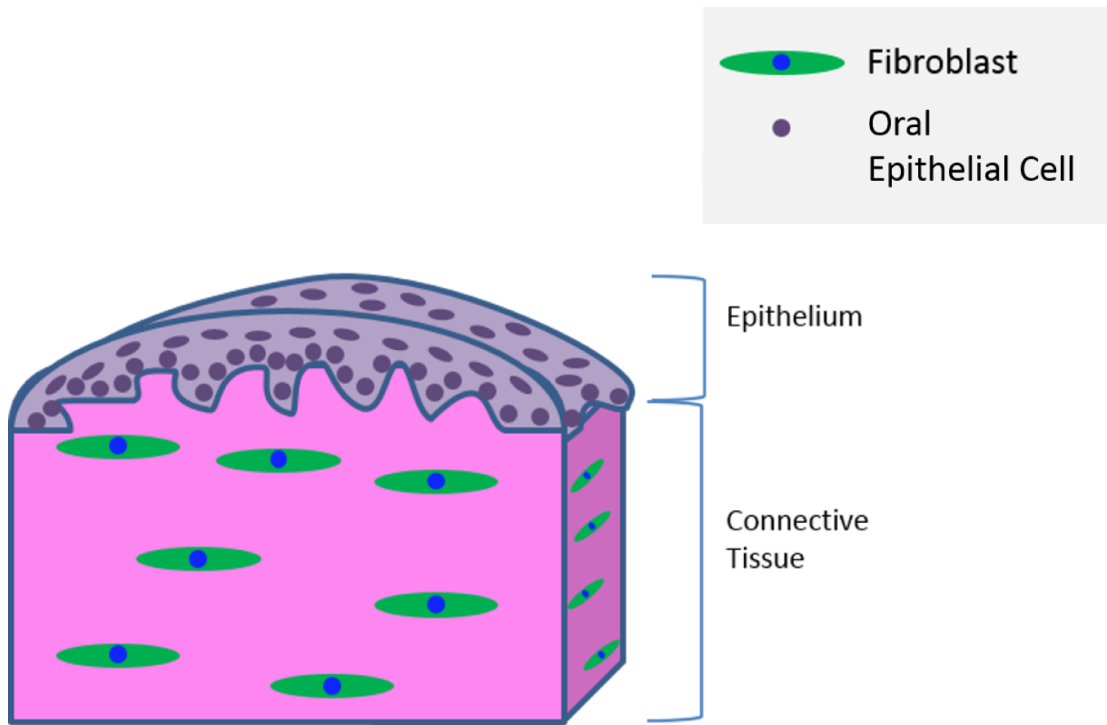
Human gingival fibroblasts (hGFs) were isolated and cultured from clinically healthy gingival tissue received from patients undergoing routine dental surgery at Western University Schulich School of Medicine and Dentistry Oral Surgery Clinic with informed patient consent. hGFs were cultured from both male and female patients aged 15 to 79

years of age. Excised gingival tissue was isolated in Dulbecco's Modified Eagle Medium (DMEM) (Gibco, Cat # 11995-065, Carlsbad, CA, USA) supplemented with 10% fetal bovine serum (FBS) (Gibco, Cat # 12483-020) and antibiotic-antimicotic (AA) (100 U/mL penicillin, 100 µg/mL streptomycin and 0.25 µg/mL amphotericin B; Gibco, Cat # 15240-062) at 4°C. Tissue was rinsed in phosphate buffered saline (PBS), pH 7.4 (Gibco, Cat # 10010-023) and the epithelium was mechanically separated from underlying connective tissue using a No. 15 scalpel blade. Connective tissue was minced and cultured on polystyrene tissue culture treated plates (Corning, Tewksbury, MA, USA) in DMEM supplemented with 10% FBS and AA (culture medium) at 37°C in a humidified atmosphere of 95% air and 5% CO₂. Once wells became confluent, gingival fibroblasts were dissociated from the growth surface using 0.05% Trypsin-EDTA (Gibco, Cat # 25300-054) and passaged 1:3 in 75 cm² polystyrene tissue culture treated flasks (Corning). For use in cell experiments, hGFs were grown to 80-90% confluence, dissociated from the growth surface, and cell number was determined using a Multisizer 3 Coulter Counter (Beckman Coulter, Mississauga, ON, Canada). Cells were used between passages 2 and 8 and in some instances frozen in liquid nitrogen prior to use. Experiments were carried out in culture media supplemented with 50 µg/mL ascorbic acid (experimental media) at 37°C in a humidified atmosphere of 95% air and 5% CO₂.

Gingival tissue explants (GTEs) were used directly for certain experiments. The tissue was cut on five faces, leaving the surface epithelium undisturbed, using a No. 15 scalpel blade into 2 mm³ blocks composed of connective tissue and attached epithelium as illustrated in Figure 2.1. GTEs were used immediately for experiments.

Figure 2.1 – Gingival tissue explant as an *ex vivo* experimental system.

Gingival tissue was cut into cubes along five faces, with the exception of the epithelial surface, into 2 mm³ blocks to be used for experiments.



2.2.2 Electrospun Fibrous Polycaprolactone Scaffolds Loaded with bFGF

Scaffolds were fabricated in, and obtained from the laboratory of Dr. Jianjun Guan (The Ohio State University, Columbus, OH, USA). Briefly, scaffolds were created using a two-stream electrospinning and electro spraying apparatus. Scaffolds were created by electrospinning a positively charged solution of PCL onto a negatively charged rotating collecting mandrel to form a fibrous construct. Simultaneously during fabrication, a second positively charged stream was used to electro spray microspheres with a core-shell structure consisting of a basic fibroblast growth factor core and a shell of poly (lactide-co-glycolide). The result was a fibrous construct composed of PCL fibers with uniform distribution of PLGA microspheres with a bFGF core throughout. The bFGF solution had a concentration of 150 $\mu\text{g}/\text{mL}$ and contained 0.05 wt % heparin to protect the bFGF from denaturation. The rate at which the bFGF solution was injected during the fabrication process was altered to produce scaffolds with different amounts of bFGF. An injection rate of 0.1 mL/hour and 0.7 mL/hour both with constant 1 mL/hour injection rate of PLGA created scaffolds with low bFGF and high bFGF loading, respectively. The constant injection rate of PLGA in low and high bFGF loaded scaffolds maintained a uniform density and distribution of the microspheres within the scaffold (Guo, Elliott et al. 2012). As a control, a scaffold without bFGF loading was also tested.

The scaffolds were characterized (Guo, Elliott et al. 2012) and found to have a sustained bFGF release over a 28 day period in PBS at 37°C. Approximately 50 mg pieces of scaffold released 35 ng and 20 ng for the high bFGF and low bFGF loading, respectively, over the 28 day period. The kinetics of bFGF release were found to occur in two stages with a relatively fast and nonlinear release in the first seven days (25 ng for the high bFGF scaffold, and 15 ng for the low bFGF scaffold) followed by the remainder being released relatively slower with a linear release profile in the days following.

Prior to use in experiments, the scaffolds were cut into appropriate sizes and sterilized in 70% ethanol for 20 minutes at room temperature (RT) and washed three times for 5 minutes in sterile water followed by one wash in experimental media for *in vitro* experiments and an additional wash in sterile water for *in vivo* experiments.

2.2.3 Human Gingival Fibroblast Attachment

Scaffolds were cut into 6 mm disks using a disposable biopsy punch (Integra Miltex, York, PA, USA) and sterilized. Scaffolds were placed into 96 well plates (Corning) and hGFs were seeded onto the scaffold surface at a density of 3.5×10^4 cells/cm². Cells were cultured on the scaffolds for 1, 2, 4 or 24 hours at which time they were gently rinsed once with PBS to remove non-adherent cells and fixed using 4% paraformaldehyde (PFA) in PBS at RT for 10 minutes. Cell seeded constructs were rinsed three times with PBS and dehydrated through a graded series of ethanol (50%, 70% and 90%) followed by three changes of anhydrous ethanol for 10 minutes per step. To preserve cell morphology, cell seeded constructs were immersed in hexamethyldisilazane (HMDS) (Sigma-Aldrich, St. Louis, MO, USA) for 15 minutes, air dried for 30 minutes and stored in a desiccator overnight. Samples were coated with 5 nm osmium metal using a Filgen OPC80T Osmium Plasma Coater (Filgen, Midori-ku, Nagoya, Japan) and visualized by scanning electron microscopy (SEM) using a Hitachi 3400-N Variable Pressure Scanning Electron Microscope (Hitachi, Mississauga, ON, Canada) to acquire images using an acceleration voltage of 2.00 kV. Photoshop 7.0 software (Adobe Systems Incorporated, San Jose, CA, USA) was used to pseudocolour attached cells.

2.2.4 Gingival Fibroblast Cell Number

Scaffolds seeded with hGFs at a density of 7×10^3 cells/cm² in 96-well plates were cultured for 1, 5 or 9 days with the addition of 50 μ L experimental media every 2 days. Cell number on the scaffolds at each time point was determined using a CyQUANT® Cell Proliferation Assay kit (Molecular Probes, Carlsbad, CA, USA) (Jones, Gray et al. 2001). At each experimental time point the media was gently removed and scaffolds were rinsed in PBS to remove non-adherent cells and residual media. Scaffolds were transferred to a 500 μ L microcentrifuge tube (Port City Diagnostics, Wilmington, NC, USA) and stored at -80°C until the end of the experimental culture period. Once all experimental time points were frozen, the assay was conducted according to manufacturer's specifications. Briefly, scaffolds were thawed and incubated with 250 μ L CyQUANT® GR working solution for 5 minutes at RT with vigorous vortexing. 200 μ L

of the incubated working solution was transferred to a 96-well microplate. A standard curve was created from a 1×10^6 hGF cell pellet frozen at the beginning of the experiment. Sample fluorescence was measured using a Safire² microplate reader (Tecan, Männedorf, Switzerland) at an excitation wavelength of 480 nm and an emission wavelength of 520 nm.

2.2.5 *Ex-Vivo* Explant Cultures

Gingival tissue explant blocks were placed on sterilized 6 mm scaffold disks in 3.5 cm diameter polystyrene dishes (Corning), oriented such that the surface epithelium was not in contact with the scaffold surface, and cultured submerged in experimental media for 3 weeks. Half of the media was removed and replaced every two days for the duration of the experiment taking care not to disrupt explant tissue. Explant tissue and scaffolds were fixed in 10% neutral buffered formalin (Sigma-Aldrich) at 4°C overnight. Samples were prepared for SEM (as described above) and for frozen sections.

Samples to be used for frozen sections were prepared for embedding by rinsing in PBS once for 15 minutes, 4% sucrose (Sigma-Aldrich) in PBS three times for 15 minutes and sinking in 30% sucrose in PBS at 4°C overnight. The following day, samples were rinsed in 30% sucrose in water three times for 15 minutes and sunk in a 50:50 mixture of 30% sucrose in water and VWR Premium Frozen Section Compound (VWR International, Radnor, PA, USA) for 1 hour at RT. For embedding, the samples were sunk in VWR Premium Frozen Section Compound and placed in an embedding mold such that sections along the face of the block cut along the length of the scaffold. Samples were frozen in liquid nitrogen until almost completely frozen then left on dry ice for 20 minutes to complete freezing. Samples were stored in sealed containers at -20°C for short term storage.

Frozen blocks were sectioned at 10 μ m using a Leica CM3050 S cryostat (Leica, Wetzlar, Germany). Sections containing explanted tissue were mounted on Superfrost Plus slides (Fisher Scientific, Waltham, MA, USA), air dried at RT and stored at -20°C until ready to be stained.

Three sections per sample, at least 50 μm apart, were stained for vimentin to visualize the location of cells of mesenchymal origin. Additional sections were stained for keratin 17 to localize epithelial cells. Sections were rehydrated in PBS for 30 minutes at RT. Endogenous peroxidase activity was quenched with 3% hydrogen peroxide (H_2O_2) in methanol for 5 minutes. Non-specific antibody binding was blocked using 10% horse serum for 30 minutes at RT prior to application of the primary antibody against vimentin (clone EPR3776, Abcam, Cambridge, England, UK) at a 1:400 dilution or keratin 17 (A2175, NeoBiolab, Cambridge, MA, USA) at a dilution of 1:100. Sections were incubated with the primary antibody at 4°C overnight. Sections were rinsed three times in PBS to remove unbound antibodies and sections were incubated for 30 minutes at RT with ImmPRESS HRP Anti-Rabbit Ig (Peroxidase) reagent (Vector Laboratories, Burlingame, CA, USA). Unbound reagent was rinsed from the section using PBS and 3, 3'-diaminobenzidine (DAB) peroxidase substrate (Vector Laboratories) was used to develop the reagent according to manufacturer's instructions. Colour development was stopped by rinsing sections with water. Negative control sections were made by omitting the primary antibody. All sections were counterstained using Harris Modified Hematoxylin Solution (Sigma-Aldrich). Stained sections were imaged using an Axio Imager M1 microscope (Zeiss, Oberkochen, Germany) and AxioImager software. ImageJ 1.48v software (National Institutes of Health, Bethesda, MD, USA) was used to calculate the distance of each vimentin-positive cell from the surface of the scaffold.

2.2.6 Immunocytochemical Analysis

Scaffolds seeded with hGFs at a density of 8.8×10^4 cells/cm² in 96-well plates were cultured for 3 or 7 days with the addition of 50 μL experimental media every 2 days. Cells were fixed with 4% PFA in PBS for 10 minutes, rinsed three times with PBS and blocked with 1% bovine serum albumin (BSA) in PBS for 30 minutes. Scaffolds were incubated with primary antibodies diluted 1:100 in 1% BSA in PBS against the extracellular matrix (ECM) proteins biglycan (ab54855, Abcam), decorin (ab54728, Abcam) and fibronectin (EP5, Santa Cruz Biotechnology, Dallas, TX, USA) at 4°C overnight. Scaffolds were gently washed with PBS five times for 10 minutes each and blocked with 1% BSA in PBS for 5 minutes. Scaffolds were then incubated, protected

from light, for 90 minutes at RT with Alexa Fluor 488 Goat Anti-Mouse IgG antibody (Molecular Probes) at a 1:200 dilution. Following incubation, the scaffolds were washed five times for 10 minutes in PBS and mounted on glass coverslips using Vectashield Mounting Medium (Vector Laboratories) with 4', 6-diamidino-2-phenylindole (DAPI). Samples were imaged using an Axio Observer.Z1 fluorescence microscope (Zeiss). Axiovision Software Release 4.8.0.0 was used to capture images. Negative control samples were prepared with the omission of the primary antibody and used to set the threshold for fluorescence detection (Appendix D, F, H). Due to the thickness of the samples being imaged, z-stacks were acquired and extended depth of focus was employed using the Axiovision software.

2.2.7 Human Gingival Fibroblast Extracellular Matrix Gene Expression

Scaffolds seeded with hGFs at a density of 2×10^5 cells/cm² in 96-well plates were cultured for 3 or 7 days with the addition of 50 μ L experimental media every 2 days. Total RNA was isolated using TRIzol Reagent (Ambion, Carlsbad, CA, USA). Isolated RNA was purified using a PureLink RNA Mini Kit (Ambion) according to the manufacturer's directions. Quantitative real-time reverse transcription polymerase chain reaction (RT-qPCR) was used to determine the gene expression level of biglycan (*BGN*, Hs00959141_g1) and fibronectin (*FNI*, Hs01549958_m1). 15 μ L reactions containing: 3-15 ng RNA; qScript XLT One-Step RT-qPCR ToughMIX master mix reagent (Quanta Biosciences, Gaithersburg, MD, USA); TaqMan Gene Expression Assay (Life Technologies, Carlsbad, CA) containing PCR primers for *FNI*, *BGN* or *18S* and a FAM dye labelled TaqMan probe; and RNase free water. Thermal cycling conditions for amplification were 30 minutes at 48°C (reverse transcription), 10 minutes at 95°C (polymerase activation) followed by 40 cycles of each 15 seconds at 95°C and 1 minute at 60°C (melt and anneal/extend, respectively). A dilution series was created from pooled RNA samples to test the efficiency of each target gene expression assay primer and probe set compared to the reference gene, *18S*. Gene expression levels of *FNI* and *BGN* were normalized to the levels of endogenous *18S* rRNA. Data are presented as a

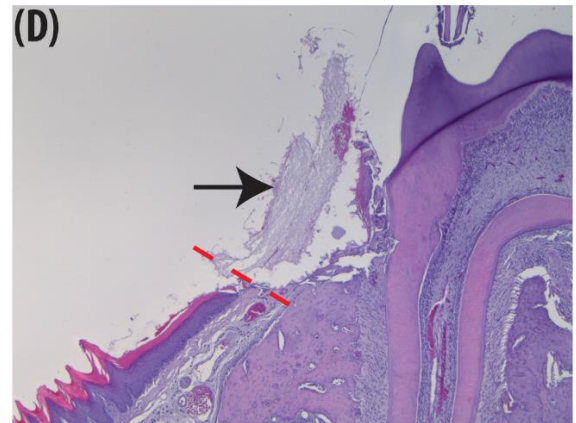
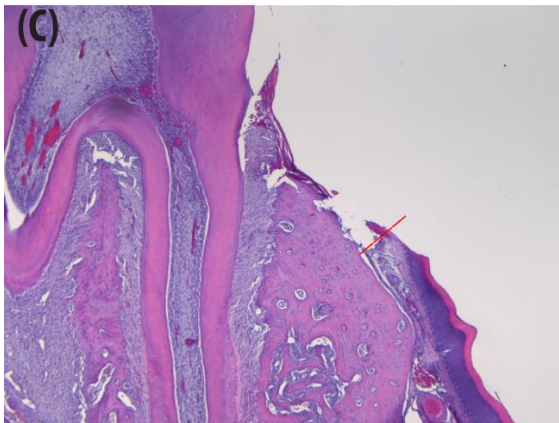
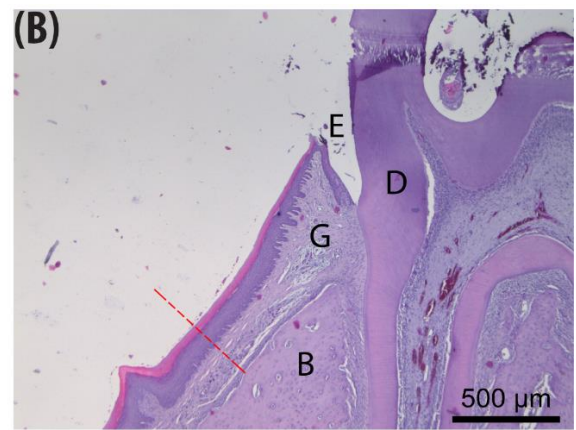
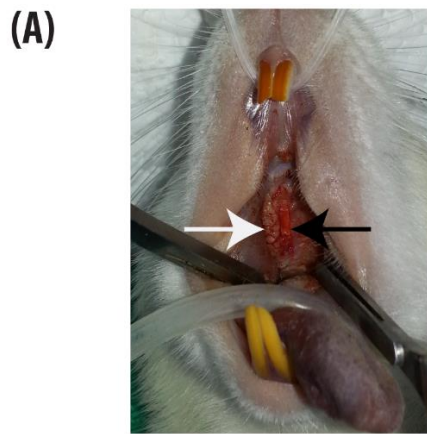
relative quantification of gene expression of samples relative to the PCL alone scaffold at day 3 using the $2^{-\Delta\Delta CT}$ method (Livak and Schmittgen 2001).

2.2.8 Rat Gingivectomy Model

Fifteen adult female Wistar rats aged 8 to 20 weeks weighing between 160 and 370 g were used in experiments (a generous gift from the lab of Dr. Stephen Sims, Western University, London, ON, Canada). All animal procedures were approved by the University Council on Animal Care of Western University. Gingivectomy was performed on the maxillary palatal gingiva or mandibular buccal gingiva by one operator (Figure 2.2). Animals were anesthetized by intraperitoneal injection of Ketamine-Xylazine (75 mg/kg Ketamine and 10 mg/kg Xylazine). A small, round dental instrument was used to disrupt the junctional epithelium and a No. 15 scalpel blade was used to raise a full-thickness 900 μm wide gingival flap along the first, second and third molars. The No. 15 scalpel blade was then used to excise the soft connective tissue flap and a small dental blade was used to thoroughly remove any remaining soft connective tissue on the tooth or bone. To maintain hemostasis, cotton swabs were held over the wound with slight pressure. Wounds received either PCL alone, low bFGF or high bFGF scaffolds or no scaffold (empty defect) as a control (n = 6 wounds receiving low bFGF and high bFGF scaffolds and n = 9 wounds receiving PCL alone scaffold or an empty defect). Two sterilized scaffold strips 1 mm x 3 mm in size were placed into the experimental surgical wounds on top of one another to create a double layer and held in place with a small amount of Vetbond tissue adhesive (Figure 2.2). A subset of animals (n = 3) with empty defects and PCL alone scaffolds were euthanized by carbon dioxide inhalation immediately following surgery completion to serve as a day 0 baseline. Remaining animals received 0.5 mg/kg Buprenorphine by subcutaneous injection twice daily for 48 hours post-surgery as an analgesic. Animals were maintained on a standard lab chow powdered food diet and were allowed food and water *ad libitum* for the duration of the experiment.

Figure 2.2 - Gingivectomy in a rat model and scaffold placement.

Gingivectomy was performed in adult female Wistar rats. Soft gingival tissue was removed and two layers of sterilized scaffolds were placed in the defect. A) Macroscopic view of scaffold placement in the gingival wound. White arrow – Molars, Black arrow – Scaffold placement. B) Uninjured gingival tissue. B – Alveolar bone, G – Gingiva, D – Dentin, E – Enamel space. Dashed red line demarcates approximate location of wound edge to be created following gingivectomy. C) Immediately following gingivectomy in an empty defect. Dashed red line indicates wound edge. D) Immediately following gingivectomy in a PCL alone treated defect. Dashed red line indicates wound edge. Black arrow indicates the scaffold.

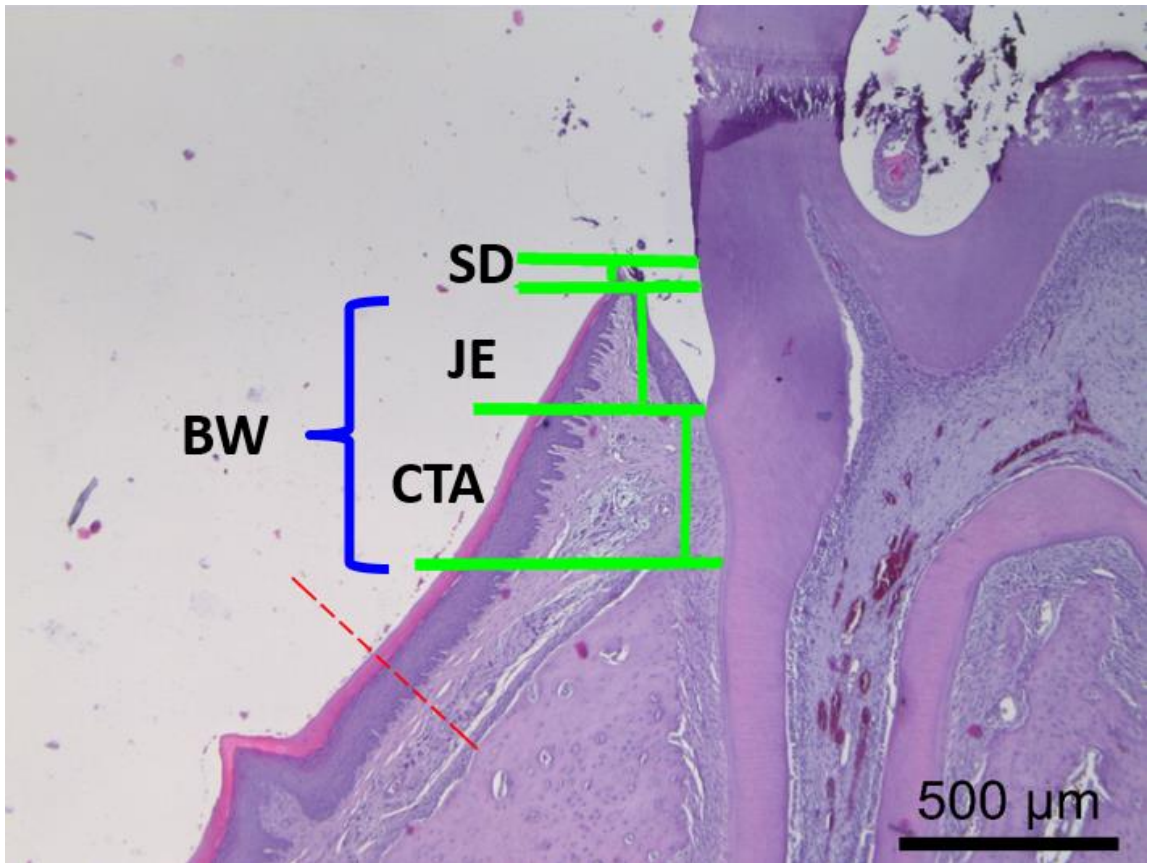


Animals were euthanized 3 (n = 6) or 7 (n = 6) days post-gingivectomy by carbon dioxide inhalation. Heads were fixed in 10% neutral buffered formalin (Sigma) overnight at 4°C. Jaws were excised and tissues were subsequently decalcified at 4°C for 48 hours in two changes of Cal-Ex Decalcifier (Fisher Chemical, Waltham, MA, USA). Molars were processed *en bloc* for frozen sections or by routine paraffin embedding. Serial 5 µm sections were taken in the mesio-distal plane encompassing the second molar.

Sections were rehydrated and stained with hematoxylin (Sigma) and eosin (alcoholic; Leica) (H&E), Van Gieson, and Masson's Trichrome. Images were taken with a Leica DM100 light microscope (Leica). Histomorphometric analysis of H&E stained sections of the wounds was completed using ImageJ 1.48v software (National Institutes of Health, USA) to measure the epithelial migration distance, the area of regenerated gingival connective tissue, and biologic width; as indicated by connective tissue attachment and junctional epithelium length (Khuller and Sharma 2009) (Figure 2.3). Connective tissue attachment was measured from the crest of the alveolar bone to the apical most epithelial attachment. Junctional epithelium length was measured from the most apical epithelial attachment to the bottom of the gingival sulcus. Biologic width was the combined measurement of connective tissue attachment and junctional epithelium length (Figure 2.3).

Figure 2.3 - Biologic width.

Measurements of biologic width were made on H&E stained sections of rat gingival wounds. Measurement parameters are indicated on uninjured tissue. Horizontal green lines demarcate boundaries between which measurements are made, vertical lines indicate distances measured. Biologic width (BW) is the combined measurement of connective tissue attachment (CTA) and junctional epithelium length (JE). Sulcular depth (SD) is indicated, however does not contribute to the biologic width measurement. Red dashed line demarcates the approximate location of the wound edge which would be created following gingivectomy.



Immunohistochemical staining for arginase-1 (V-20:sc-18354, Santa Cruz), alpha smooth muscle actin (α -SMA) (clone 1A4, A5228, Sigma-Aldrich) and proliferating cell nuclear antigen (PCNA) (ab2426, Abcam) was performed to visualize M2 phenotype macrophages, myofibroblasts (α -SMA positive cells not associated with blood vessels) and proliferating cells in the wound area, respectively. Sections were rehydrated, permeabilized using 0.1% Triton X-100 in PBS for 5 minutes at RT, rinsed in PBS and blocked using 10% horse serum. Sections were incubated with primary antibodies against arginase-1, α -SMA and PCNA diluted 1:100 in 10% horse serum for 1 hour at room temperature. Sections were rinsed in PBS and incubated, protected from light, for 1 hour at RT with an appropriate Cy5 conjugated secondary antibody. Sections were rinsed with PBS to remove unbound antibody and mounted using Vectashield Mounting Medium with DAPI. Sections were imaged using an AxioImager.M2m (Zeiss) with Zen software (Zeiss). Negative control sections were created in which the primary antibody was omitted and used to set the threshold level for fluorescence detection (Appendix L). ImageJ 1.48v software (National Institutes of Health, USA) was used to quantify the number of myofibroblasts and proliferating cells in the wound area.

2.2.9 Statistical Analysis

Data are presented as mean \pm SD of triplicate experiments. Statistical analysis was performed using GraphPad Prism software version 5.01 for Windows (GraphPad Software, San Diego, CA, USA). Data were analyzed using a two-way ANOVA with Bonferroni's post-test, with the exception of biologic width calculations which were analyzed using a one-way ANOVA with Kuskal-Wallis post-test. A p-value of less than 0.05 was considered statistically significant.

2.3 Results

2.3.1 Attachment and Morphology of hGFs on PCL Electrospun Scaffolds Loaded With bFGF

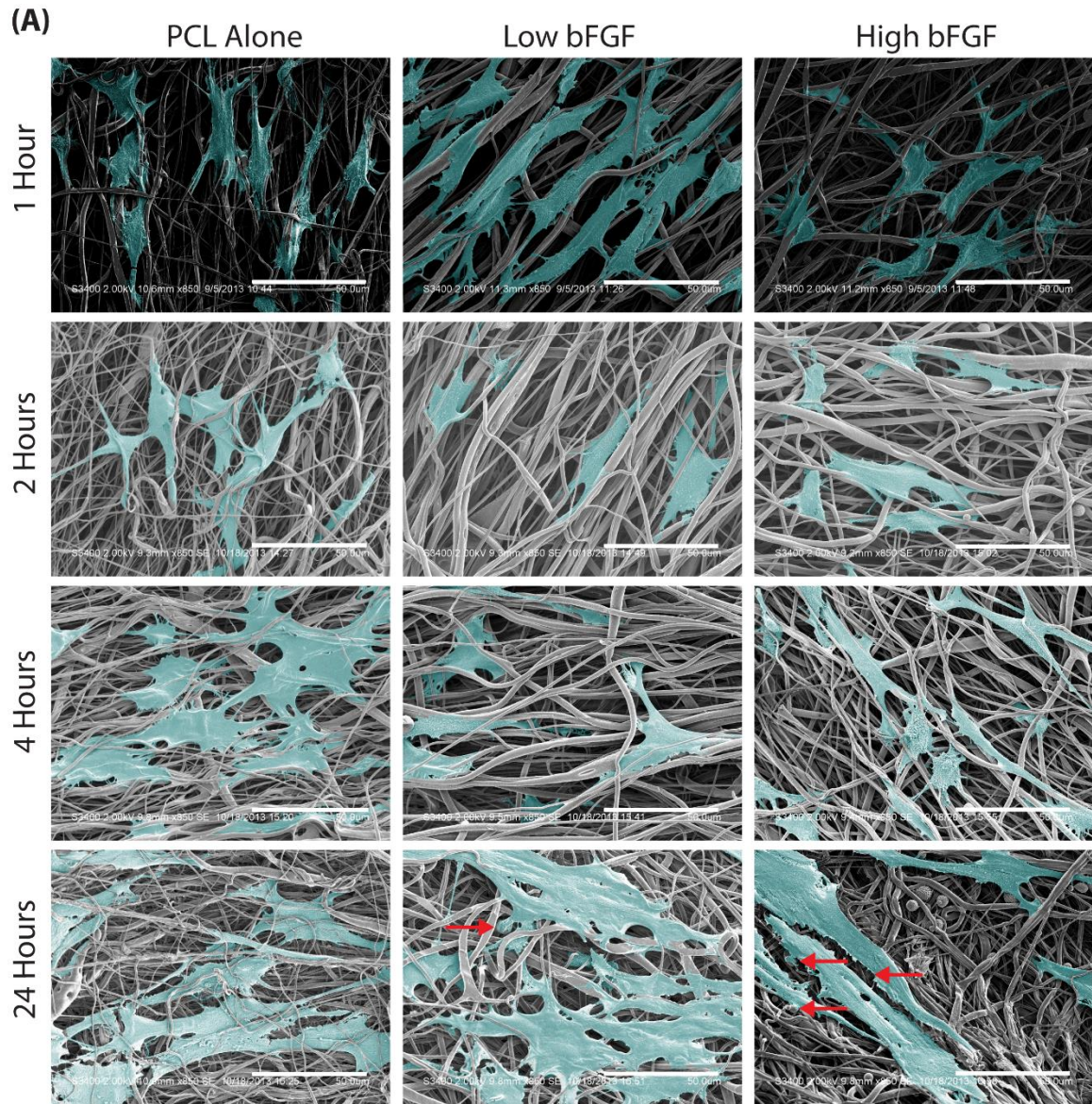
SEM was used to visualize hGF attachment, spreading and morphological changes on scaffolds with and without bFGF loaded microspheres. hGFs attached within 1 h and began spreading, with extension of cellular processes along the scaffold fibers evident on all scaffold types (Figure 2.4A). Cells attached to and spanned across multiple fibers within the scaffolds, but remained on the surface of the scaffolds. By 2 h both cell processes and cell bodies began penetrating the scaffolds, and were evident under the top fiber layer (Figure 2.4B). Cell morphology was observed to be influenced by the underlying fiber architecture of the scaffolds. By 24 h cells on scaffolds containing bFGF were seen to make contact with the microspheres (Figure 2.4B).

2.3.2 bFGF Loaded PCL Electrospun Scaffolds Increase hGF Cell Number

Increase in hGF cell number on each scaffold was assessed at 1, 5, or 9 days post-seeding. All three scaffolds supported an increase in cell number as DNA content on each of the three scaffolds increased with time (Figure 2.5). At 5 days post-seeding, the low bFGF loaded scaffold significantly increased cell number compared to the PCL alone scaffold and the high bFGF loaded scaffold for one of the patient cells tested. At 9 days post-seeding, the scaffold with low bFGF loading significantly increased cell number compared to the PCL alone scaffold for two of the patient cells tested while the hGFs from the third patient showed a significantly larger cell number on the scaffold with high bFGF loading (Figure 2.5).

Figure 2.4 - hGF attachment and morphology.

A) SEM micrographs show hGFs (pseudo-coloured blue) attached to and spread along the scaffold fibers on PCL electrospun scaffolds both with and without bFGF microspheres at 1 hour. The scaffold architecture influenced cell morphology. Red arrows indicate cell contact with bFGF loaded microspheres. Scale bar = 50 μm B) Higher magnification SEM micrographs showing cells contacting the fibers of the scaffold with both large and small cell processes in as little as 1 hour. By 2 hours, cell processes were seen extending down into the scaffold and cell bodies were seen below the superficial fibers. Red arrows indicate cell contact with bFGF loaded microspheres. Scale bar = 30 μm (1 and 24 hours), Scale bar = 20 μm (2 and 4 hours). Images are representative of a single experiment.



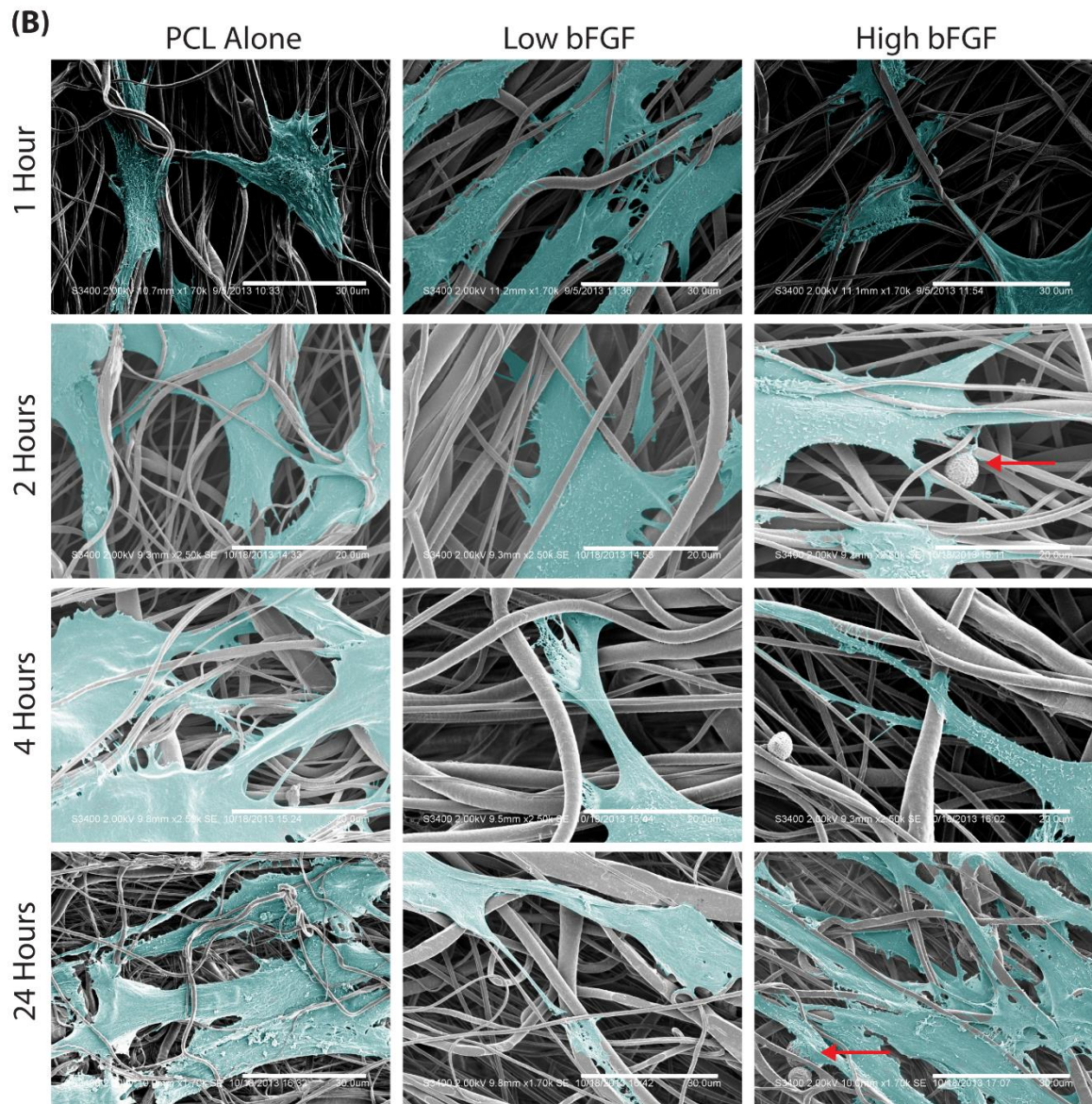
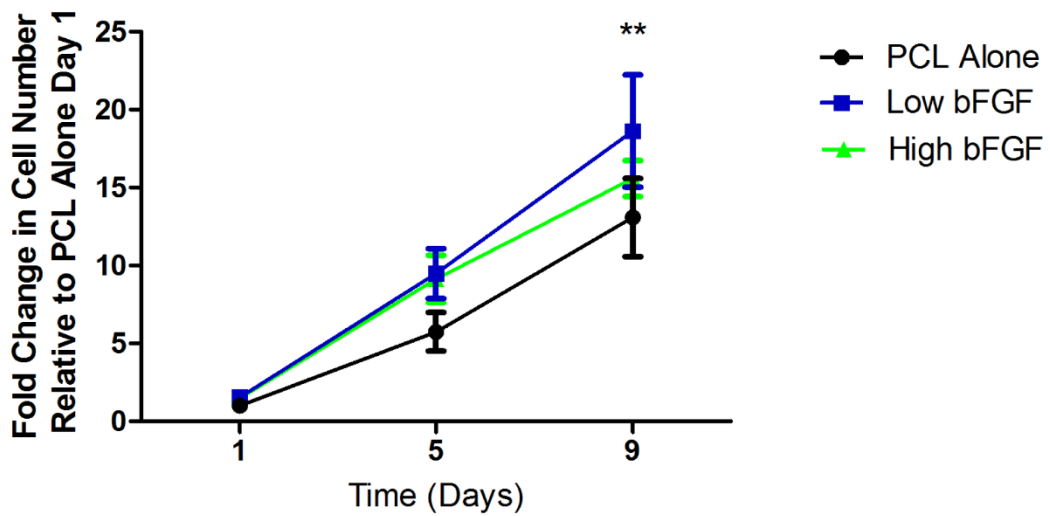
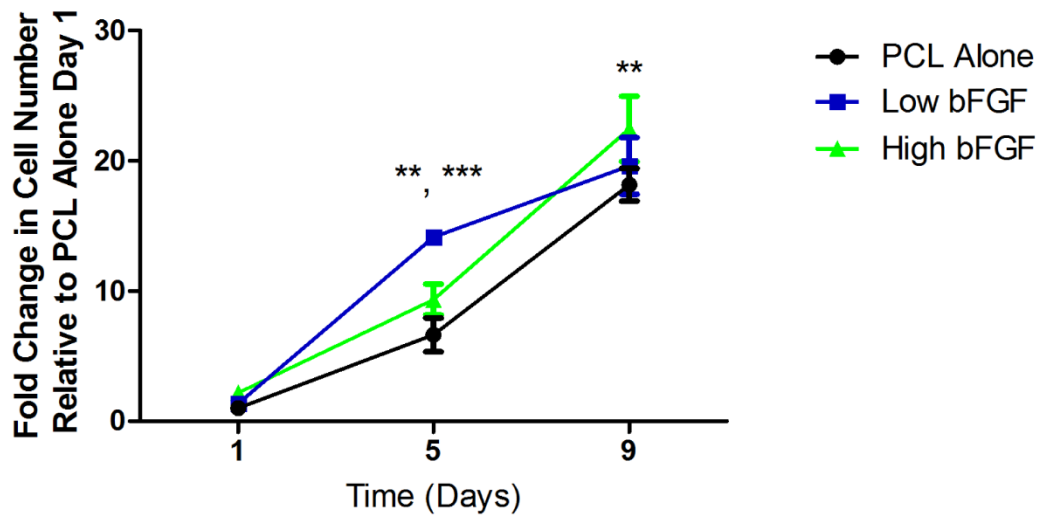
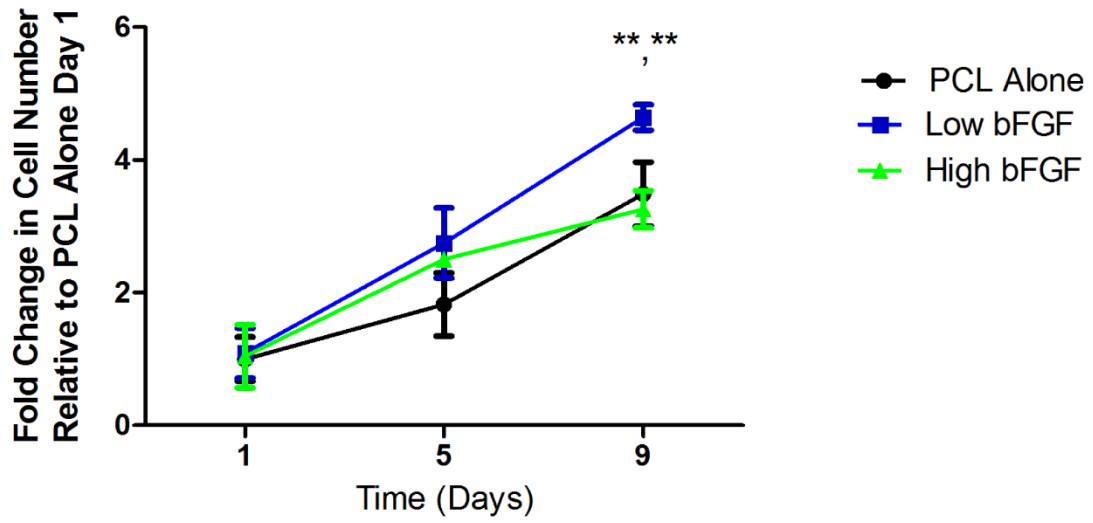


Figure 2.5 - hGF cell number.

hGFs were seeded onto all three scaffold types and cultured for 1, 5 or 9 days. Cell number at each time point was determined by quantification of DNA using a CyQUANT® assay. Data are presented as mean \pm SD of the fold change in cell number relative to the PCL alone scaffold at day 1. Data are presented as individual donor patient cells with three experimental replicates. Two-way ANOVA with Bonferroni's post-test was conducted to compare means, * $p < 0.05$, ** $p < 0.01$, *** $p < 0.001$.



2.3.3 Interaction of Gingival Explant Tissue with PCL Electrospun Scaffolds Loaded with bFGF

In the next experiments, gingival tissue explants were cultured on the surface of PCL electrospun scaffolds with and without bFGF microspheres for three weeks. Cells grew out from the explants on all scaffold surfaces and appeared as cell sheets on the top of the scaffold fibers. Sheets on the scaffolds containing bFGF appeared more confluent (Figure 2.6B, C), whereas on the PCL alone scaffold (Figure 2.6A) cells are more sparsely distributed on the scaffold surface.

To further assess cell growth and migration on and into the scaffolds, sections of gingival tissue explants cultured on the scaffolds for three weeks were cut and cell type assessed using vimentin immunoreactivity, which allows separation of cells of mesenchymal origin and epithelial cells. Vimentin-positive cells had migrated into the scaffolds with and without bFGF from the explants (Figure 2.7A). Scaffolds with high bFGF loading had significantly more cells than scaffolds with low bFGF loading or with no bFGF loading for at least one depth from the scaffold surface in all three patient tissues ($p < 0.05$) (Figure 2.7B). Two of the three patient tissues showed significantly more cells in the high bFGF scaffold as compared to the scaffold without bFGF for several depths from the scaffold surface ($p < 0.05$) while the third patient tissue showed this trend, however it was not statistically significant (Figure 2.7B).

In some instances the epithelium from the explanted gingival tissue migrated along the exterior surface of the tissue at the interface between the tissue and the scaffold. The epithelial cell phenotype was assessed by non-reactivity to vimentin and positive labeling for keratin 17 (Figure 2.8). In both instances, the epithelial cells showed minimal migration into the interior of the scaffold, staying on the surface of both the PCL alone and high bFGF loaded scaffold. The epithelial sheet on the high bFGF loaded scaffold qualitatively was thicker than the epithelial sheet migrating along the PCL alone scaffold.

Figure 2.6 - SEM of gingival tissue explants.

Gingival tissue explants consisting of gingival connective tissue and attached epithelium were cultured on the surface of PCL electrospun scaffolds with and without bFGF loading for 3 weeks. SEM micrographs show cells (pseudo-coloured blue) on the surface of the scaffold adjacent to the gingival tissue explants (pseudo-coloured purple). A) PCL alone scaffold. B) Low bFGF scaffold. C) High bFGF scaffold. Images are representative of a single experiment using tissue from one patient. Scale bars = 500 μm .

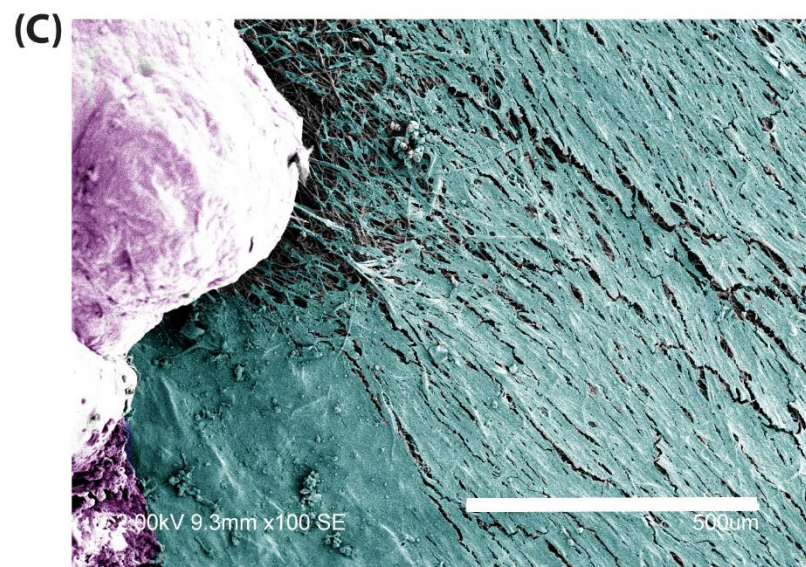
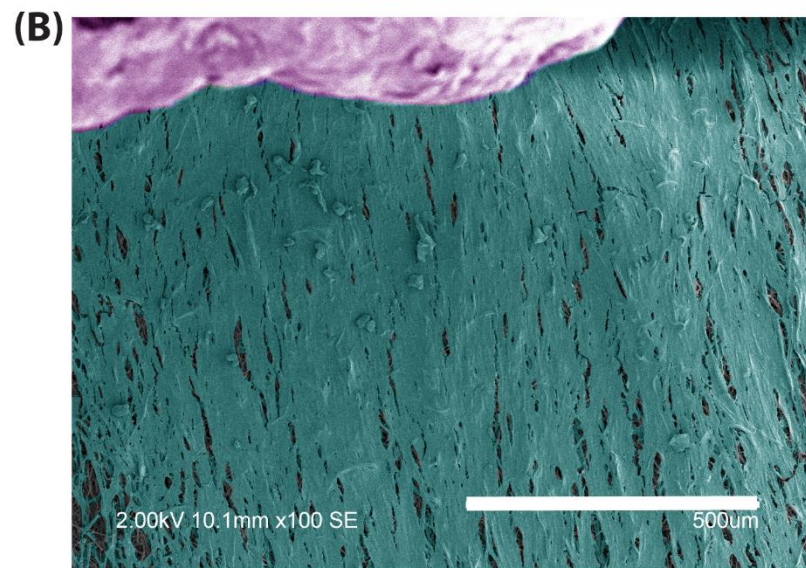
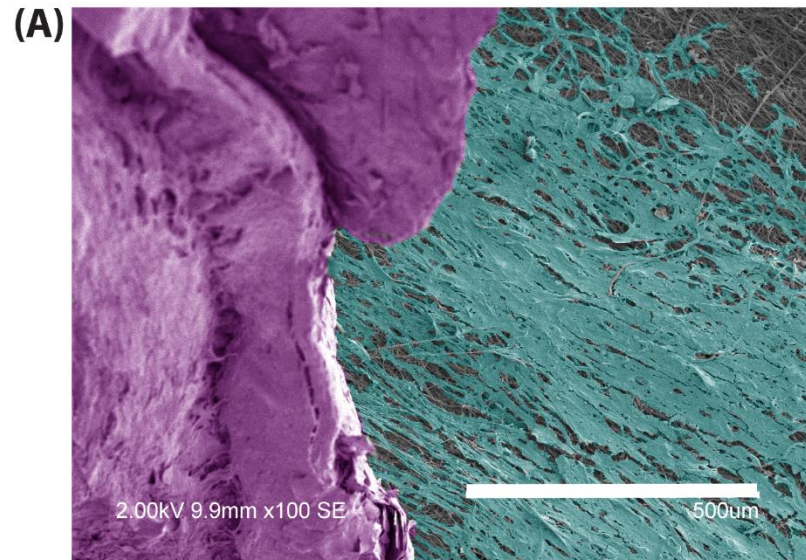


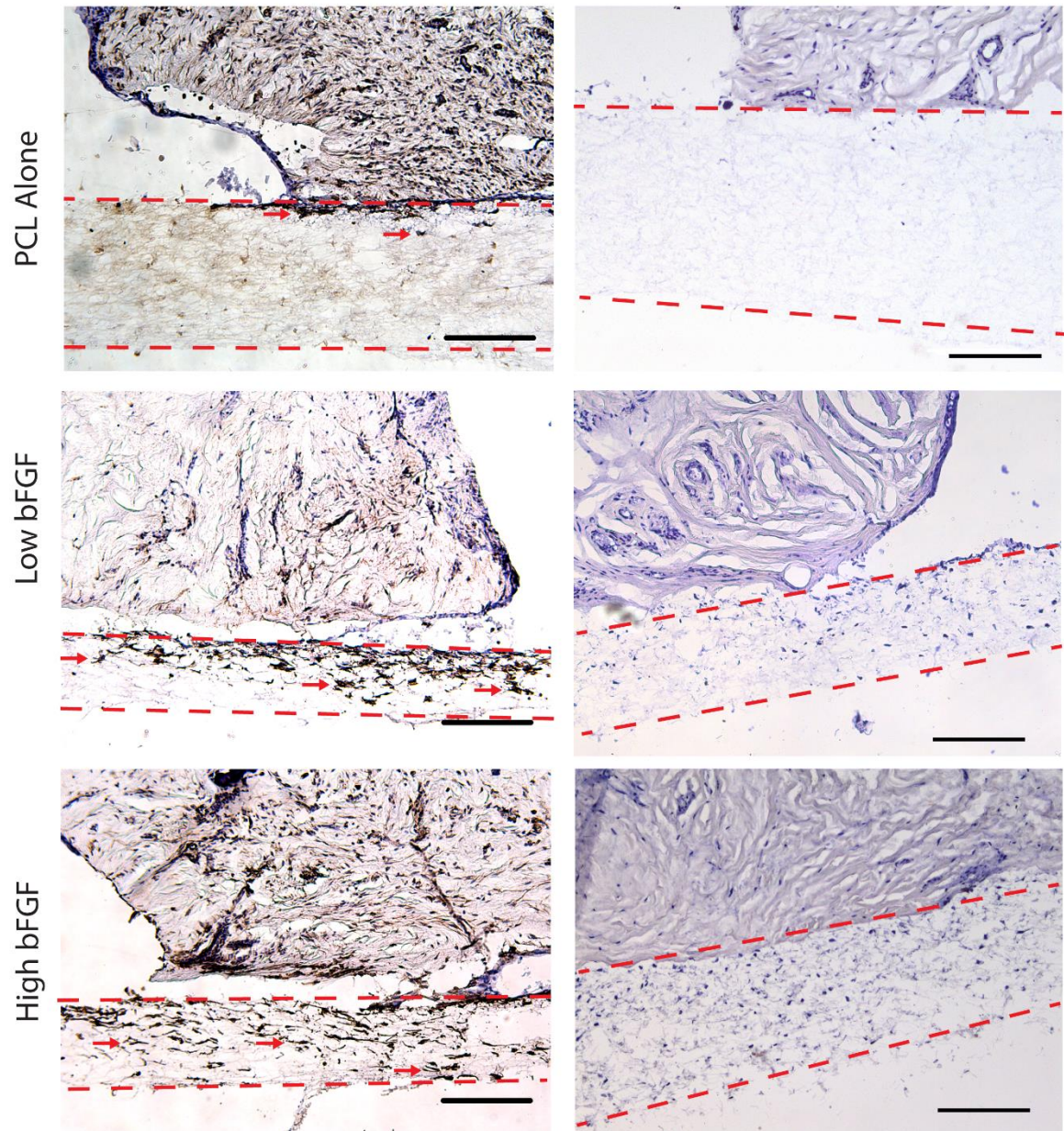
Figure 2.7 - Population of the PCL electrospun scaffolds by cells from gingival tissue explants.

A) Vimentin-positive cells were observed within the interior of the scaffolds both with and without bFGF. Red dashed lines delineate the PCL scaffolds. Red arrows indicate vimentin-positive cells within the scaffolds. Images are representative of three patient tissues with three experimental replicates. Scale bars = 200 μm . B) The distance each vimentin-positive cell was located from the surface of the scaffold was measured for three separate patient tissues. Scaffolds with high bFGF loading had significantly more cells than scaffolds with no bFGF or low bFGF for at least one depth from the scaffold surface in all three patient tissues. * $p < 0.05$, ** $p < 0.01$, *** $p < 0.001$. Two-way ANOVA with Bonferroni post-test was conducted to compare means. Data presented for each patient as mean \pm SD of three sections from three experimental replicates.

(A)

Vimentin

No Primary Antibody



(B)

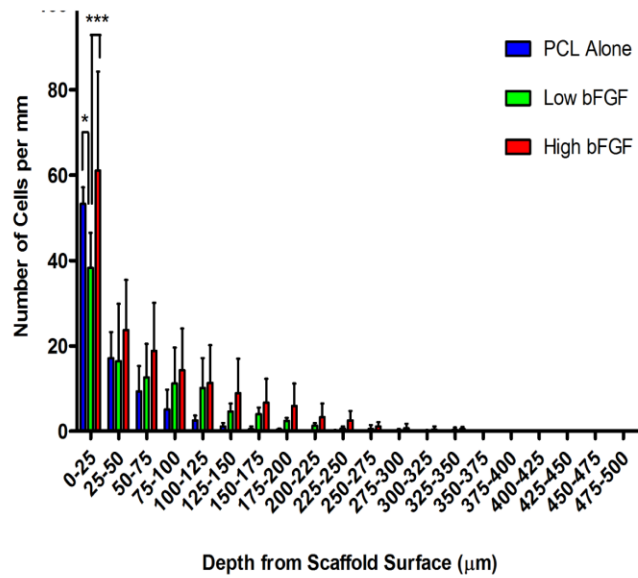
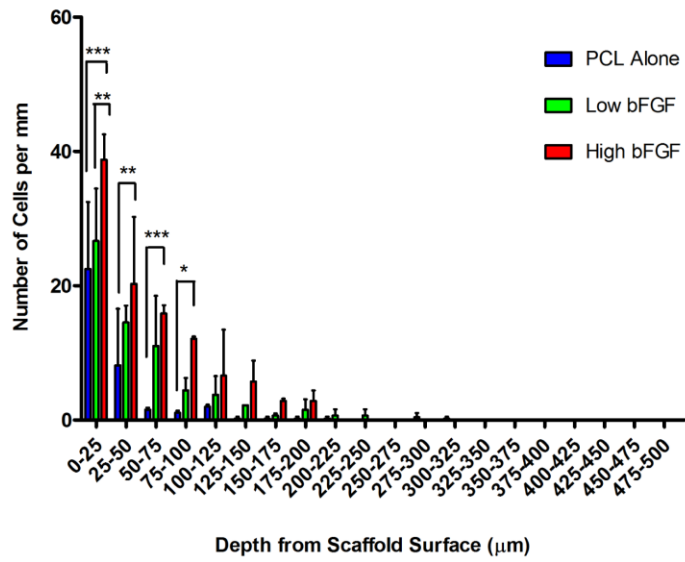
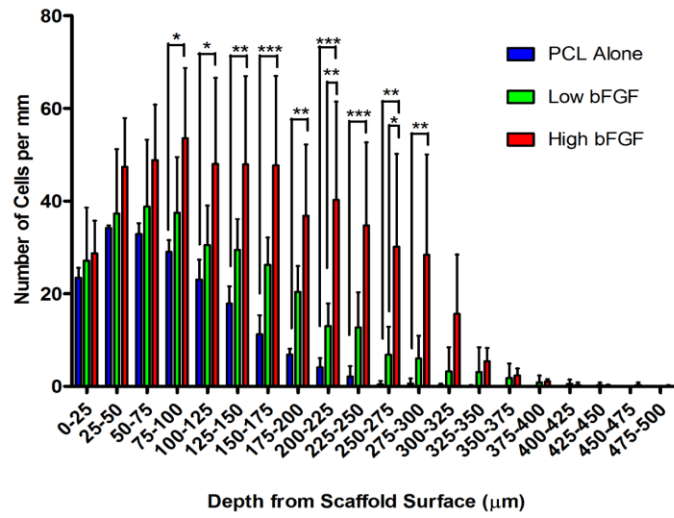
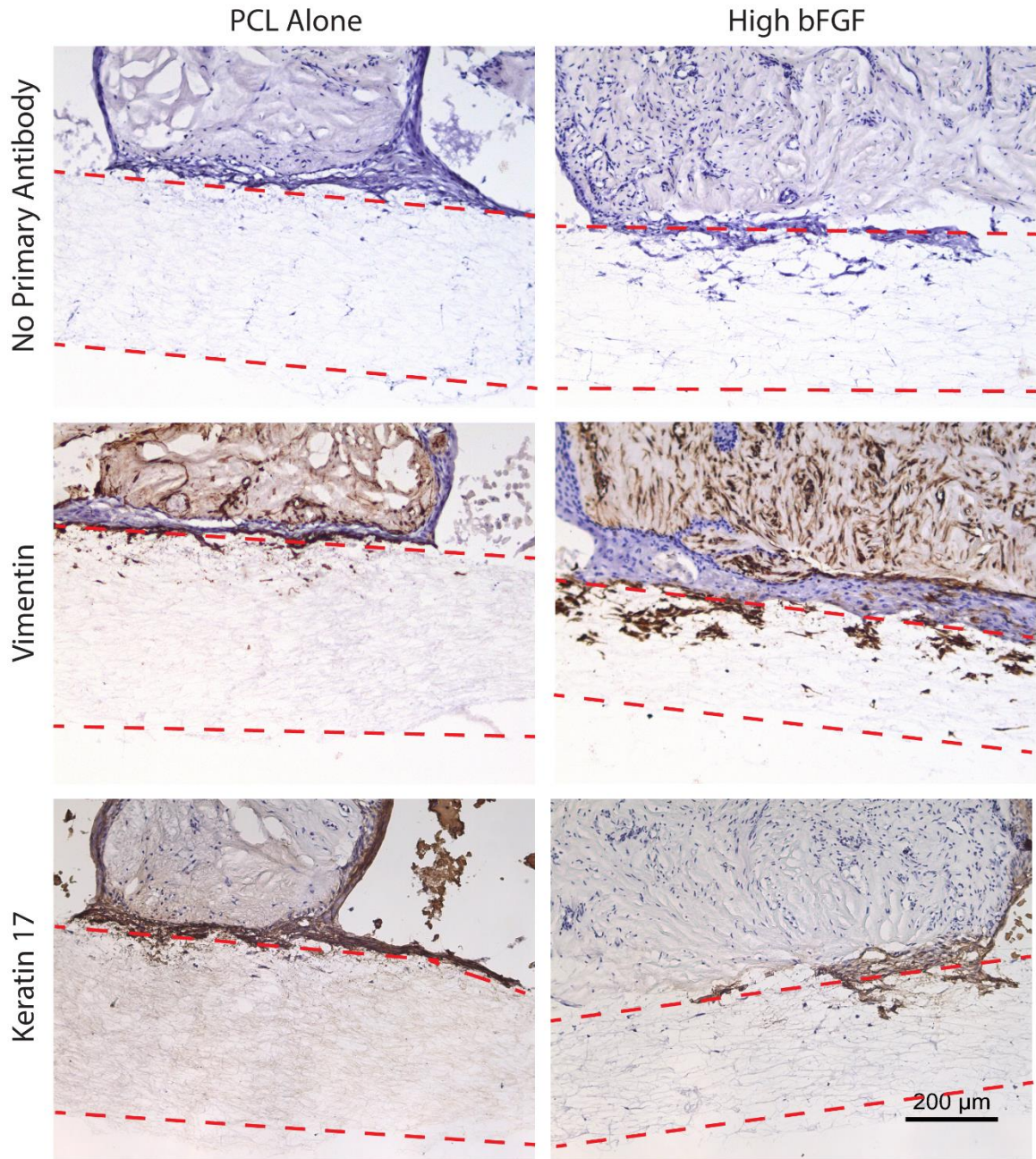


Figure 2.8 - PCL electrospun scaffolds as a barrier to oral epithelial cells.

When epithelial cells from the explant tissue migrated to the interface between the tissue and the scaffold, epithelial cells migrated along the surface of the scaffold with minimal penetration into the scaffolds. Vimentin staining, excluding epithelial cells, and keratin 17 staining, a marker of epithelial cells, showed minimal scaffold penetration by epithelial cells both in the presence and absence of bFGF microspheres. Red dashed lines delineate the PCL scaffold.



2.3.4 hGF ECM Secretion is Modulated by bFGF on PCL Electrospun Scaffolds

We next investigated whether addition of bFGF to the scaffolds influenced secretion and deposition of fibronectin, biglycan, and decorin by hGF cells seeded onto the scaffolds. Localization of all three ECM proteins on the surface of each scaffold was initially visualized with fluorescent microscopy at low magnification (Appendix C, E, G) to qualitatively assess deposition across a large scaffold area. Higher magnification images were taken to assess deposition on the surface of the scaffold associated with the cells. Fibronectin deposition was evident on all scaffold types after 3 days (Figure 2.9). By 7 days of culture, fibronectin deposition on the surface of the scaffold remained evident on all three of the scaffold types.

Biglycan immunoreactivity was observed on the surface of the scaffolds after 3 days of culture although remained intracellular with little evidence of secretion into the ECM (Figure 2.10). Biglycan appeared most prominent on the PCL alone scaffold and was diminished in the presence of bFGF release. After 7 days of culture, biglycan immunoreactivity remained intracellular.

At 3 days post-seeding, decorin immunoreactivity is observed on all of the scaffold types (Figure 2.11). Decorin immunoreactivity appeared to be most prominent in the presence of bFGF and was mainly associated with the cells. After 7 days of culture, decorin remained associated with the cells.

Figure 2.9 - Fibronectin immunoreactivity on the scaffold surface.

The secretion and deposition of the structural ECM protein fibronectin by hGFs cultured on the scaffold was visualized on the scaffold surface using immunocytochemistry; fibronectin (green), nuclei (blue). Fibronectin deposition is evident after 3 days on all three scaffold types. After 7 days, fibronectin deposition remains evident on the surface of all three scaffold types. Images are representative of three independent experiments.

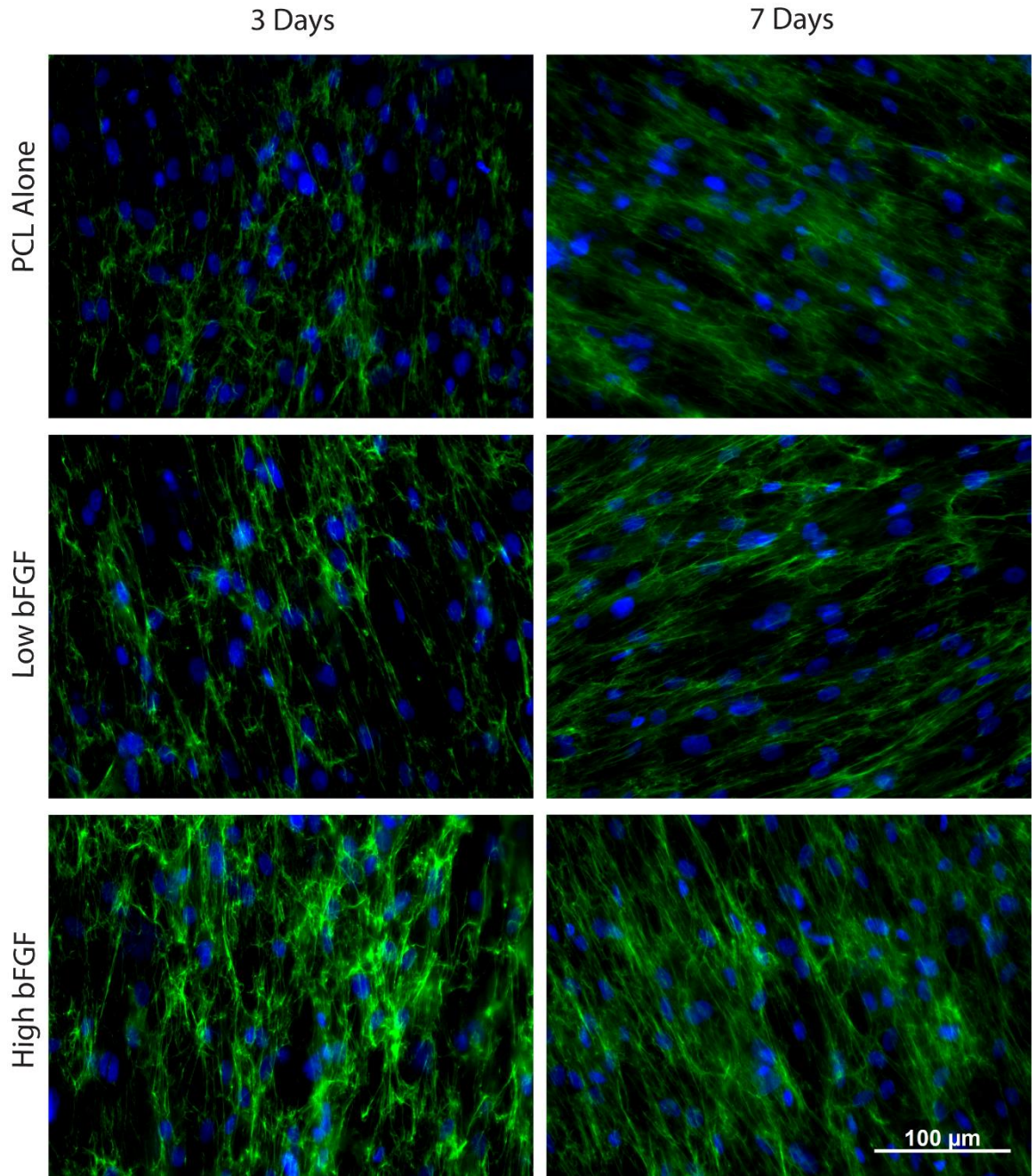


Figure 2.10 - Biglycan immunoreactivity on the scaffold surface.

The secretion and deposition of the small ECM proteoglycan biglycan by hGFs cultured on the scaffolds was visualized on the scaffold surface using immunocytochemistry; biglycan (green), nuclei (blue). Biglycan immunoreactivity was observed intracellularly after 3 days on all three scaffold types. Biglycan appears most prominent on PCL alone scaffolds and appears to be diminished in the presence of increasing concentrations of bFGF. After 7 days of culture, biglycan remains intracellular.

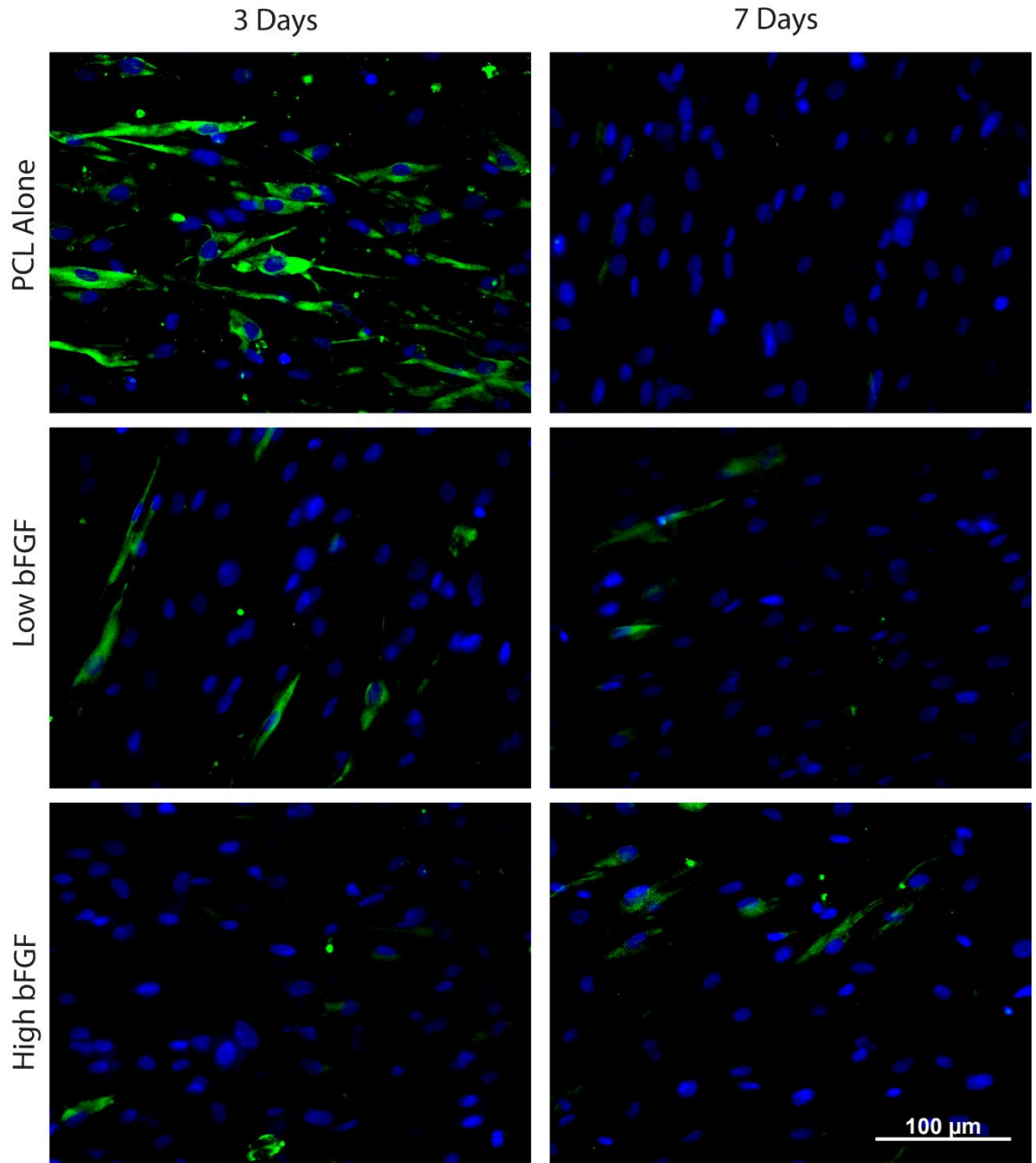
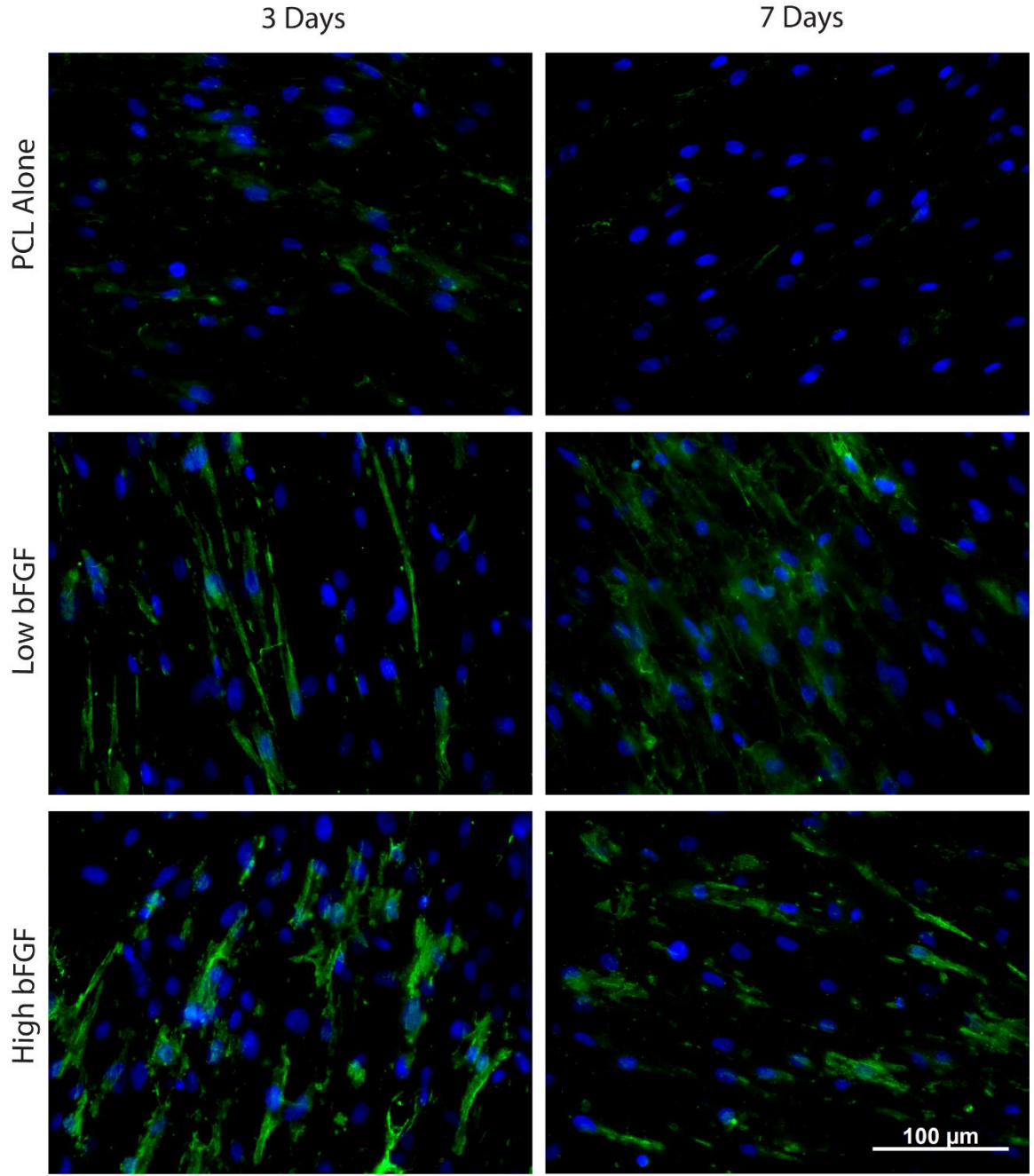


Figure 2.11 - Decorin immunoreactivity on the scaffold surface.

The secretion and deposition of the small ECM proteoglycan decorin by hGFs cultured on the scaffolds was visualized on the surface of the scaffold using immunocytochemistry; decorin (green), nuclei (blue). Decorin is observed on all three scaffold types at day 3 however appears most prominent in the presence of bFGF. Decorin remains associated with the cells after 7 days.



2.3.5 Effect of PCL Electrospun Fibrous Scaffolds Loaded with bFGF Microspheres on Fibronectin and Biglycan mRNA

Relative mRNA levels of fibronectin (Figure 2.12A) and biglycan (Figure 2.12B) were assessed following culture on PCL electrospun scaffolds with and without bFGF microspheres for 3 or 7 days. At both 3 and 7 days, neither fibronectin nor biglycan mRNA levels on scaffolds with low or high bFGF loaded microspheres was observed to be significantly different from that of the PCL alone scaffold (Figure 2.12A, B).

2.3.6 Localization of M2 Macrophages in Rat Gingival Wounds Treated with PCL Electrospun Scaffolds

The next set of experiments were conducted to assess the effect of each scaffold type on the rate of wound healing in a rat model following gingivectomy. We first determined the effect of each scaffold type on inflammatory cells, in particular the M2 or alternatively activated macrophage phenotype, in healing rat gingival tissue following gingivectomy. At 3 days, macrophages were observed primarily in the region of the developing granulation tissue in all treatments (Figure 2.13). At 7 days, M2 macrophage populations appeared more prominent and were observed in the connective tissue around the crest of the alveolar bone in wounds treated with PCL alone and bFGF loaded scaffolds, whereas accumulation was predominantly located underneath the junctional epithelium at the junction of the epithelium with the tooth surface in untreated wounds.

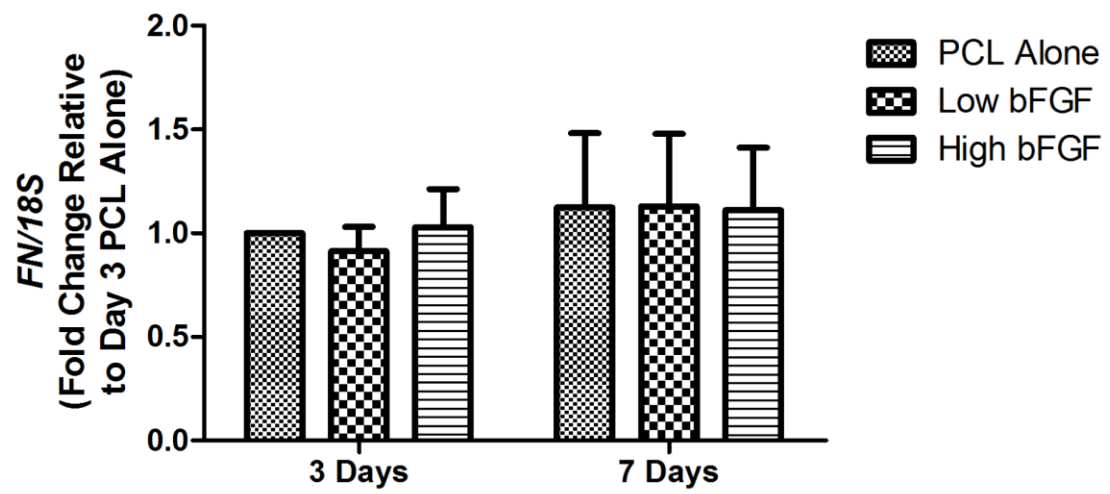
2.3.7 Proliferating Cells in Rat Gingival Wounds Treated with PCL Electrospun Scaffolds

To determine the effect of the scaffolds on the proliferation of cells in healing rat gingival tissue, sections were stained for proliferating cell nuclear antigen (PCNA), a marker of active DNA replication (Figure 2.14A). At 3 days post-wounding, proliferating cells were observed in the connective tissue at the wound edge for all treatments (Figure 2.14B). In addition, proliferating cells were observed in the basal epithelial cell layer in all treatments. At 7 days post-wounding, proliferating cells are evident in the connective tissue and basal epithelial cells in all treatment groups (Figure 2.14B). Proliferating cells were quantified and no significant differences were observed between treatments at 3 or 7 days post-wounding (Figure 2.14C)

Figure 2.12 - Influence of PCL electrospun scaffolds loaded with bFGF on fibronectin and biglycan mRNA levels.

hGFs were seeded and cultured on PCL electrospun fibrous scaffolds with and without bFGF microspheres for 3 or 7 days. RNA was isolated and qRT-PCR was performed using primers specific for *FN* and *BGN*. mRNA levels were normalized to endogenous *18S* ribosomal RNA levels. A) Release of bFGF from the microspheres did not significantly alter the levels of fibronectin mRNA from that of the PCL alone scaffold at 3 or 7 days. B) Release of bFGF from the microspheres did not significantly alter the levels of biglycan mRNA from the PCL alone scaffold at either 3 or 7 days. Graphs represent mean \pm SD of three independent experiments conducted with different patient cells, with three replicates per experiment. Effect of treatments were analyzed via a two-way ANOVA with a Bonferroni post-test to compare differences between means, $p < 0.05$.

(A)



(B)

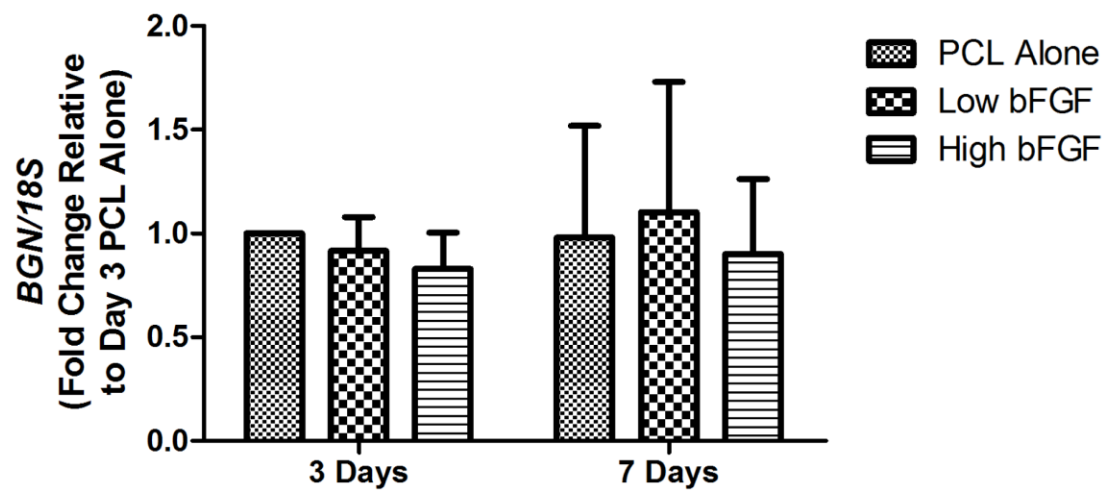
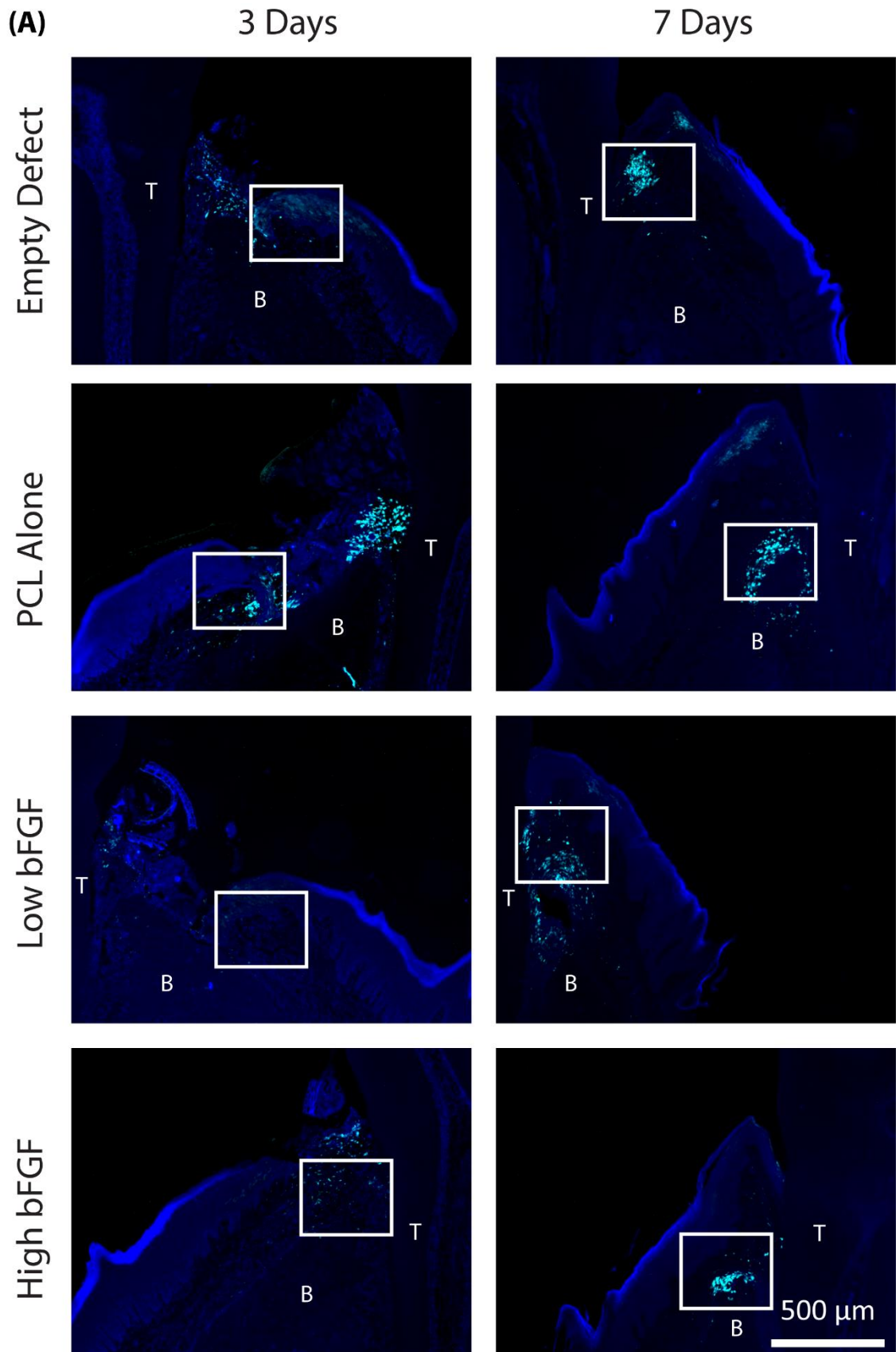


Figure 2.13 - M2 macrophage localization following *in vivo* gingivectomy.

Gingivectomy was performed in rats, and wounds were treated with scaffold membranes of PCL alone, low bFGF loaded, high bFGF loaded or no treatment (empty defect). Localization of arginase 1 (cyan), a marker of M2 macrophages, was visualized with immunohistochemistry using a Cy5 conjugated secondary antibody with Hoechst dye counterstaining (blue) to visualize nuclei in the tissue and imaged with fluorescent microscopy. Images are representative of three individual experiments. A) Arginase 1 is observed in the granulation tissue at 3 days and in the connective tissue of the gingiva at 7 days. In wounds treated with scaffolds, M2 macrophage populations are localized around the crest of the alveolar bone. T – Tooth, B – Alveolar bone. B) Higher magnification images of the areas in A) indicated by white boxes. M2 macrophages become more abundant at 7 days and in wounds treated with all three scaffold types, M2 macrophages are localized around the crest of the alveolar bone, whereas in the empty defect they are localized under the junctional epithelium.



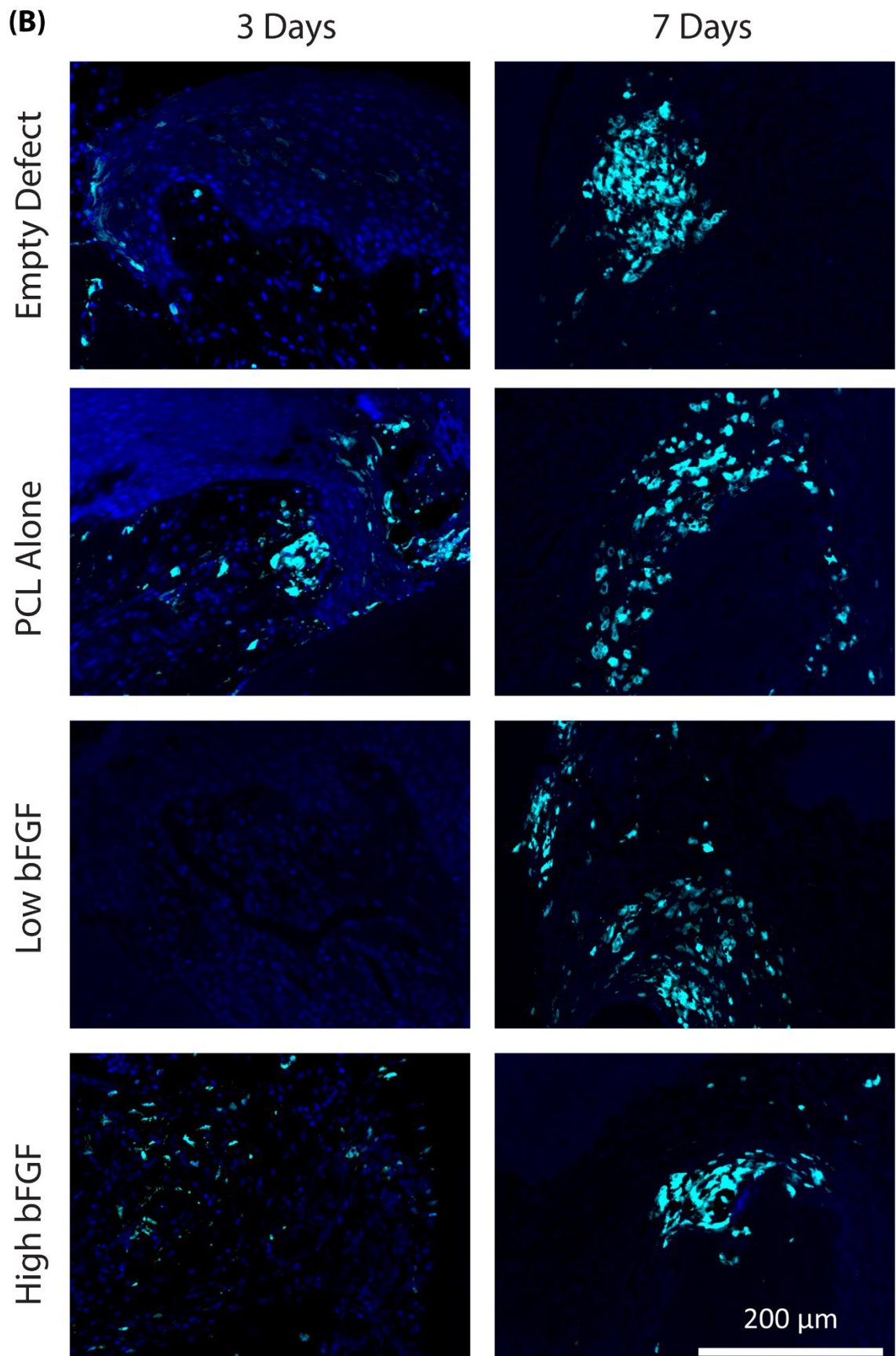
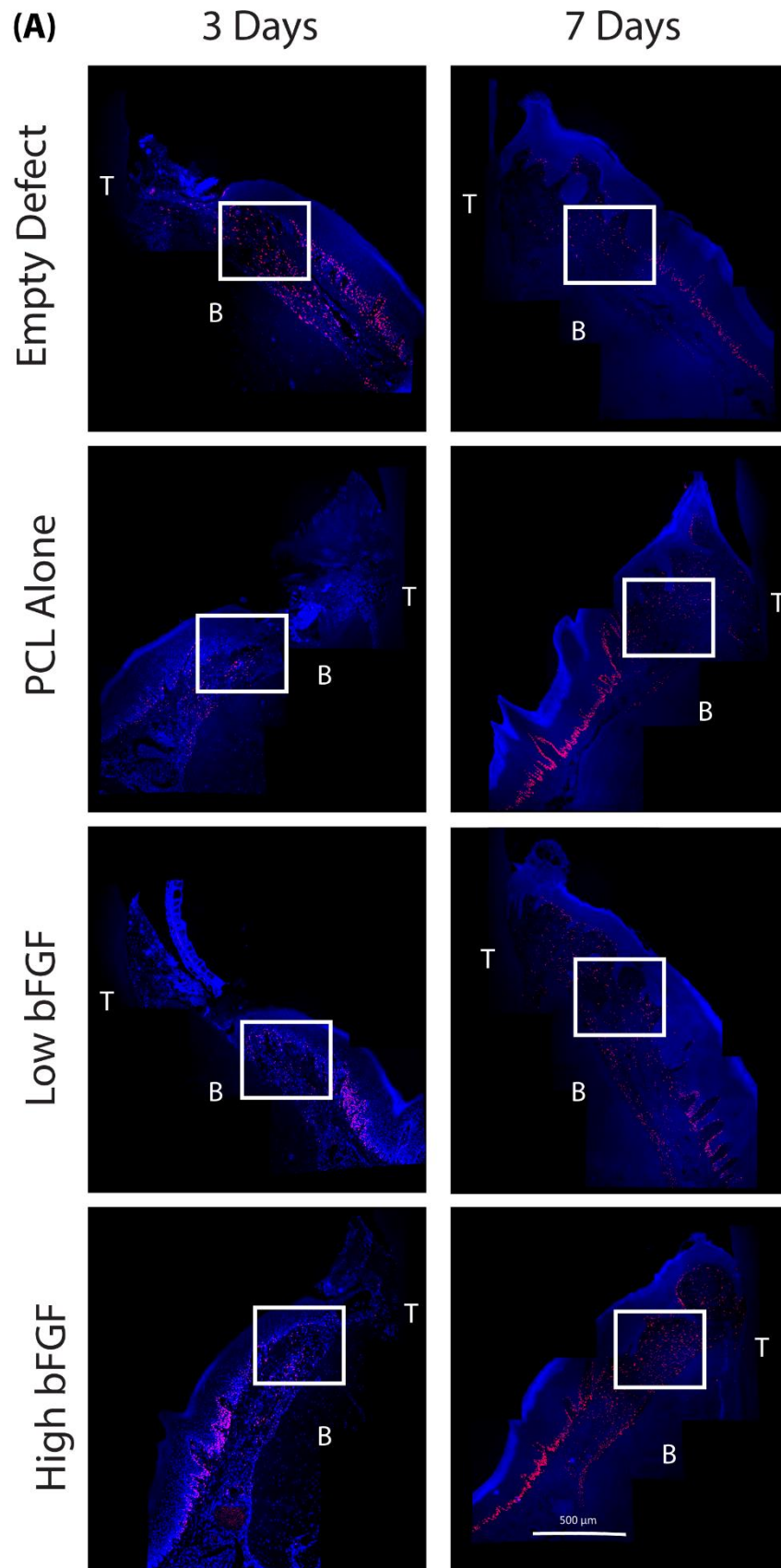
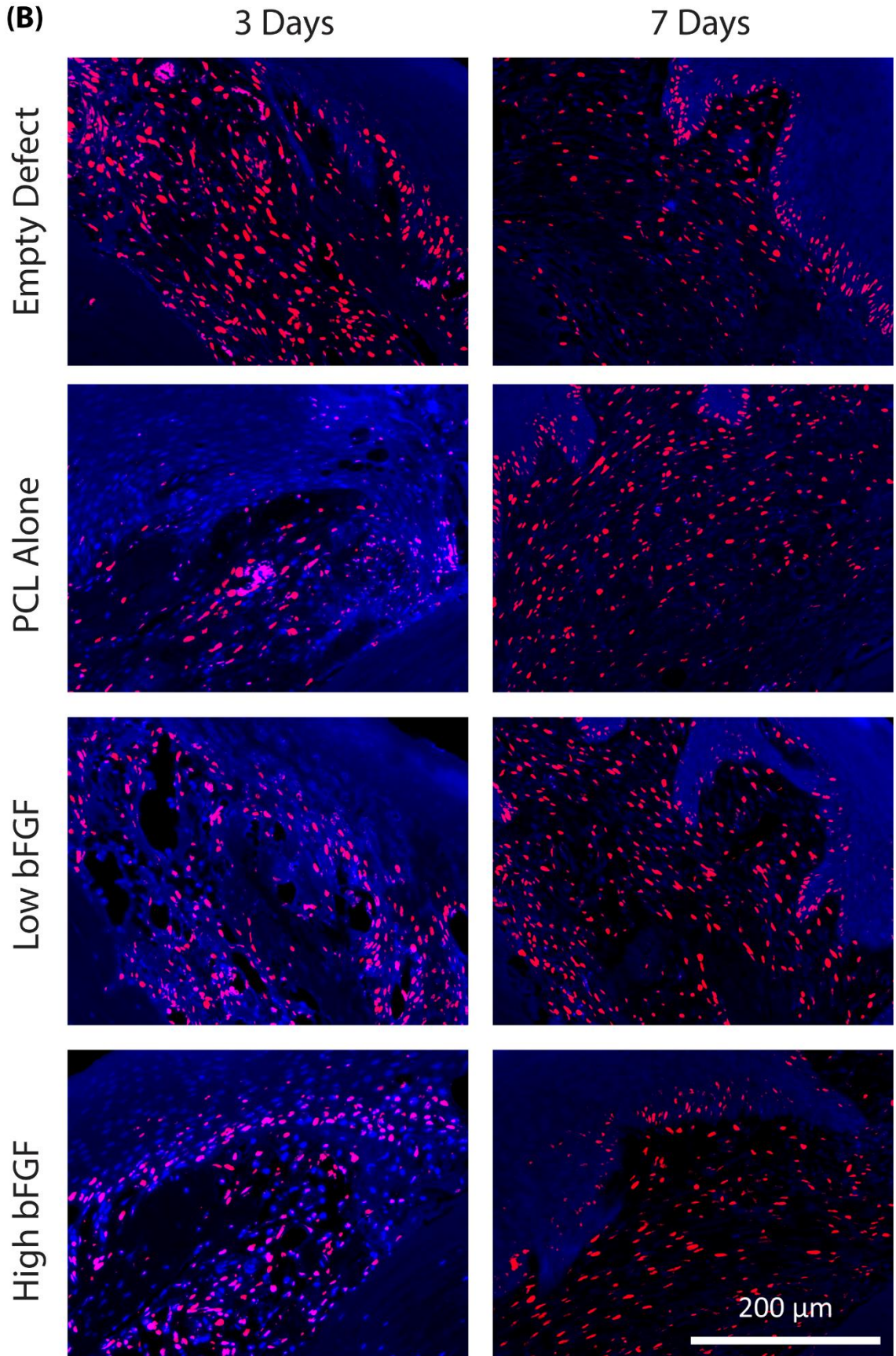


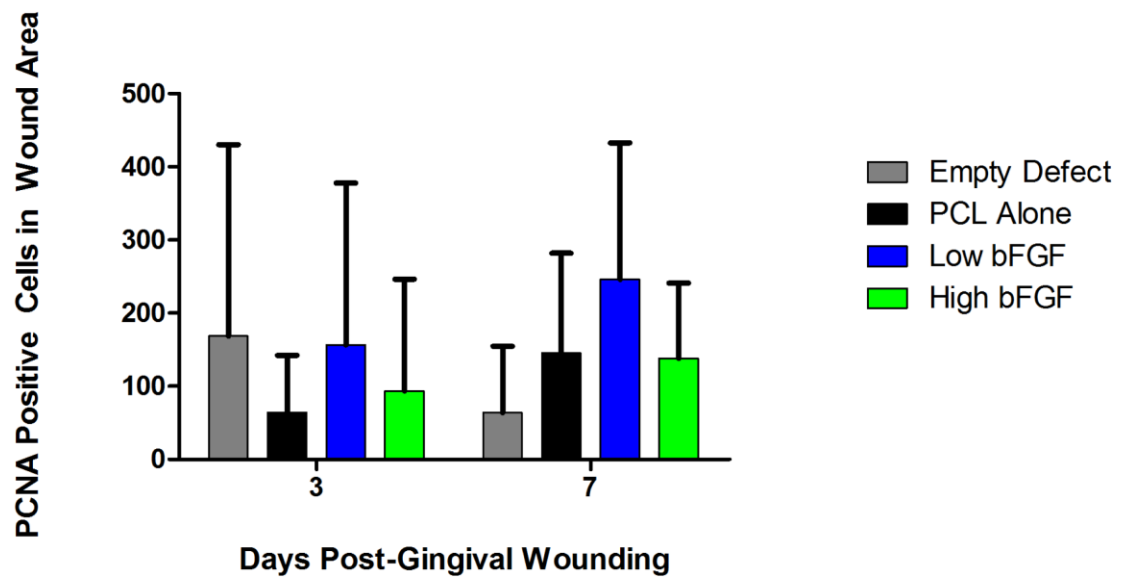
Figure 2.14 - Cell proliferation following *in vivo* gingivectomy.

Gingivectomy was performed in rats, and defects were treated with scaffold membranes of PCL alone, low bFGF loaded, high bFGF loaded or no treatment (empty defect). Sections were labelled with a primary antibody for PCNA and visualized with an appropriate Cy5 conjugated secondary antibody (red) with Hoechst dye counterstain (blue) to visualize nuclei in the tissue. Images are representative of three independent experiments. A) Proliferating cells were observed in the connective tissue and basal epithelial layer for all treatments at both 3 and 7 days post-wounding. T – Tooth, B – Alveolar bone. Scale bar = 500 μm . B) Higher magnification images of the areas in A) indicated by white boxes. Proliferating cells are evident in the connective tissue and basal epithelial cell layer at both 3 and 7 days for all treatments. C) The number of PCNA positive cells in the wound was quantified at 3 and 7 days post-wounding and plotted as mean \pm SD of three independent experiments. Two-way ANOVA with a Bonferroni post-test was used to compare means. No significant difference in the number of PCNA positive cells in the healing wounds were observed between treatments at either 3 or 7 days.





(C)



2.3.8 Myofibroblasts in Rat Gingival Wounds Treated with PCL Electrospun Scaffolds

Myofibroblasts in healing rat gingival tissue were visualized by immunostaining for α -SMA and identified as α -SMA positive fibroblasts in the connective tissue not in the vasculature (Figure 2.15A, B, Appendix K). Myofibroblasts were observed in the wound area at 3 days for all treatments and became more abundant at 7 days for all treatments (Figure 2.15C).

2.3.9 Collagen Deposition in Rat Gingival Wounds Treated with PCL Electrospun Scaffolds

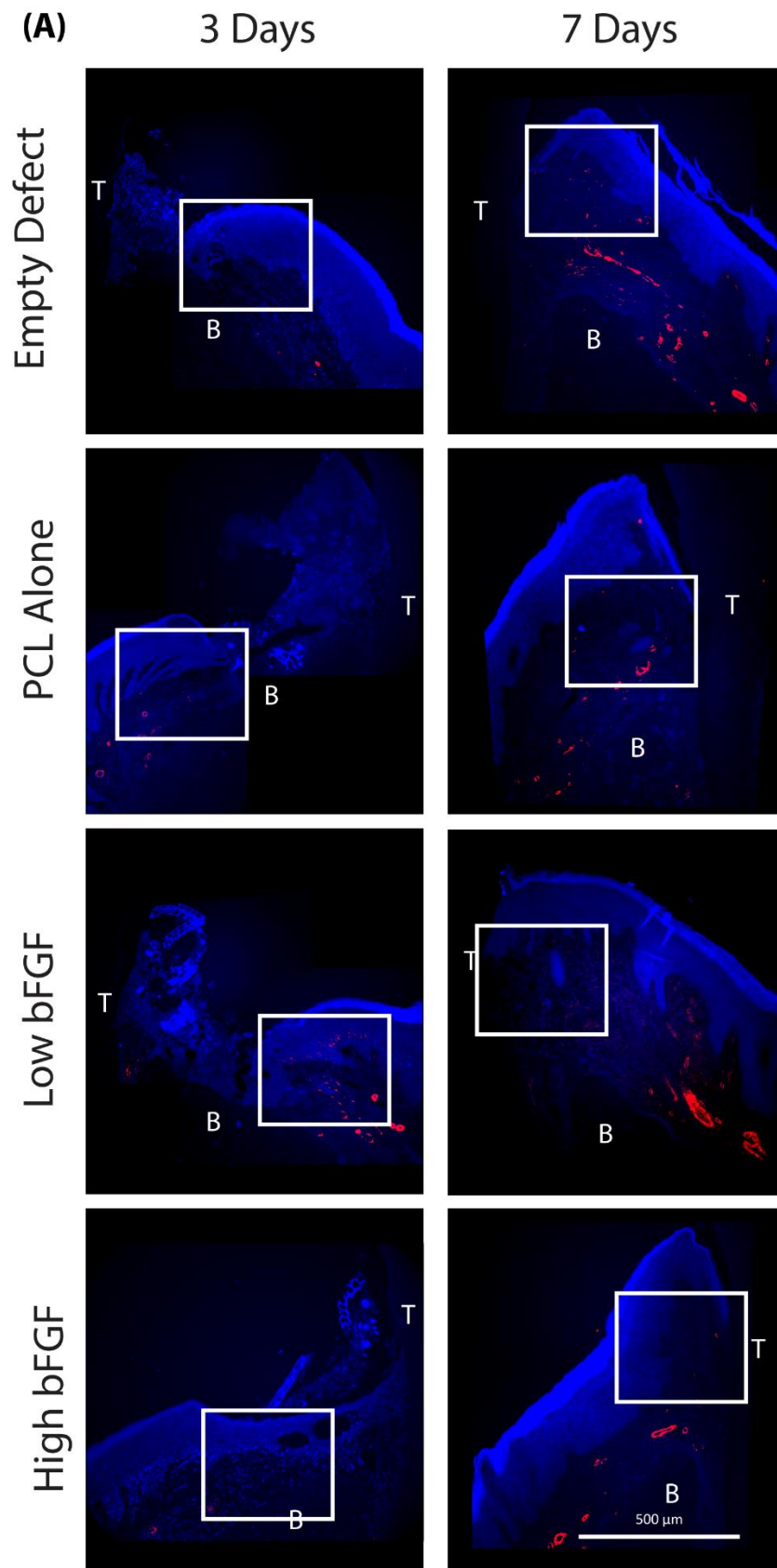
To visualize the deposition of collagen in healing rat gingival tissue following gingivectomy, sections were stained with Van Gieson's stain (Figure 2.16A, B) and Masson's trichrome (Figure 2.16C, D). In addition, collagen was visualized in uninjured tissue and immediately following gingivectomy (Appendix J). At day 3, the original wound margin is visible using both stains as indicated by the termination of the pre-existing thick collagen fibers in the connective tissue. At 7 days, dense collagen accumulation is noted in the newly formed connective tissue of untreated wounds and wounds treated with scaffolds containing bFGF. Black arrows indicate areas of dense collagen accumulation. In the high bFGF treated wound collagen fibers are seen to extend into the free gingiva.

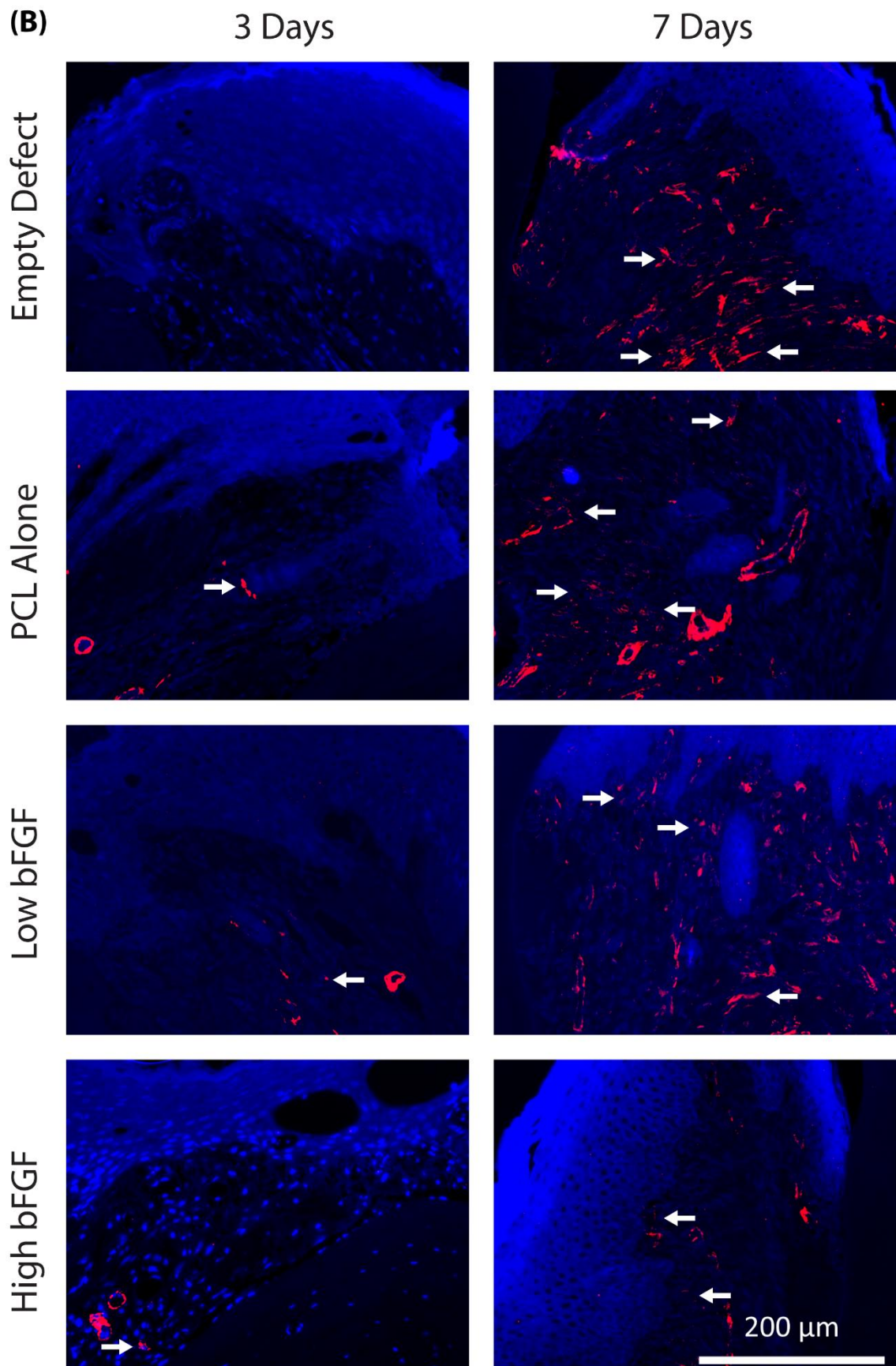
2.3.10 Connective Tissue Area in Rat Gingival Wounds Treated with PCL Electrospun Scaffolds

Gingival wounds were assessed at 3 and 7 days post-wounding to quantify the amount of newly formed connective tissue in the wound area (Figure 2.17A). 3 days post-wounding granulation tissue was observed in the wound area for all scaffold treatments and the empty defect (Figure 2.17B). At 7 days, the general architecture of the gingival connective tissue appeared to be restored in all treatment groups (Figure 2.17A). Connective tissue area was quantified and no difference was observed between treatment groups (Figure 2.17B).

Figure 2.15 - Myofibroblast populations following *in vivo* gingivectomy.

Gingivectomy was performed in rats, and defects were treated with scaffold membranes of PCL alone, low bFGF loaded, high bFGF loaded or no treatment (empty defect). A) Sections were labelled with a primary antibody for α -SMA and visualized with an appropriate Cy5 conjugated secondary antibody (red) with Hoechst dye counterstain (blue) to visualize nuclei in the tissue. T – Tooth, B – Alveolar bone. Scale bar = 500 μ m. B) Higher magnification images of the areas in A) indicated by white boxes. The number of α -SMA positive myofibroblasts not associated with vasculature in the wound area were quantified at 3 and 7 days post-wounding and plotted as mean \pm SD of three independent experiments. Two-way ANOVA with Bonferroni's post-test was used to compare means. No significant difference in the number of myofibroblasts in the healing wounds were observed between treatments at either 3 or 7 days.





(C)

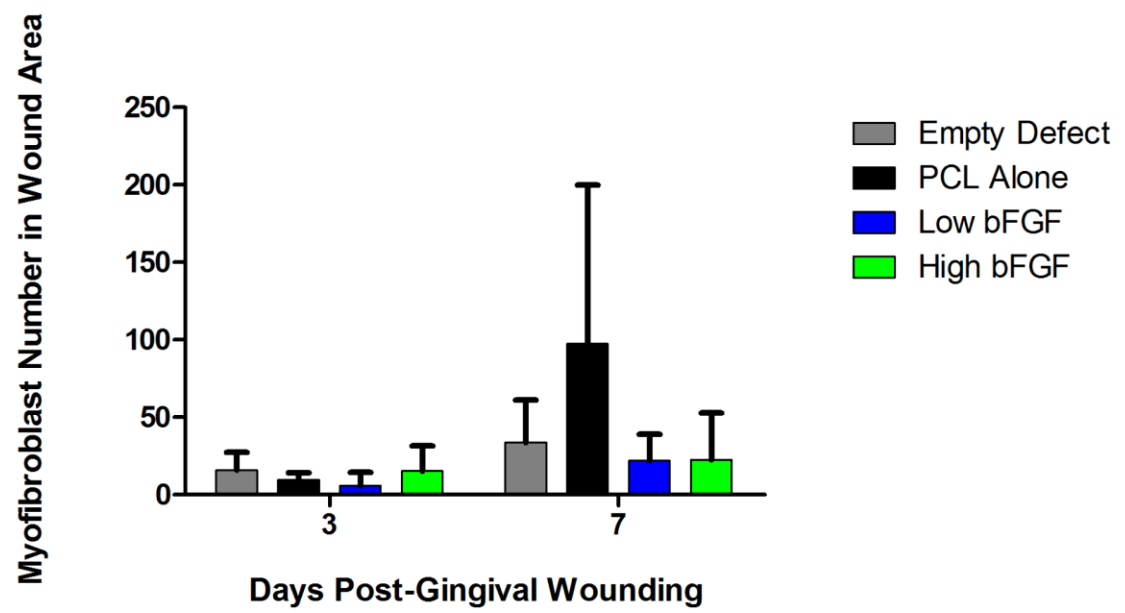
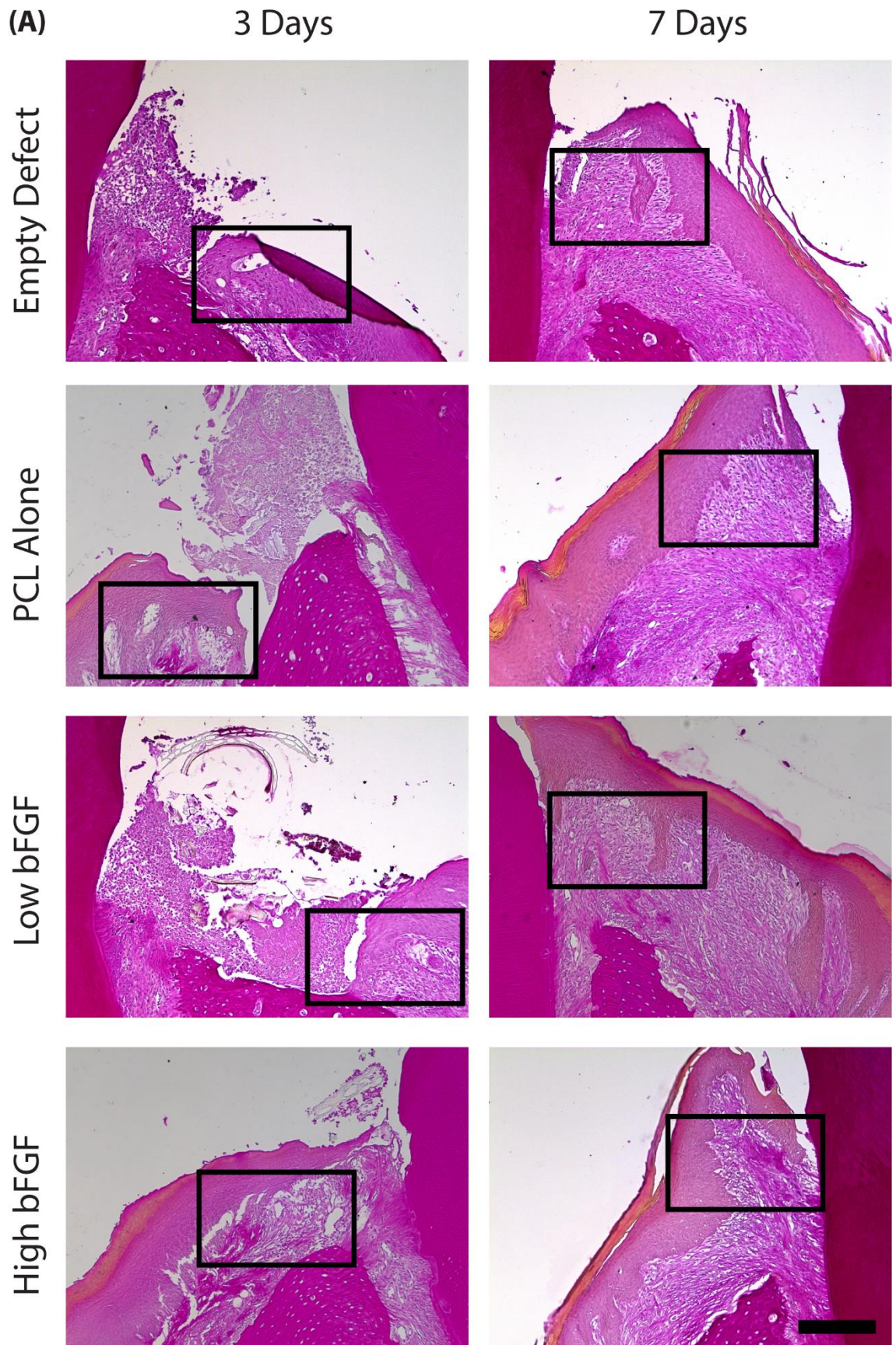
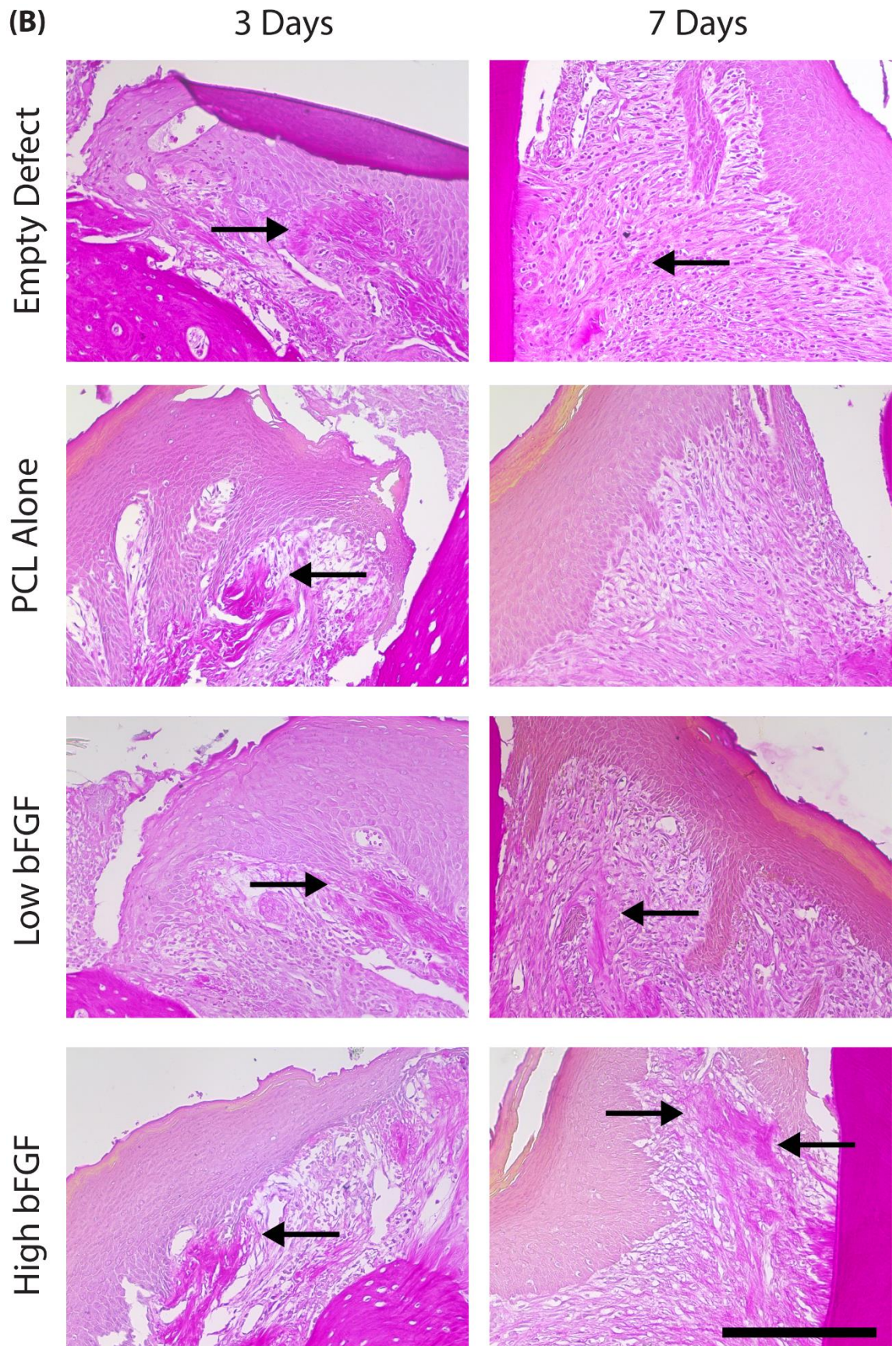
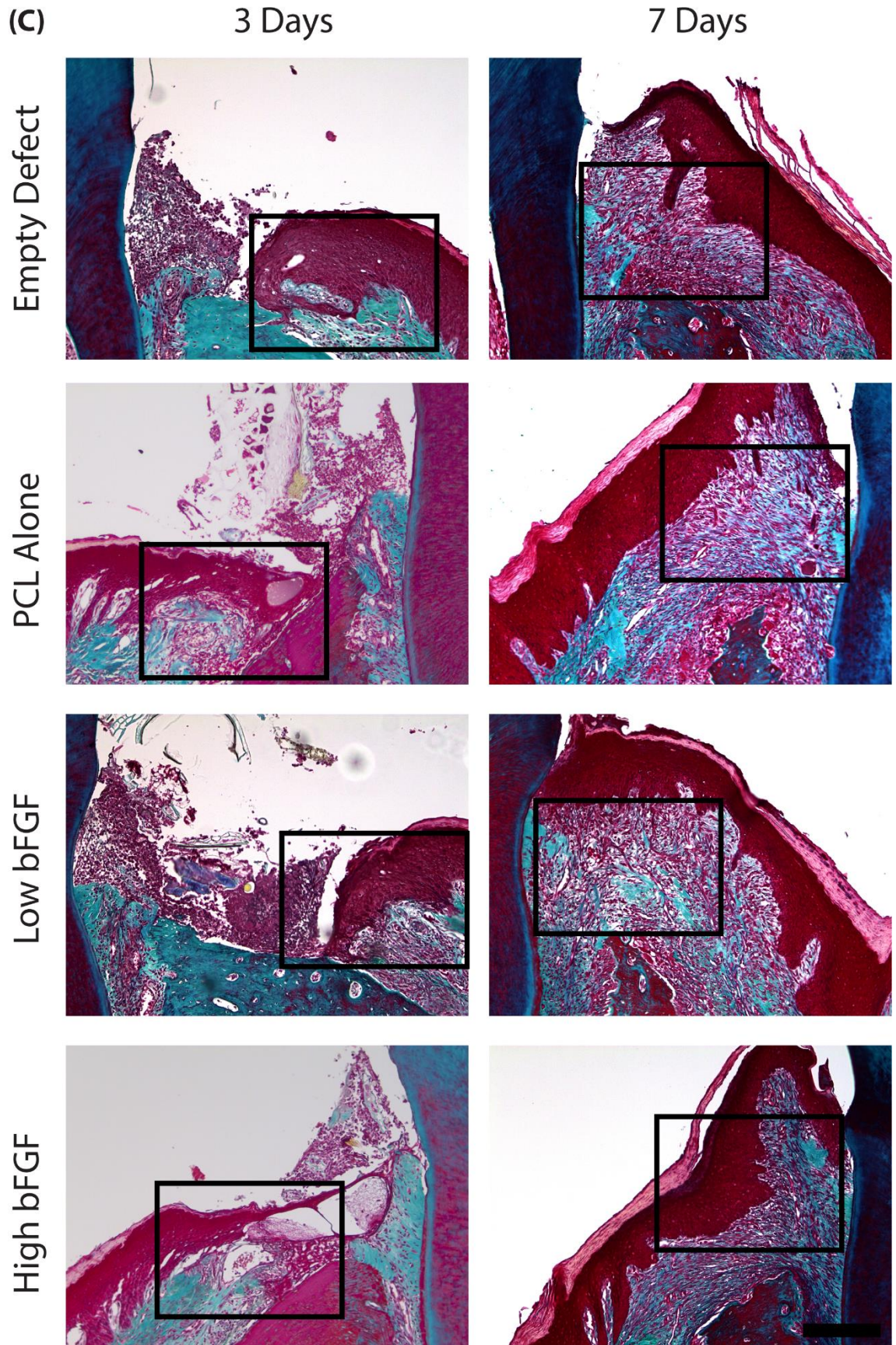


Figure 2.16 - Collagen deposition following *in vivo* gingivectomy.

Gingivectomy was performed in rats, and defects were treated with scaffold membranes of PCL alone, low bFGF loaded, high bFGF loaded or no treatment (empty defect). A) Collagen was visualized at 3 and 7 days post-gingivectomy using Van Gieson's staining (pink). B) Higher magnification images of the areas indicated in A) by the black boxes. C) Masson's trichrome staining was used to visualize collagen (blue) in the healing rat gingival wounds. D) Higher magnification images of the areas indicated in C) by the black boxes. Images are representative of three independent experiments. Scale bars = 200 μm . At day 3 for all treatments, the boundary of the created wounds is visible as indicated by the termination of the pre-existing dense collagen fibers in the gingival connective tissue, labelled with black arrows [B), D)]. 7 days post-wounding, areas of dense collagen fibers in the newly formed tissues of the untreated and bFGF scaffold treated wounds were visible, as indicated by black arrows [B), D)].





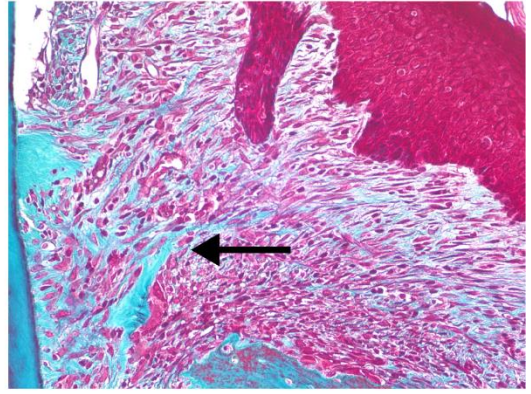
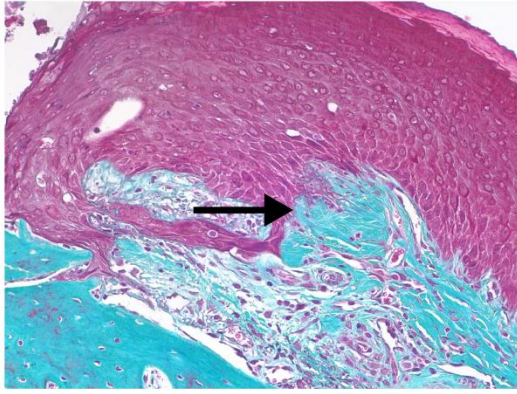


(D)

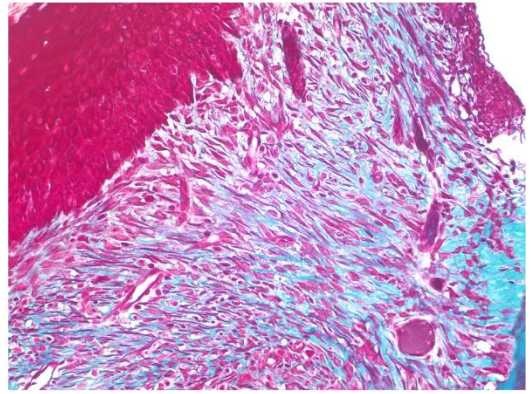
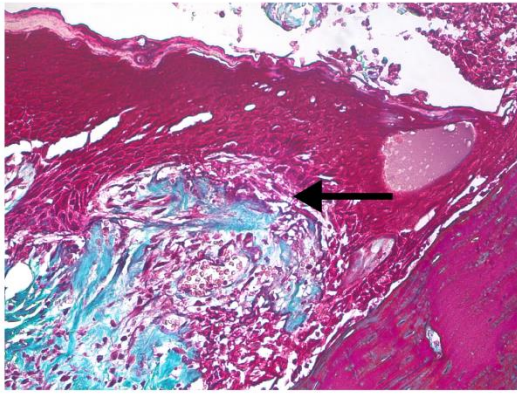
3 Days

7 Days

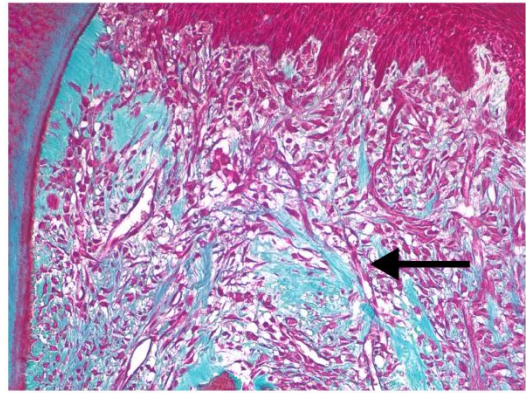
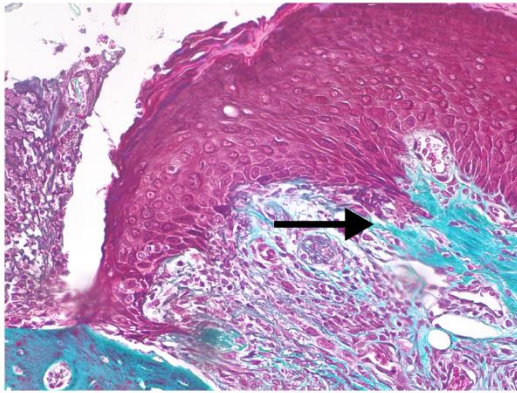
Empty Defect



PCL Alone



Low bFGF



High bFGF

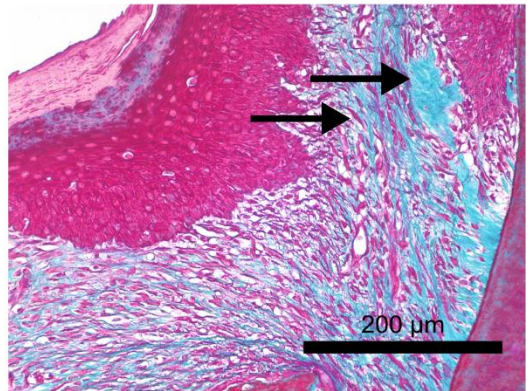
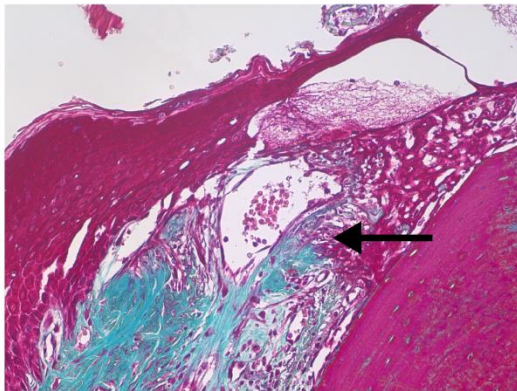
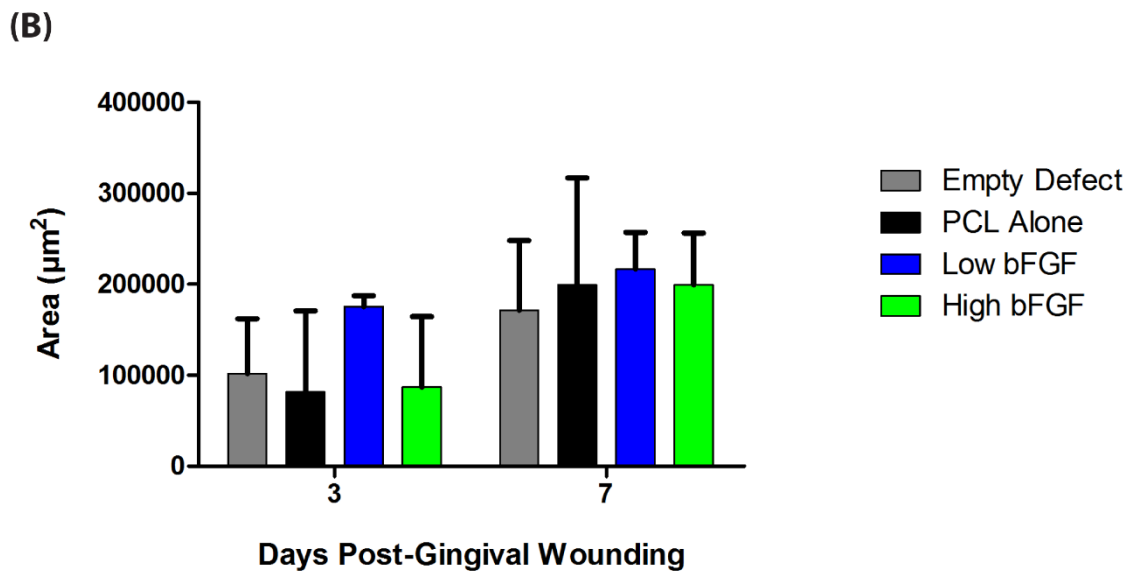
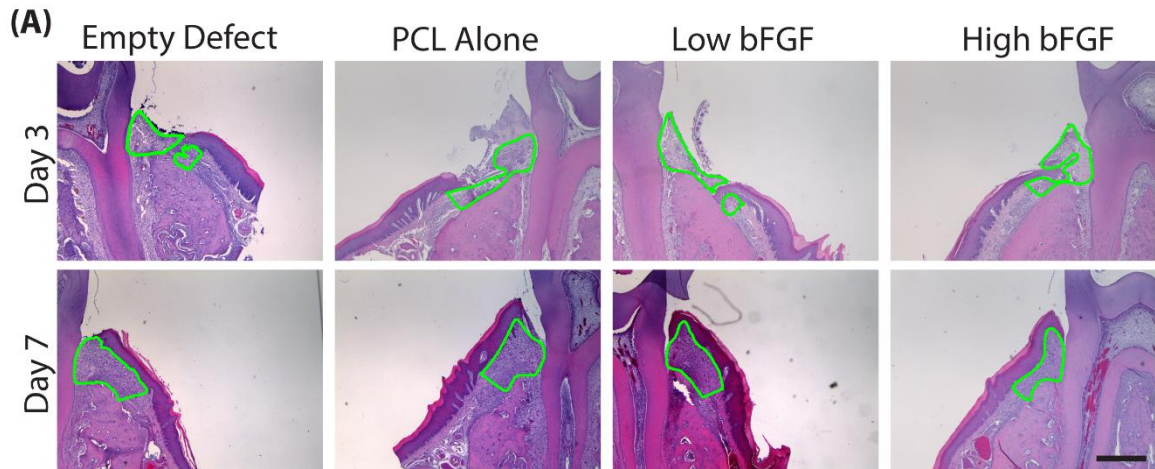


Figure 2.17 - Connective tissue area following *in vivo* gingivectomy.

Gingivectomy was performed in rats, and defects were treated with scaffold membranes of PCL alone, low bFGF loaded, high bFGF loaded or no treatment (empty defect). A) Area of newly formed tissue in the gingival connective tissue was quantified from H&E stained histological sections at 3 and 7 days post-wounding. Solid green line indicates the quantified area of newly formed tissue. Scale bar = 500 μm . B) Newly formed tissue area was quantified and plotted as mean \pm SD of three individual experiments. Newly formed tissue was observed in the wound area at day 3 for all treatments with increased tissue area observed at day 7. Two-way ANOVA with Bonferroni's post-test was used to compare means. No significant difference in regenerated connective tissue area was seen between treatments.



2.3.11 Epithelial Migration in Rat Gingival Wounds Treated with PCL Electrospun Scaffolds

The distance the epithelium had migrated from the original wound location was measured in the healing rat gingival tissue from H&E stained sections (Figure 2.18A). At 3 days post-gingivectomy, the epithelium was observed to have migrated towards the tooth from the location of the original wound in all treatment groups (Figure 2.18B). Epithelial migration increased with time and was greater at 7 days than at 3 days for all treatments. At day 7 the epithelium in all treatment groups was observed to contact the tooth (Figure 2.18A).

2.3.12 Biologic Width of Rat Gingival Wounds Treated with PCL Electrospun Scaffolds

Histomorphometric analysis of H&E stained rat gingival wound sections was conducted to determine the biologic width of the healing tissue at 7 days, as at 3 days none of the wounds were reepithelialized (Figure 2.19A). Connective tissue attachment was measured from the crest of the alveolar bone to the most coronal attachment of connective tissue to the tooth. No statistically significant difference in connective tissue attachments between treatments was observed (Figure 2.19B).

Junctional epithelium length was measured as the second component of the biologic width of the gingiva. A junctional epithelium was present for all treatments (Figure 2.19A). No statistically significant difference in the length of the junctional epithelium was observed between treatments (Figure 2.19C).

The biologic width of the gingiva was calculated by the addition of the connective tissue attachment to the junctional epithelium length. Biologic width between treatments was not significantly different at day 7 and all groups were observed to have a biological width similar to that of healthy, uninjured gingival tissue (Figure 2.19D).

Figure 2.18 - Epithelium length following *in vivo* gingivectomy.

Gingivectomy was performed in rats, and defects were treated with scaffold membranes of PCL alone, low bFGF loaded, high bFGF loaded or no treatment (empty defect). A) The length of the epithelium was measured from the original wound from H&E stained histological sections at 3 and 7 days post-wounding. Solid green line indicates distance migrated. Scale bar = 500 μm . B) Migration distance was measured and plotted as mean \pm SD of three individual experiments. The epithelium migrated from the original wound towards the tooth at day 3 with epithelial migration distance increasing at day 7 for all treatments. Two-way ANOVA with Bonferroni's post-test was used to compare means. No significant difference in epithelial migration distance was seen between treatments at 3 or 7 days.

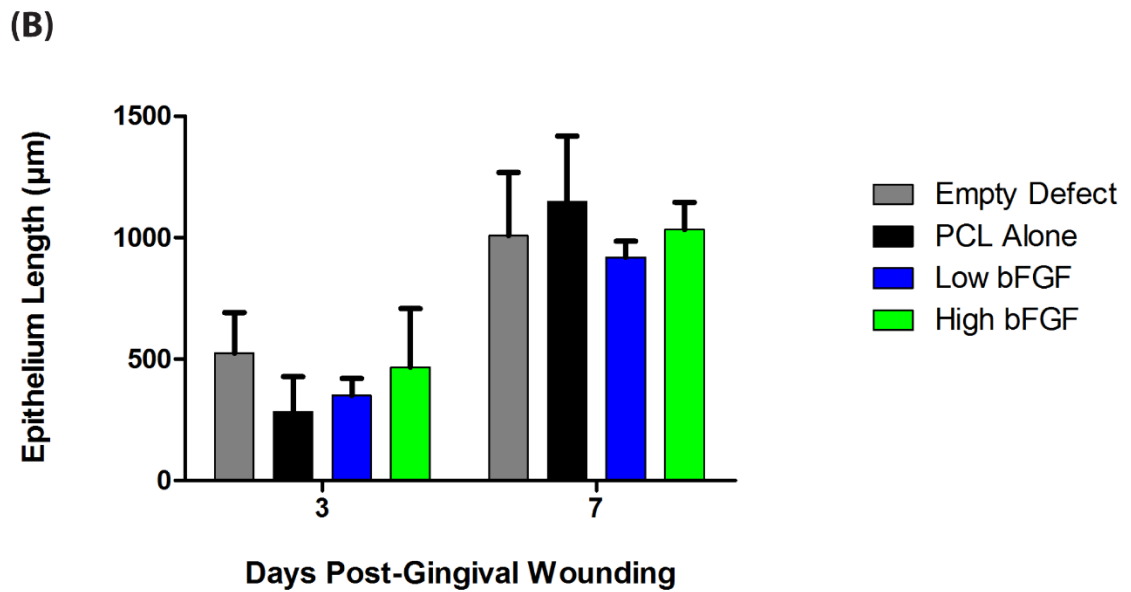
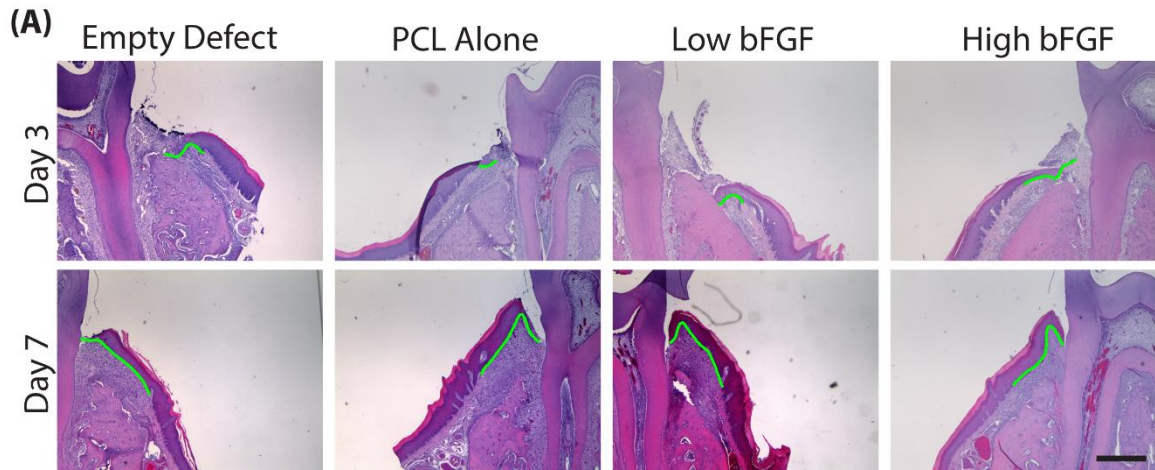
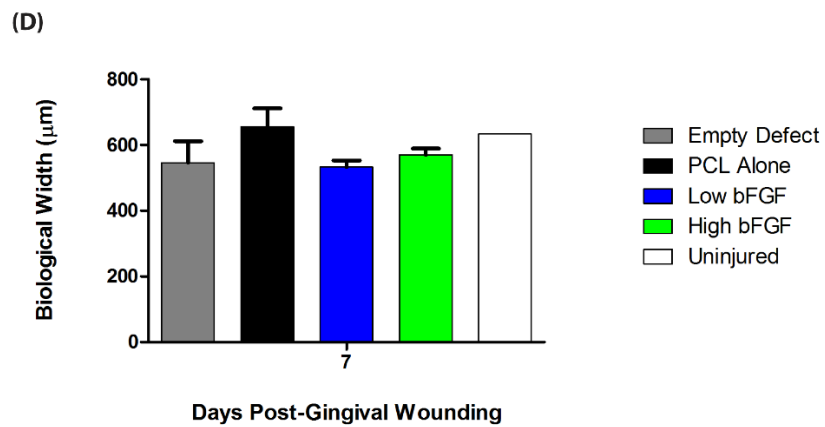
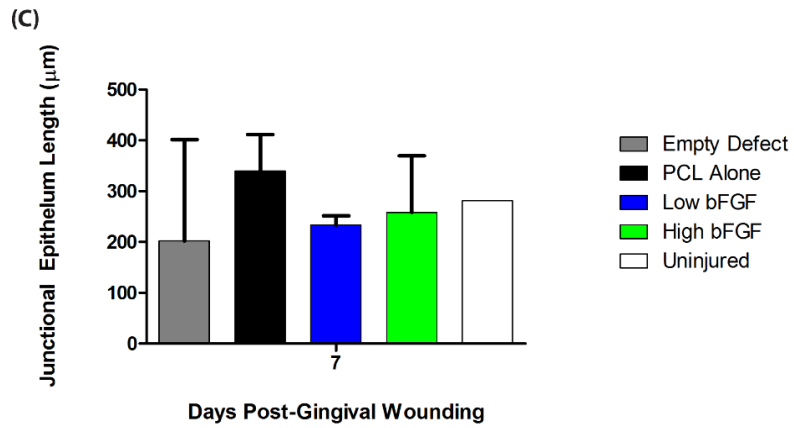
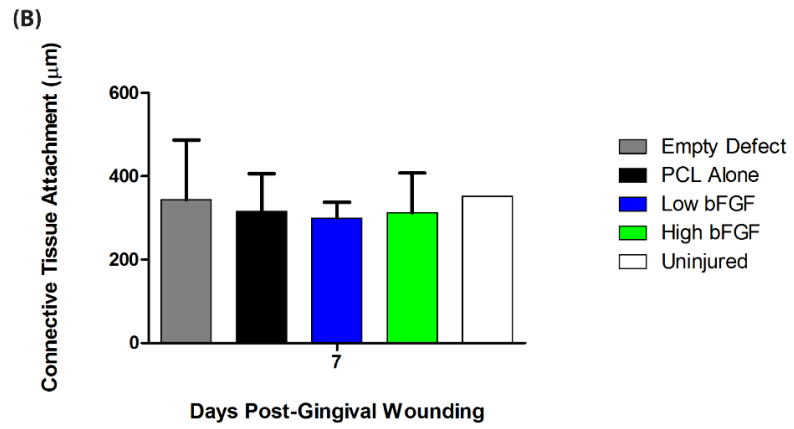
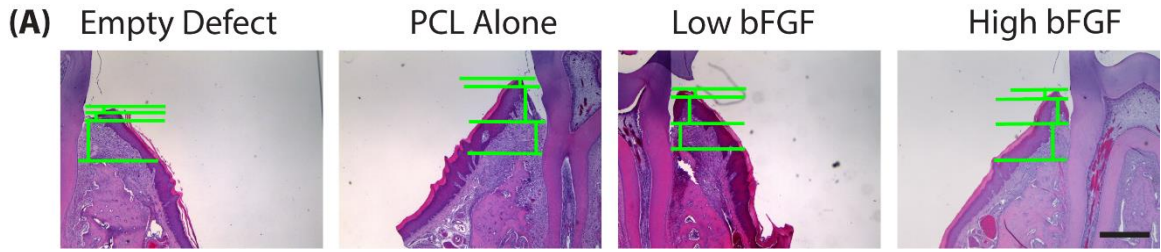


Figure 2.19 - Biologic width measurement following *in vivo* gingivectomy.

Following gingivectomy in rats, defects were treated with scaffold membranes of PCL alone, low bFGF loaded, high bFGF loaded or no treatment (empty defect). A) Biologic width measurements were made from H&E stained histological sections at 7 days post-wounding as at 3 days the wounds were not reepithelialized. Horizontal solid green lines indicate demarcations between measured components as outlined in the methods. Measured distances are indicated by vertical solid green lines on each section. Scale bar = 500 μm . B) Connective tissue attachment was measured and plotted as mean \pm SD of three individual experiments. One-way ANOVA with Kruskal-Wallis post-test was used to compare means. Connective tissue attachment was observed at 7 days for all treatments with no significant difference between treatments. C) Junctional epithelium length was measured and plotted as mean \pm SD of three individual experiments. One-way ANOVA with Kruskal-Wallis post-test was used to compare means. At day 7 a junctional epithelium was present for all treatments with no significant difference in length between treatments. D) Biological width was calculated as the sum of connective tissue attachment and junctional epithelium length and plotted as mean \pm SD of three independent experiments. One-way ANOVA with Kruskal-Wallis post-test was used to compare means. No significant difference in biological width was observed between treatments.



2.4 Discussion

GTR employs a cell occlusive barrier membrane to prevent the oral epithelium migrating along the tooth root into periodontal defects, precluding connective tissue attachment to the tooth (Karring, Nyman et al. 2000, Polimeni, Xiropaidis et al. 2006). The use of an occlusive barrier membrane for GTR is not optimal as it physically separates the periodontal defect from the gingival connective tissue, the latter representing a rich source of vascular beds (Bartold, Walsh et al. 2000) and potentially cell populations such as pericytes and mesenchymal progenitor cells which could contribute significantly to periodontal healing (Fournier, Larjava et al. 2013). Therefore the development of membranes that would allow gingival connective tissue integration, while maintaining a barrier to the oral epithelium, would be extremely advantageous. In this study, using hGFs, human gingival explants and *in vivo* rat models, we investigated the efficacy of a porous electrospun fibrous PCL scaffold with microspheres containing bFGF as a potential new material for periodontal GTR applications.

We utilized polycaprolactone (PCL) as the base polymer for the modified barrier membrane for several key reasons. Firstly, it is FDA-approved, which allows for faster clinical translation, and it is already used as a root-end filling material in endodontics (de Souza Filho, Gallina et al. 2012). Secondly, as we have done, it can readily be electrospun into fibers to produce a scaffold rather than an impermeable membrane. In addition, although it is not biodegradable in physiological systems, it is bioresorbable through hydrolysis of its ester linkages, which typically occurs over a 12-month period (Woodruff and Huttmacher 2010). As periodontal tissues are slow to regenerate, hydrolysis over a 12-month period is advantageous.

To assess the efficacy of the scaffold, we first investigated the *in vitro* response of hGFs to the scaffolds. SEM revealed that hGFs attached to the fibers of all scaffold types within 1 hour following seeding on the scaffold surface. The observation of broad cell extensions and cell spreading indicates strong attachment to the scaffold fibers as non-adherent fibroblasts display a more rounded morphology (Rosen and Culp 1977). Both cell alignment and orientation are strongly influenced by the underlying topography, in this case, multiple fibers under each cell (Brunette, Kenner et al. 1983, Brunette 1986,

Hamilton, Oakley et al. 2009). Cellular orientation in response to aligned electrospun fibers has been noted for several different cell types and scaffold materials (Baker and Mauck 2007, Murugan and Ramakrishna 2007, Nisbet, Forsythe et al. 2009, Shang, Yang et al. 2010). Fiber diameter is a significant factor influencing fibroblast alignment with the greatest degree of alignment observed along fibers of 10 μm diameter (Hwang, Park et al. 2009). The PCL electrospun scaffolds used in this study had a fiber diameter of $7.4 \pm 2.0 \mu\text{m}$ (Guo, Elliott et al. 2012) and although smaller than 10 μm , still influence hGF morphology. The significance of cell alignment is considerable, as it is known to alter downstream cellular processes including proliferation and differentiation, and matrix deposition (Chou, Firth et al. 1995, Glass-Brudzinski, Perizzolo et al. 2002).

In gingival wound healing, fibroblasts proliferate and migrate into the wound site. PCL electrospun scaffolds with and without bFGF support an increase in hGF population growth *in vitro* as indicated by an increase in cell number on all three scaffold types tested, in a temporal manner. bFGF is a potent mitogen of fibroblast cells (Gospodarowicz 1974) and the addition of bFGF microspheres to the scaffold significantly increases the cell number of hGFs cultured on the scaffold. This suggests that the addition of bFGF microspheres to PCL electrospun scaffolds enhances the scaffold bioactivity. Variability in the degree of cell number increase was observed between patients, which could be attributed to donor patient age (Bartold, Boyd et al. 1986, Caceres, Oyarzun et al. 2014). Future studies will focus on an increased analysis of cells isolated from patients of different ages. As gingival recession and periodontal disease predominantly affect more elderly populations, it will be important to quantify if bFGF release would be effective in the induction of proliferation in cells from patients in this age range.

As they enter the wound site, hGFs contribute to granulation tissue formation and synthesize ECM components to replace the provisional matrix (Aukhil 2000, Hakkinen, Uitto et al. 2000). Fibronectin is the first component of granulation tissue secreted by fibroblasts (Hakkinen, Uitto et al. 2000) and is found in the gingival tissue in health (Connor, Aubin et al. 1984, Steffensen, Duong et al. 1992). hGFs cultured on all three scaffold types were observed to secrete fibronectin onto the scaffold surface after 3 days

and 7 days of culture on the scaffold. Fibronectin deposition was organized predominantly in the direction of the cell long axis. It has been previously demonstrated that fibronectin deposition can be altered by variations in substratum topography, such that our observations are not unexpected (den Braber, de Ruijter et al. 1998). Fibronectin mRNA transcript levels were not significantly altered by the release of bFGF from the microspheres on the PCL electrospun scaffolds, which was unexpected as bFGF has been shown to increase fibronectin expression in a dose-dependent manner (Xie, Bian et al. 2008).

Decorin, a small leucine-rich proteoglycan, is a major component of gingival connective tissue where it associates with type I collagen fiber bundles (Hakkinen, Oksala et al. 1993). Decorin is secreted by fibroblasts in culture where it associates with fibronectin (Schmidt, Robenek et al. 1987). Decorin production by hGFs cultured on PCL electrospun scaffolds was visible at 3 days and was most notable on the scaffold containing high bFGF microspheres. Following 7 days of culture, decorin production appeared localized to the cells, suggesting cells are not actively secreting the proteoglycan. This is consistent with previous findings that bFGF upregulates decorin gene expression in dermal fibroblasts (Tan, Hoffren et al. 1993). Finally, we assessed deposition of biglycan, a small leucine-rich proteoglycan that makes up a minor component of human gingival connective tissue where it associates with type I collagen fiber bundles in the deep connective tissue (Hakkinen, Oksala et al. 1993, Alimohamad, Habijanac et al. 2005). Biglycan production by hGFs on PCL electrospun scaffolds was evident after 3 and 7 days and appeared to be attenuated in a bFGF dose-dependent manner. Biglycan gene expression of hGFs cultured on the electrospun PCL scaffolds was not significantly altered by the release of bFGF from the microspheres. Interestingly, previous studies have shown that bFGF downregulates biglycan gene expression in dermal fibroblasts *in vitro*, suggesting that gingival fibroblasts may differ in response to bFGF (Tan, Hoffren et al. 1993). Overall, our data demonstrates that PCL scaffolds with or without bFGF support matrix fibrillogenesis, which will be an important determinant of regeneration of the connective tissue.

Ex-vivo gingival explant cultures more closely mimic the *in situ* environment, as cells would be required to migrate through the collagenous ECM of the tissue to enter the scaffold. Therefore, we next investigated whether cells would migrate from explants onto the scaffold and whether this was influenced by the presence of bFGF. SEM analysis demonstrated that cell outgrowth from gingival tissue explants was evident on the surface of all scaffold types. In tissue sections, bFGF release significantly promoted scaffold infiltration by mesenchymal cells (vimentin⁺ cells) compared to PCL alone scaffolds, with increased cell number correlated with higher bFGF concentrations. We chose bFGF primarily because it is a potent chemotactic agent for fibroblast cells (Buckley-Sturrock, Woodward et al. 1989) and based on the increased cell number seen within the scaffolds containing both low and high bFGF, it appears to function when released from the microspheres. However, bFGF is also a potent mitogen for fibroblast cells (Gospodarowicz 1974) and cell proliferation within the scaffold cannot be eliminated as a contributing factor to the increase in cell population in the presence of bFGF microspheres. To investigate the individual contribution of migration and proliferation to scaffold population in future studies, proliferation of cells within the explant tissue will be inhibited using mitomycin C (Tomasz 1995). However, as we hypothesized, mesenchymal cells from the gingival connective tissue are able to infiltrate the scaffolds through the pores.

Oral epithelial cells are known to migrate quickly *in vivo* (Hamilton, Chehroudi et al. 2007). As highlighted previously, conventional GTR membranes are cell-occlusive and are designed to block this aggressive migration into the pocket (Needleman, Worthington et al. 2006). While the scaffolds supported the infiltration of mesenchymal cells, they excluded the infiltration of oral epithelial cells. Oral epithelial cells found at the interface between the scaffold and the explant tissue were observed to migrate along the surface of the scaffold as a sheet with minimal infiltration below the surface of the scaffold. We attribute this to the pore size of the scaffolds ($17.1 \pm 8.3 \mu\text{m}$ with pore size ranging from $6.8 - 47.2 \mu\text{m}$ (Guo, Elliott et al. 2012)). The function of epithelial cells *in vivo* is to form coverings and linings over tissues. *In vitro* epithelial cells tend not to migrate into pitted topographies and rather form coverings over pits with dimensions of $45 \mu\text{m}^2$ openings (Hamilton, Chehroudi et al. 2007). bFGF stimulates the proliferation of

gingival epithelial cells in a dose-dependent manner, however the stimulation is somewhat attenuated in the presence of serum (Takayama, Yoshida et al. 2002). In the current study, epithelial cells did not penetrate scaffolds even in the presence of bFGF release from the microspheres, however on high bFGF loaded scaffolds the epithelial layer appeared larger, likely in a state of hyperproliferation. Both topical and sustained release of bFGF in palatal wound healing *in vivo* has been shown to accelerate wound epithelialization and increase the proliferation of basal epithelial cells (Oda, Kagami et al. 2004, Ayvazyan, Morimoto et al. 2011). The morphology of the healing epithelial layer following topical application of bFGF was found to be morphologically similar to that of the control wounds (Oda, Kagami et al. 2004), however bFGF administration using a sustained method increased the epithelial ridges observed as compared to the control (Ayvazyan, Morimoto et al. 2011). The sustained release of bFGF from the microspheres in the PCL electrospun scaffolds used in this study may account for the observed differences in epithelial sheet thickness from the tissue explants. Of particular significance is the observation that the PCL electrospun scaffold excludes oral epithelial cells. This result has significant implications for membrane design as it demonstrates that it is not necessary for GTR membranes to be completely cell-occlusive to prevent the migration of the oral epithelium. As has been previously demonstrated, the strict occlusion of the gingival connective tissue from a regenerating periodontal defect is not a critical requirement for the successful regeneration of periodontal structures (Wikesjo, Lim et al. 2003); however, occlusion of the oral epithelium is (Linghorne and O'Connell 1950). Our scaffolds accomplish this as indicated by the infiltration of and population by cells of mesenchymal origin while simultaneously maintaining a barrier to oral epithelial cells.

Based on their efficacy *in vitro*, we next assessed each scaffold type in a rat gingivectomy model, with healing responses at 3 and 7 days investigated. The initial stage of wound healing is characterized by an inflammatory response and inflammatory responses are commonly elicited following the implantation of biomaterials (Polimeni, Xiropaidis et al. 2006, Garg, Pullen et al. 2013). The regenerative, alternatively activated M2 phenotype macrophages are typically associated with tissue repair and the polarization of macrophages to the M2 phenotype is influenced by scaffold architecture, therefore we

investigated the M2 macrophage response following treatment with PCL electrospun scaffolds (Fairweather and Cihakova 2009, Garg, Pullen et al. 2013). In all wounds, M2 macrophage populations were prominent in the connective tissue at 7 days post-wounding and were localized under the junctional epithelium in untreated wounds. However, in scaffold treated wounds, M2 macrophage populations were observed around the crest of the alveolar bone, although the presence of bFGF appeared to have no effect on macrophage persistence. Although bFGF is not proinflammatory, studies have shown that under inflammatory conditions in dermal tissues bFGF potentiates the recruitment of inflammatory cells (Zittermann and Issekutz 2006). However, our results are consistent with the observation that the addition of bFGF to a collagen scaffold implanted in rat palatal submucoperiosteal tissue did not alter the inflammatory response. The scaffolds used in this study had a mean pore diameter of $17.1 \pm 8.3 \mu\text{m}$ with pore size ranging from $6.8 - 42.7 \mu\text{m}$ (Guo, Elliott et al. 2012) which has been shown in other studies to be favourable for M2 macrophage polarization in the early inflammatory response (Garg, Pullen et al. 2013). In addition, scaffolds with aligned fibers minimized host response compared to randomly oriented fibers (Cao, McHugh et al. 2010).

We next assessed whether the presence of bFGF within the scaffolds influenced cell proliferation. In the healing gingival tissue, proliferating cells were observed in the epithelium and connective tissue for all treatments at both 3 and 7 days post-wounding. The presence of bFGF at both low and high loading did not significantly alter the number of proliferating cells at either 3 or 7 day post-wounding compared to both the empty defect and the PCL alone scaffold. Since bFGF is a potent mitogen and exhibits stimulatory effects on gingival epithelial cell proliferation, increased cell proliferation in healing rat gingival wounds treated with PCL electrospun scaffolds containing bFGF would be expected (Gospodarowicz 1974, Takayama, Yoshida et al. 2002). The mitogenic effects of bFGF have been demonstrated following topical application to oral mucosa wounds wherein an increase in the number of proliferating basal epithelial cells was noted and at higher concentrations proliferation of cells within the connective tissue was evident (Oda, Kagami et al. 2004). Myofibroblasts, characterized by α -SMA expression, are transiently present during wound healing and contribute to matrix production and contraction, however persistence of myofibroblasts is associated with scar

formation and fibrosis (Shi, Lin et al. 2013). bFGF treatment downregulates α -SMA gene expression and induces apoptosis of both dermal and oral mucosal myofibroblasts (Funato, Moriyama et al. 1997, Funato, Moriyama et al. 1999, Shi, Lin et al. 2013). In the current study, myofibroblasts in the healing rat gingiva treated with PCL electrospun scaffolds were observed at 3 days and became more abundant at 7 days. The presence of bFGF on the scaffolds did not significantly alter the number of myofibroblasts observed in the healing rat gingival wounds. This is unexpected as bFGF induces the apoptosis of myofibroblasts and studies have shown that the addition of bFGF to collagen scaffolds implanted in the submucosal tissue of the rat palate reduce the number of myofibroblasts observed within and around the scaffold at 7 and 14 days following implantation (Funato, Moriyama et al. 1997, Funato, Moriyama et al. 1999, Jansen, van Kuppevelt et al. 2009). It is possible that the scaffolds used in this study may show an effect at a later time point, such as 14 days post-wounding, as myofibroblast differentiation in a healing wound generally occurs around day 6 and populations accumulate until day 15 where myofibroblasts comprise 70% of granulation tissue fibroblasts (Darby, Skalli et al. 1990, Hakkinen, Uitto et al. 2000).

During granulation tissue formation, fibroblasts initially secrete fibronectin which is gradually replaced with a fibrillar type I collagen matrix (Kurkinen, Vaheri et al. 1980, Hakkinen, Uitto et al. 2000). In the present study, we investigated the collagen deposition in rat gingival wounds using histochemical staining. At 7 days post wounding, dense collagen accumulation is observed in the connective tissue of untreated wounds and wounds treated with scaffolds containing bFGF. Studies of healing rat palatal wounds found that treatment with topical bFGF application resulted in the formation of mature collagen fibers in the granulation tissue adjacent to the pre-existing fibers at 7 days post-wounding whereas mature collagen fibers were absent in untreated control wounds suggesting that bFGF may accelerate the maturation of collagen (Oda, Kagami et al. 2004). Studies looking at longer time points of 6 weeks found that following mucoperiosteal denudation of the rat palate, collagen accumulation was decreased in the submucosa of the gingiva in wounds receiving a topical application of bFGF (Choi, Kawanabe et al. 2008). In this study, collagen deposition was evident in the gingival connective tissue at 7 days and future studies using longer time points would be

of interest to investigate collagen deposition in response to scaffold membrane treatment following tissue remodeling.

Treatment with the scaffold membranes did not have a significant effect on the area of granulation tissue formed at 3 days, the area of connective tissue regenerated at 7 days or the length of the neoformed epithelium at 3 or 7 days. This is unexpected as studies have shown topical bFGF applications to rat palatal wounds increases the rate of granular tissue formation and reepithelialization of these wounds (Oda, Kagami et al. 2004). However, the concentration used for topical application was greater (0.5 and 3.0 μg) than that of the scaffold used (~25 ng cumulative release over 7 days from a 50 mg piece of high bFGF loaded scaffold (Guo, Elliott et al. 2012)). In this study, treatment with PCL scaffold membranes did not significantly affect the biologic width of the reepithelialized wound at day 7. Taken together, these results suggest that the scaffolds are biocompatible for use as a GTR membrane.

bFGF exerts its effects in a dose-dependent manner (Gospodarowicz 1974, Takayama, Murakami et al. 2001, Ayvazyan, Morimoto et al. 2011, Ma, Wang et al. 2012) therefore this study looked at two loading doses of bFGF on the PCL scaffolds. *In vitro*, high bFGF loading appeared to be more effective for population of the scaffolds by mesenchymal cells from gingival tissue explants as compared to the low bFGF loading dose, whereas experiments in which a finite cell number was seeded onto the scaffolds, the low bFGF loading dose promoted a greater increase in cell number. bFGF loading dose did not significantly alter the mRNA expression levels of fibronectin or biglycan. When tested *in vivo* the two loading doses of bFGF were not significantly different for any of the parameters tested: proliferating cell number, myofibroblast number, connective tissue area, neoformed epithelium length or biologic width. These results suggest that the loading dose of bFGF in the microspheres of PCL scaffold membranes for use in periodontal regeneration could be optimized to determine the concentration which promotes accelerated wound healing *in vivo*. In addition, for translation to clinical studies, dosing would need to be further optimized. bFGF in the microspheres was stabilized by heparin (Nissen, Shankar et al. 1999) and retains its biological activity following release from the microspheres (Guo, Elliott et al. 2012), however over time the

age of the scaffold may have contributed to a loss of bioactivity of the bFGF in the microspheres.

2.5 Conclusion

In conclusion, we have shown that PCL electrospun fibrous scaffolds are biocompatible when tested *in vitro* with hGFs as evidenced by cellular attachment, increase in cell number with time and matrix deposition, and when tested with gingival tissue explants *ex vivo* as indicated by population of the fibrous construct by mesenchymal cells. The release of bFGF from microspheres contained within the PCL scaffolds promotes the population of the scaffolds by mesenchymal cells from gingival tissue explants and increases hGF cell number on the scaffolds. Importantly, the scaffolds were found to act as a barrier to oral epithelial cells *in vitro*, as indicated by minimal epithelial cell penetration into the scaffold interior. *In vivo* all three scaffold types were found to be biocompatible in a rat model of gingival repair. These results suggest that with further optimization for *in vivo* testing, PCL electrospun scaffolds show promise as a bioactive, porous GTR membrane alternative.

2.6 Acknowledgements

The authors wish to extend special thanks to Linda Jackson-Boeters for technical assistance. DWH is a recipient of the Ontario Ministry of Research and Innovation Early Researcher Award.

2.7 References

- AAP (2001). Glossary of Periodontal Terms. Chicago, IL, The American Academy of Periodontology.
- Akman, A. C., R. S. Tigli, M. Gumusderelioglu and R. M. Nohutcu (2010). "bFGF-loaded HA-chitosan: a promising scaffold for periodontal tissue engineering." J Biomed Mater Res A **92**(3): 953-962.
- Alimohamad, H., T. Habijanac, H. Larjava and L. Hakkinen (2005). "Colocalization of the collagen-binding proteoglycans decorin, biglycan, fibromodulin and lumican with different cells in human gingiva." J Periodontol Res **40**(1): 73-86.
- Aukhil, I. (2000). "Biology of wound healing." Periodontology 2000 **22**: 44-50.
- Aurer, A. and K. Jorgic-Srdjak (2005). "Membranes for periodontal regeneration." Acta Stomat Croat **39**: 107-112.
- Ayvazyan, A., N. Morimoto, N. Kanda, S. Takemoto, K. Kawai, Y. Sakamoto, T. Taira and S. Suzuki (2011). "Collagen-gelatin scaffold impregnated with bFGF accelerates palatal wound healing of palatal mucosa in dogs." J Surg Res **171**(2): e247-257.
- Baker, B. M. and R. L. Mauck (2007). "The effect of nanofiber alignment on the maturation of engineered meniscus constructs." Biomaterials **28**(11): 1967-1977.
- Bartold, P. M., R. R. Boyd and R. C. Page (1986). "Proteoglycans Synthesized by Gingival Fibroblasts Derived From Human Donors of Different Ages." J Cell Physiol **126**: 37-46.
- Bartold, P. M., C. A. G. McCulloch, A. S. Narayanan and S. Pitaru (2000). "Tissue engineering: a new paradigm for periodontal regeneration based on molecular and cell biology." Periodontology 2000 **24**: 253-269.
- Bartold, P. M., L. J. Walsh and A. S. Narayanan (2000). "Molecular and cell biology of the gingiva." Periodontology 2000 **24**: 28-55.
- Brunette, D. M. (1986). "Fibroblasts on micromachined substrata orient hierarchically to grooves of different dimensions." Exp Cell Res **164**: 11-26.
- Brunette, D. M., G. S. Kenner and T. R. L. Gould (1983). "Grooved titanium surfaces orient growth and migration of cells from human gingival explants." J Dent Res **62**(10): 1045-1048.
- Buckley-Sturrock, A., S. C. Woodward, R. M. Senior, G. L. Griffin, M. Klagsbrun and J. M. Davidson (1989). "Differential stimulation of collagenase and chemotactic activity in fibroblasts derived from rat wound repair tissue and human skin by growth factors." J Cell Physiol **138**: 70-78.

- Caceres, M., A. Oyarzun and P. C. Smith (2014). "Defective wound-healing in aging gingival tissue." J Dent Res **93**(7): 691-697.
- Cao, H., K. McHugh, S. Y. Chew and J. M. Anderson (2010). "The topographical effect of electrospun nanofibrous scaffolds on the in vivo and in vitro foreign body reaction." J Biomed Mater Res A **93**(3): 1151-1159.
- Choi, W., H. Kawanabe, Y. Sawa, K. Taniguchi and H. Ishikawa (2008). "Effects of bFGF on suppression of collagen type I accumulation and scar tissue formation during wound healing after mucoperiosteal denudation of rat palate." Acta Odontol Scand **66**(1): 31-37.
- Chou, L., J. D. Firth, V.-J. Uitto and D. M. Brunette (1995). "Substratum surface topography alters cell shape and regulates fibronectin mRNA level, mRNA stability, secretion and assembly in human fibroblast." J Cell Sci **108**: 1563-1573.
- Connor, N. S., J. E. Aubin and A. H. Melcher (1984). "The distribution of fibronectin in rat tooth and periodontal tissues: an immunofluorescence study using a monoclonal antibody." J Histochem Cytochem **32**(6): 565-572.
- Darby, I., O. Skalli and G. Gabbiani (1990). "Alpha-smooth muscle actin is transiently expressed by myofibroblasts during experimental wound healing." Lab Invest **63**(1): 21-29.
- de Souza Filho, F. J., G. Gallina, L. Gallottini, R. Russo and E. M. Cumbo (2012). "Innovations in endodontic filling materials: guttapercha vs Resilon." Curr Pharm Des **18**(34): 5553-5558.
- den Braber, E. T., J. E. de Ruijter, L. A. Ginsel, A. F. von Recum and J. A. Jansen (1998). "Orientation of ECM protein deposition, fibroblast cytoskeleton, and attachment complex components on silicone microgrooved surfaces." J Biomed Mater Res **40**: 291-300.
- Dong, Y., S. Liau, M. Ngiam, C. K. Chan and S. Ramakrishna (2009). "Degradation behaviors of electrospun resorbable polyester nanofibers." Tissue Eng Part B Rev **15**(3): 333-351.
- Eke, P. I., B. A. Dye, L. Wei, G. O. Thornton-Evans and R. J. Genco (2012). "Prevalence of periodontitis in adults in the United States: 2009 and 2010." J Dent Res **91**(10): 914-920.
- Fairweather, D. and D. Cihakova (2009). "Alternatively activated macrophages in infection and autoimmunity." J Autoimmun **33**(3-4): 222-230.
- Fournier, B. P., H. Larjava and L. Hakkinen (2013). "Gingiva as a source of stem cells with therapeutic potential." Stem Cells Dev **22**(24): 3157-3177.

Funato, N., K. Moriyama, Y. Baba and T. Kuroda (1999). "Evidence for apoptosis induction in myofibroblasts during palatal mucoperiosteal repair." J Dent Res **78**(9): 1511-1517.

Funato, N., K. Moriyama, H. Shimokawa and T. Kuroda (1997). "Basic fibroblast growth factor induces apoptosis in myofibroblastic cells isolated from rat palatal mucosa." Biochem Biophys Res Commun **240**: 21-26.

Garg, K., N. A. Pullen, C. A. Oskeritzian, J. J. Ryan and G. L. Bowlin (2013). "Macrophage functional polarization (M1/M2) in response to varying fiber and pore dimensions of electrospun scaffolds." Biomaterials **34**(18): 4439-4451.

Glass-Brudzinski, J., D. Perizzolo and D. M. Brunette (2002). "Effects of substratum surface topography on the organization of cells and collagen fibers in collagen gel cultures." J Biomed Mater Res **61**: 608-618.

Gospodarowicz, D. (1974). "Localisation of a fibroblast growth factor and its effect alone and with hydrocortisone on 3T3 cell growth." Nature **249**: 123-127.

Gospodarowicz, D., N. Ferrara, L. Schweigerer and G. Neufe (1987). "Structural characterization and biological functions of fibroblast growth factor." Endocr Rev **8**(2): 95-114.

Guo, X., C. G. Elliott, Z. Li, Y. Xu, D. W. Hamilton and J. Guan (2012). "Creating 3D angiogenic growth factor gradients in fibrous constructs to guide fast angiogenesis." Biomacromolecules **13**(10): 3262-3271.

Hakkinen, L., O. Oksala, T. Salo, F. Rahemtulla and H. Larjava (1993). "Immunohistochemical localization of proteoglycans in human periodontium." J Histochem Cytochem **41**(11): 1689-1699.

Hakkinen, L., V.-J. Uitto and H. Larjava (2000). "Cell biology of gingival wound healing." Periodontology 2000 **24**: 127-153.

Hamilton, D. W., B. Chehroudi and D. M. Brunette (2007). "Comparative response of epithelial cells and osteoblasts to microfabricated tapered pit topographies in vitro and in vivo." Biomaterials **28**(14): 2281-2293.

Hamilton, D. W., C. Oakley, N. A. Jaeger and D. M. Brunette (2009). "Directional change produced by perpendicularly-oriented microgrooves is microtubule-dependent for fibroblasts and epithelium." Cell Motil Cytoskeleton **66**(5): 260-271.

Hughes, F. J., M. Ghuman and A. Talal (2010). "Periodontal regeneration: a challenge for the tissue engineer?" Proc Inst Mech Eng H **224**(12): 1345-1358.

Hwang, C. M., Y. Park, J. Y. Park, K. Lee, K. Sun, A. Khademhosseini and S. H. Lee (2009). "Controlled cellular orientation on PLGA microfibers with defined diameters." Biomed Microdevices **11**(4): 739-746.

Jansen, R. G., T. H. van Kuppevelt, W. F. Daamen, A. M. Kuijpers-Jagtman and J. W. Von den Hoff (2009). "FGF-2-loaded collagen scaffolds attract cells and blood vessels in rat oral mucosa." J Oral Pathol Med **38**(8): 630-638.

Jones, L. J., M. Gray, S. T. Yue, R. P. Haugland and V. L. Singer (2001). "Sensitive determination of cell number using the CyQUANT cell proliferation assay." J Immunol Methods **254**: 85-98.

Karring, T., S. Nyman, J. Gottlow and L. Laurell (2000). "Development of the biological concept of guided tissue regeneration - animal and human studies." Periodontology **2000** **1**: 26-35.

Khuller, N. and N. Sharma (2009). "Biologic Width: Evaluation and Correction of its Violation." J Oral Health Comm Dent **3**(1): 20-25.

Kitamura, M., M. Akamatsu, M. Machigashira, Y. Hara, R. Sakagami, T. Hirofuji, T. Hamachi, K. Maeda, M. Yokota, J. Kido, T. Nagata, H. Kurihara, S. Takashiba, T. Sibutani, M. Fukuda, T. Noguchi, K. Yamazaki, H. Yoshie, K. Ioroi, T. Arai, T. Nakagawa, K. Ito, S. Oda, Y. Izumi, Y. Ogata, S. Yamada, H. Shimauchi, K. Kunimatsu, M. Kawanami, T. Fujii, Y. Furuichi, T. Furuuchi, T. Sasano, E. Imai, M. Omae, S. Yamada, M. Watanuki and S. Murakami (2011). "FGF-2 stimulates periodontal regeneration: results of a multi-center randomized clinical trial." J Dent Res **90**(1): 35-40.

Kitamura, M., K. Nakashima, Y. Kowashi, T. Fujii, H. Shimauchi, T. Sasano, T. Furuuchi, M. Fukuda, T. Noguchi, T. Shibutani, Y. Iwayama, S. Takashiba, H. Kurihara, M. Ninomiya, J. Kido, T. Nagata, T. Hamachi, K. Maeda, Y. Hara, Y. Izumi, T. Hirofuji, E. Imai, M. Omae, M. Watanuki and S. Murakami (2008). "Periodontal tissue regeneration using fibroblast growth factor-2: randomized controlled phase II clinical trial." PLoS One **3**(7): e2611.

Kurkinen, M., A. Vaheri, P. J. Roberts and S. Stenman (1980). "Sequential appearance of fibronectin and collagen in experimental granulation tissue." Lab Invest **43**(1): 47-51.

Linghorne, W. J. and D. C. O'Connell (1950). "Studies in the regeneration and reattachment of supporting structures of the teeth: I. Soft tissue reattachment." J Dent Res **29**(4): 419-428.

Livak, K. J. and T. D. Schmittgen (2001). "Analysis of relative gene expression data using real-time quantitative PCR and the 2(-Delta Delta C(T)) Method." Methods **25**(4): 402-408.

Lowery, J. L., N. Datta and G. C. Rutledge (2010). "Effect of fiber diameter, pore size and seeding method on growth of human dermal fibroblasts in electrospun poly(epsilon-caprolactone) fibrous mats." Biomaterials **31**(3): 491-504.

Ma, Q., W. Wang, P. K. Chu, S. Mei, K. Ji, L. Jin and Y. Zhang (2012). "Concentration- and time-dependent response of human gingival fibroblasts to fibroblast growth factor 2 immobilized on titanium dental implants." Int J Nanomedicine **7**: 1965-1976.

- Murakami, M. and M. Simons (2008). "Fibroblast growth factor regulation of neovascularization." Curr Opin Hematol **15**(3): 215-220.
- Murakami, S., S. Takayama, K. Ikezawa, Y. Shimabukuro, M. Kitamura, T. Nozaki, A. Terashima, T. Asano and H. Okada (1999). "Regeneration of periodontal tissues by basic fibroblast growth factor." J Periodont Res **34**: 425-430.
- Murakami, S., S. Takayama, M. Kitamura, Y. Shimabukuro, K. Yanagi, K. Ikezawa, T. Saho, T. Nozaki and H. Okada (2003). "Recombinant human basic fibroblast growth factor (bFGF) stimulates periodontal regeneration in class II furcation defects created in beagle dogs." J Periodont Res **38**: 97-103.
- Murugan, R. and S. Ramakrishna (2007). "Design strategies of tissue engineering scaffolds with controlled fiber orientation." Tissue Eng **13**(8): 1845-1866.
- Nam, Y. S. and T. G. Park (1999). "Porous biodegradable polymeric scaffolds prepared by thermally induced phase separation." J Biomed Mater Res **47**: 8-17.
- Needleman, I., H. V. Worthington, E. Giedrys-Leeper and R. Tucker (2006). "Guided tissue regeneration for periodontal infra-bony defects." Cochrane Database Syst Rev **19**(2).
- Nisbet, D. R., J. S. Forsythe, W. Shen, D. I. Finkelstein and M. K. Horne (2009). "Review paper: a review of the cellular response on electrospun nanofibers for tissue engineering." J Biomater Appl **24**(1): 7-29.
- Nissen, N. N., R. Shankar, R. L. Gamelli, A. Singh and L. A. Dipietro (1999). "Heparin and heparan sulphate protect basic fibroblast growth factor from non-enzymic glycosylation." J Biochem **338**: 637-642.
- Nugent, M. A. and R. V. Iozzo (2000). "Fibroblast growth factor-2." Int J Biochem Cell Biol **32**: 115-120.
- Oda, Y., H. Kagami and M. Ueda (2004). "Accelerating effects of basic fibroblast growth factor on wound healing of rat palatal mucosa." J Oral Maxofac Surg **62**: 73-80.
- Pham, Q. P., U. Sharma and A. G. Mikos (2006). "Electrospinning of polymeric nanofibers for tissue engineering applications: A review." Tissue Eng **12**(5): 1197-1211.
- Pihlstrom, B. L., B. S. Michalowicz and N. W. Johnson (2005). "Periodontal diseases." Lancet **366**(9499): 1809-1820.
- Polimeni, G., A. V. Xiropaidis and U. M. E. Wikesjo (2006). "Biology and principles of periodontal wound healing/regeneration." Periodontology 2000 **41**: 30-47.
- Rosen, J. J. and L. A. Culp (1977). "Morphology and cellular origins of substrate-attached material from mouse fibroblasts." Exp Cell Res **107**: 139-149.

Schmidt, G., H. Robenek, B. Harrach, J. Glössl, V. Nolte, H. Hörmann, H. Richter and H. Kresse (1987). "Interaction of small dermatan sulfate proteoglycan from fibroblasts with fibronectin." J Cell Biol **104**: 1683-1691.

Schroeder, H. E. and M. A. Listgarten (1997). "The gingival tissues: the architecture of periodontal protection." Periodontology 2000 **13**: 91-120.

Shang, S., F. Yang, X. Cheng, X. F. Walboomers and J. A. Jansen (2010). "The effect of electrospun fibre alignment on the behaviour of rat periodontal ligament cells." Eur Cell Mater **19**: 180-192.

Shi, H. X., C. Lin, B. B. Lin, Z. G. Wang, H. Y. Zhang, F. Z. Wu, Y. Cheng, L. J. Xiang, D. J. Guo, X. Luo, G. Y. Zhang, X. B. Fu, S. Bellusci, X. K. Li and J. Xiao (2013). "The anti-scar effects of basic fibroblast growth factor on the wound repair in vitro and in vivo." PLoS One **8**(4): e59966.

Steffensen, B., A. H. Duong, S. B. Milam, C. L. Potempa, W. B. Winborn, V. L. Magnuson, D. Chen, G. Zardeneta and R. J. Klebe (1992). "Immunohistological localization of cell adhesion proteins and integrins in the periodontium." J Periodontol **63**: 584-592.

Takayama, S., S. Murakami, Y. Shimabukuro, M. Kitamura and H. Okada (2001). "Periodontal regeneration by fgf-2 (bfgf) in primate models." J Dent Res **80**(12): 2075-2079.

Takayama, S., J. Yoshida, H. Hirano, H. Okada and S. Murakami (2002). "Effects of basic fibroblast growth factor on human gingival epithelial cells." J Periodontol **73**: 1467-1473.

Tan, E. M. L., J. Hoffren, S. Rouda, S. Greenbaum, J. W. Fox, J. H. Moore and G. R. Dodge (1993). "Decorin, versican and biglycan gene expression by keloid and normal dermal fibroblasts: differential regulation by basic fibroblast growth factor." Exp Cell Res **209**: 200-207.

Tigli, R. S., A. C. Akman, M. Gumusderelioglu and R. M. Nohutcu (2009). "In vitro release of dexamethasone or bFGF from chitosan/hydroxyapatite scaffolds." J Biomater Sci Polym Ed **20**(13): 1899-1914.

Tomasz, M. (1995). "Mitomycin C: small, fast and deadly (but very selective)." Chem Biol **2**(9): 575-579.

Wikesjo, U. M. E., W. H. Lim, R. C. Thomson and W. R. Hardwick (2003). "Periodontal repair in dogs: gingival tissue occlusion, a critical requirement for GTR?" J Clin Periodontol **30**: 655-664.

Wikesjo, U. M. E. and K. A. Selvi (1999). "Periodontal wound healing and regeneration." Periodontology 2000 **19**: 21-39.

Woodruff, M. A. and D. W. Hutmacher (2010). "The return of a forgotten polymer-Polycaprolactone in the 21st century." Progress in Polymer Science **35**(10): 1217-1256.

Xie, J., H. Bian, S. Qi, Y. Xu, J. Tang, T. Li and X. Liu (2008). "Effects of basic fibroblast growth factor on the expression of extracellular matrix and matrix metalloproteinase-1 in wound healing." Clin Exp Dermatol **33**(2): 176-182.

Zhang, S. (2003). "Fabrication of novel biomaterials through molecular self-assembly." Nat Biotechnol **21**(10): 1171-1178.

Zittermann, S. I. and A. C. Issekutz (2006). "Basic fibroblast growth factor (bFGF, FGF-2) potentiates leukocyte recruitment to inflammation by enhancing endothelial adhesion molecule expression." Am J Pathol **168**(3): 835-846.

Chapter 3

3 General Discussion

3.1 Summary and Conclusions

Objective #1: To characterize the influence of PCL electrospun fibrous scaffolds loaded with bFGF microspheres on human gingival fibroblasts *in vitro* and gingival tissue *ex vivo*

- a. Assess human gingival fibroblast attachment, proliferation and matrix synthesis and deposition on PCL electrospun scaffolds loaded with bFGF

In this study, hGFs were found to attach and spread on all three scaffold types with cell morphology being influenced by the fibers of the scaffold. All three scaffolds supported an increase in hGF cell number temporally with bFGF loading promoting an increase in cell number. Qualitative assessment of ECM deposition on the surface of the scaffolds using immunocytochemistry revealed that hGFs secreted a fibronectin matrix onto the scaffolds both with and without bFGF loading, whereas biglycan and decorin remained mainly intracellular on all scaffolds. bFGF did not alter the deposition of fibronectin appreciably, however appeared to reduce biglycan immunoreactivity and increase decorin immunoreactivity. Neither bFGF concentration significantly altered fibronectin or biglycan mRNA levels.

- b. Assess cell infiltration from gingival tissue explants into PCL electrospun scaffolds loaded with bFGF

In this set of experiments, cells of mesenchymal origin, vimentin⁺, were found to populate the PCL electrospun scaffolds with cell density increasing in a bFGF dose-dependent manner. Oral epithelial cells from the explant tissue were found to remain on the surface of the scaffold with little penetration into the scaffold interior observed on both PCL alone and high bFGF loaded scaffolds.

Taken together, these results suggest that the PCL electrospun scaffolds loaded with bFGF are able to act as an epithelial cell-occlusive membrane while facilitating interaction with hGFs and mesenchymal cells.

Objective #2: Assess the influence of PCL electrospun fibrous scaffolds loaded with bFGF microspheres on the rate of wound healing following gingivectomy in a rat model

In a rat gingivectomy model, treatment with PCL electrospun scaffolds localized populations of alternatively activated M2 phenotype macrophages around the crest of the alveolar bone. Scaffolds both with and without bFGF loading did not significantly change the number of proliferating cells or myofibroblasts in the healing wound. Collagen deposition was observed in the regenerating gingival connective tissue at day 7 in wounds treated with scaffolds loaded with bFGF. The area of newly formed connective tissue, epithelial length and biologic width did not show any significant difference in wounds treated with any scaffold type. The results of this study suggest that PCL scaffolds both with and without bFGF loading are biocompatible in a model of gingival healing.

3.2 Contributions to the Current State of Knowledge

3.2.1 General Significance

Periodontal diseases are highly prevalent in the Western population and require surgical intervention to halt disease progression and induce regeneration of the lost tissues. GTR procedures are currently used as a surgical method to regenerate the periodontium, but the membranes currently employed are cell-occlusive and when used clinically, results have been variable and unpredictable (Chen and Jin 2010). Functionally excluding the gingival connective tissue from the regenerating defect is suboptimal as it excludes the rich vascular plexus, pericytes and progenitor cells of the gingival connective tissue which could aid in the regeneration of the damaged periodontium (Schroeder and Listgarten 1997, Fournier, Larjava et al. 2013). Exclusion of the oral epithelium from the regenerating periodontal defect is a requirement for the formation of a new connective tissue attachment to the tooth root (Polimeni, Xiropaidis et al. 2006), but exclusion of the

collagenous gingival connective tissue itself arises only from the need to block oral epithelial migration (Wikesjo, Lim et al. 2003). Therefore the focus of this work was the development of a fibrous and bioresorbable scaffold as an alternative to cell-occlusive barrier membranes to allow recruitment of mesenchymal cells from the gingival connective tissue while maintaining a barrier to oral epithelial cells. We demonstrate that PCL electrospun scaffolds allow the infiltration of mesenchymal cells while simultaneously posing a barrier to oral epithelial cell infiltration, with the addition of bFGF promoting mesenchymal cell population and an increase in hGF cell number on the scaffolds. *In vivo*, the scaffolds were biocompatible in terms of the polarization of macrophages to a healing M2 phenotype, collagen deposition, connective tissue regeneration and biological width restoration.

3.2.2 Role of Scaffold Architecture in Determining Cellular Responses

It has been established that cells cultured on three dimensional substrates show numerous behavioral alterations including changes in adhesion, cytoskeletal organization, proliferation, morphology, and differentiation compared to cells in two dimensional culture (Friedl and Brocker 2000, Hakkinen, Harunaga et al. 2011, Rampichova, Chvojka et al. 2013). Furthermore, the physical properties of the scaffolds themselves, such as fiber diameter, fiber orientation, and porosity play a significant role in the regulation of cellular morphology, proliferation, alignment, and migration of cells (Liu, Ji et al. 2009, Shang, Yang et al. 2010). Fibroblast cells show preferential orientation along fibers of 10 μm diameter (Hwang, Park et al. 2009) with hGFs showing alignment along the 7.4 ± 2.0 μm fibers under investigation in this thesis. Porosity of the scaffold is another feature which has significant effects upon cell behavior. Optimal porosity allows for exchange of nutrients and wastes within the three dimensional scaffold facilitating development of a microenvironment for cellular growth (Rampichova, Chvojka et al. 2013). For optimal cell proliferation, a pore size of between 6 -20 μm has been established for fibroblast cells. As shown in this thesis, hGF cell number increases with time on the PCL electrospun scaffolds (pore size 17.1 ± 8.3 μm , pore size range of 6.8 – 42.7 μm). Porosity also dictates the level of matrix production by cells. Larger pore sizes result in

cells attaching to single fibers slowing ECM production as opposed to cells spanning across multiple fibers (Lowery, Datta et al. 2010). As demonstrated in this thesis, hGFs attach to and span across multiple scaffold fibers and secrete a fibronectin matrix. Porosity strongly influences cell migration into the interior of the scaffold, with small pore sizes excluding cells (Lowery, Datta et al. 2010). The PCL electrospun scaffolds under study in this thesis allow for infiltration of mesenchymal cells into the scaffold interior and, of particular significance in terms of GTR membrane design, the scaffolds were observed to exclude oral epithelial cells. As we have previously demonstrated, oral epithelial cells do not migrate into topographies of $45 \mu\text{m}^2$ (Hamilton, Chehroudi et al. 2007). Thus *in vitro* testing suggests that the porous, fibrous nature of the PCL electrospun scaffold shows improvement over current cell-occlusive GTR membranes in that it allows for attachment, cell number increase, and matrix deposition of hGFs and infiltration of mesenchymal cells while maintaining a barrier to oral epithelial cells.

3.2.3 Role of bFGF in Scaffold Bioactivity

bFGF is a potent mitogen of mesoderm derived cells and a potent chemotactic agent for fibroblasts (Gospodarowicz 1974, Buckley-Sturrock, Woodward et al. 1989). Topical application of bFGF has been shown to accelerate oral wound healing (Fujisawa, Miyamoto et al. 2003, Oda, Kagami et al. 2004), however this method of application in periodontal defects is problematic as high concentrations of the growth factor are required to overcome the short half-lives resulting from enzymatic degradation and quick metabolization following application (Sun, Qu et al. 2012). Suitable carriers are needed for the temporally sustained release of growth factors at a defect site. In this thesis bFGF was stabilized with heparin and encapsulated in PLGA microspheres which were electrospayed throughout the thickness of the fibrous PCL scaffold. This method of growth factor delivery allows for a slow and temporally sustained release of the growth factor as the PLGA shell degrades (Guo, Elliott et al. 2012). bFGF release from the microspheres increased the bioactivity of the scaffolds when tested *in vitro* as indicated by increased hGF number on scaffolds containing bFGF and increased mesenchymal cell density from gingival tissue explants. Comparison of the two loading doses of bFGF suggest that the high loading dose of bFGF was more effective for scaffold population by

mesenchymal cells from *ex vivo* gingival tissue explants, whereas the low loading dose promoted the greatest increase of hGF cell number on the scaffolds. In addition, high bFGF loading was found to dramatically upregulate versican mRNA expression levels at 14 days of culture in previous experiments. Taken together, these results suggest that bFGF release from the scaffolds increased their bioactivity when tested *in vitro*.

3.2.4 PCL Electrospun Scaffolds Loaded with bFGF for Tissue Repair

As the PCL electrospun scaffolds proved to be oral epithelial cell occlusive and allowed for infiltration of mesenchymal tissue *in vitro* they were subsequently tested for their ability to promote gingival tissue regeneration. The gingiva is a critical component of the periodontium that functions to protect the underlying structures of the periodontium from the multitudes of bacterial species present in the oral environment (Schroeder and Listgarten 1997). This is accomplished through the junctional epithelium of the gingiva forming a functional seal around the teeth along with adequate connective tissue attachment to the roots of the teeth. If the gingiva becomes compromised, due to the repeated inflammatory insult associated with periodontitis, regeneration of the lost functional structure requires therapeutic intervention, such as GTR (Karring, Nyman et al. 2000). GTR procedures are based upon the concept of cell occlusion, specifically the oral epithelium, from a regenerating periodontal defect to allow for the reformation of connective tissue attachment to the tooth root (Karring, Nyman et al. 2000). This is accomplished using occlusive membranes which also exclude the gingival connective tissue eliminating the rich vascular plexus and associated progenitor cells of the connective tissue from contributing to periodontal regeneration (Schroeder and Listgarten 1997, Wikesjo, Lim et al. 2003, Fournier, Larjava et al. 2013). In this thesis we have demonstrated that PCL electrospun fibrous scaffolds are biocompatible when used as an alternative GTR membrane in terms of macrophage polarization to a reparative M2 phenotype, collagen deposition, connective tissue area regenerated, and connective tissue attachment, however the role of bFGF release from the scaffolds on the healing process remains to be fully quantified.

In addition to their use in periodontal regeneration, the scaffolds may also serve to facilitate dermal wound healing. bFGF accelerates and plays a role in the reduction of scar formation, which is a common clinical problem associated with dermal wound healing (Akita, Akino et al. 2008, Shi, Lin et al. 2013). Sustained release of bFGF from the scaffold may regulate the apoptosis of myofibroblasts and regulate ECM deposition thus lessening scar formation (Shi, Lin et al. 2013). In addition, the scaffolds may be useful at promoting wound healing in diabetic patients, both in dermal and oral mucosal tissues, as topical bFGF application is shown to be effective at promoting wound healing in chronic diabetic wounds (Tan, Xiao et al. 2008). One of the complications of diabetes is deficiencies in wound healing characterized by impairment of the inflammatory response, granulation tissue formation and angiogenesis (Desta, Li et al. 2010). Fibroblasts show increased apoptosis in diabetic gingival wounds which is postulated to play a role in the impaired wound healing response (Desta, Li et al. 2010). Since bFGF is a potent mitogen for fibroblast cells, sustained release of bFGF from the scaffolds in a diabetic wound may serve to increase fibroblast proliferation thus rescuing granulation tissue formation. The porous, fibrous architecture of the scaffold would serve as a support for cells infiltrating from the granulation tissue until the cells secrete their own matrix.

3.3 Future Directions

3.3.1 Adhesion Dynamics of Cellular Interaction with PCL Electrospun Scaffolds

Cells attach to and interact with the extracellular matrix through adhesion sites. These adhesion sites serve as transmembrane linkages between the extracellular matrix and the cytoskeleton (Burrige, Molony et al. 1987). Adhesion is mediated through integrins which function as cell signaling molecules and can affect a diverse range of cell functions such as migration, proliferation, differentiation, and cell polarity (Streuli 1999, Friedl and Brocker 2000, Berrier and Yamada 2007). Of particular importance is the response of cells to three dimensional substrates (Friedl, Zanker et al. 1998, Friedl and Brocker 2000), such as the PCL electrospun scaffolds under investigation in this thesis. To investigate the adhesion dynamics of hGFs on the PCL electrospun scaffolds, both with

and without bFGF, indirect immunofluorescence will be used to localize adhesion structures such as focal adhesion and focal complexes (vinculin, phosphorylated FAK, phosphorylated paxillin) and fibrillar adhesions (tensin, integrin $\alpha_5\beta_1$) (Berrier and Yamada 2007) at 3 hours, 6 hours and 7 days post-seeding. Due to the three dimensional structure of the scaffolds, confocal microscopy will be used to visualize labelled adhesion molecules thus giving information about the composition, localization, and size of the adhesions within the cell. To further assess adhesion dynamics on the scaffolds, antibody inhibition assays will be conducted. hGFs will be incubated with monoclonal antibodies to integrins $\alpha_5\beta_1$ (three dimensional adhesions) and $\alpha_v\beta_3$ (two dimensional adhesions) prior to seeding on all three scaffold types. Cells will be allowed to attach to the scaffolds for 2 and 24 hours to assess early and late attachment, respectively. At each time point non adherent cells will be gently removed by rinsing and cell number on the scaffold will be assessed using an assay to quantify DNA content, such as the CyQUANT® assay, and compared to cells incubated with vehicle alone prior to seeding.

Adhesion dynamics allow cells to interact with the underlying substratum and ECM, which in turn dictates ECM production (Mann, Tsai et al. 1999, Lowery, Datta et al. 2010). Characterization of the adhesion dynamics of hGFs on the scaffolds will allow for determination of the optimal fiber diameter of the scaffolds in order to promote matrix formation.

3.3.2 Effect of Lipopolysaccharide on hGF Interaction with PCL Electrospun Scaffolds

Wound healing and periodontal regeneration takes place under exposure to several bacterial species as the oral environment is home to several hundreds of distinct microbial species and is one of the most densely populated areas of the body by bacteria (Takahashi 2005). Bacteria and their products can have a significant impact on wound healing and cellular response, and thus should be considered when modelling gingival wound healing *in vitro*. *Porphyromonas gingivalis* (*P. gingivalis*) has been implicated in the etiology of periodontitis (Moore and Moore 1994) and lipopolysaccharide (LPS), a bacterial cell wall component, has been postulated to be a likely candidate for activation of the host inflammatory response (Kocgozlu, Elkaim et al. 2009). Oral epithelial cells

and gingival fibroblasts produce inflammatory cytokines in response to *P. gingivalis* LPS stimulation (Wang and Ohura 2002, Kocgozlu, Elkaim et al. 2009). Fibroblasts show dose dependent responses to *Actinobacillus actinomycetemcomitans* (*A. actinomycetemcomitans*) LPS with high concentrations inhibiting DNA synthesis whereas a slight stimulation of DNA synthesis was observed when exposed to low concentrations (Hill and Ebersole 1996). Furthermore, *A. actinomycetemcomitans* LPS stimulation at high concentrations attenuated cell proliferation in response to bFGF whereas stimulation with low concentrations of *A. actinomycetemcomitans* LPS enhanced cell proliferation in response to bFGF (Hill and Ebersole 1996). The LPS of *P. gingivalis* differs structurally from that of other Gram-negative bacteria (Wang and Ohura 2002), thus future experiments to assess the effects of LPS on hGFs cultured on the PCL electrospun scaffolds will be undertaken using *P. gingivalis* LPS and *A. actinomycetemcomitans* LPS, at both low ($< 9 \mu\text{g}$) and high concentrations ($\geq 9 \mu\text{g}$). Cell number on PCL electrospun scaffolds with and without bFGF loading will be assessed in the presence of both species of LPS at both concentrations using a CyQUANT® assay to assess DNA content. These experiments will allow us to gain insight into the potential effectiveness of the scaffolds under more physiologically relevant and challenging conditions which are present during periodontal regeneration.

3.3.3 Analysis of PCL Electrospun Scaffolds on Initial and Late Wound Healing Response

In this thesis we have analyzed the initial gingival wound healing response of rats treated with PCL electrospun scaffolds both with and without bFGF loading using histological sections for morphometric analysis and assessing collagen deposition and immunohistochemistry to analyze proliferating cell number, M2 macrophage polarization and myofibroblast number. To further analyze the influence of the scaffolds on the biomolecular events occurring during gingival wound healing, scaffolds would be placed in the wounds and at 3 and 7 days post-wounding, gingival tissue would be harvested and mRNA isolated to look for changes in mRNA expression levels of ECM proteins such as collagen, fibronectin, tenascin-C, biglycan, decorin and versican. In addition, α -SMA mRNA expression levels could be analyzed to assess myofibroblast presence in the

healing wound. The protein level of the previously listed ECM molecules and α -SMA could be analyzed using Western blots following protein isolation from the tissues.

To characterize the late wound healing response, longer time-points will be used, such as 2, 4 and 6 weeks. During wound healing, myofibroblast differentiation occurs between 6 and 15 days post-wounding with maximal myofibroblast population density observed at 15 days (Darby, Skalli et al. 1990). Since bFGF has been shown to induce the apoptosis of myofibroblasts (Funato, Moriyama et al. 1997, Funato, Moriyama et al. 1999, Kanda, Funato et al. 2003) it will be of interest to analyze the effects of the PCL electrospun scaffolds loaded with bFGF on myofibroblast population in the healing rat gingival wounds at the later time points of 14 and 28 days which could be accomplished using immunohistochemistry for localization of myofibroblasts in the healing wound, or with qRT-PCR and Western blots to examine the mRNA and protein expression level of α -SMA, respectively. Although occurring to a lesser extent than in dermal tissue, gingival tissue following healing may exhibit a denser than normal collagen-rich extracellular matrix which is particularly problematic if the maxilla is not fully developed (Choi, Kawanabe et al. 2008). Since bFGF has been implicated in reducing collagen accumulation during oral wound healing (Choi, Kawanabe et al. 2008), investigation of collagen deposition at later time points would allow for assessment of the effect of the PCL electrospun scaffolds with and without bFGF on the deposition and remodeling of collagen in the healing rat gingiva. This will be accomplished using tissue sections stained with Masson's trichrome, Van Gieson's stain and picrosirius red to allow for qualitative assessment of collagen deposition. Collagen content in the healing tissues will be assessed using a hydroxyproline assay on healing tissue homogenates. As hydroxyproline is almost exclusively found in collagen, this assay will give a quantitative measure of the collagen content of the tissue (Reddy and Enwemeka 1996).

3.3.4 Assessing Cell Recruitment During Healing – Lineage Tracing to Assess the Role of Pericytes

During wound healing, extracellular matrix is deposited and the wound is contracted through the actions of myofibroblasts (Hinz and Gabbiani 2010). Interest in determining the source of myofibroblast populations in the healing wound have led to studies

implicating pericytes as a progenitor cell to the myofibroblast (Greenhalgh, Iredale et al. 2013). Pericytes are periendothelial cells found encircling the endothelial cells of the microvasculature (Greenhalgh, Iredale et al. 2013). Lineage tracing experiments have identified cells in the perivascular space which are induced upon injury and are pro-fibrotic (Dulauroy, Di Carlo et al. 2012). Since myofibroblasts contribute to wound healing and are responsible for scar formation and fibrosis which contributes to gingival recession, it is of interest to analyze their recruitment during gingival regeneration and in response to scaffold treatment. This will be accomplished using forkhead transcription factor FoxD1-Cre knock-in mice to allow for lineage tracing of pericytes. In this model, a fusion protein of Cre recombinase and GFP will be expressed under the control of the FoxD1 locus (Humphreys, Lin et al. 2010). Gingivectomy will be performed in these mice and PCL electrospun scaffolds with and without bFGF loading will be placed in the defect. At time points of 3, 7, 14 and 28 days, wounds will be assessed using histological sections to localize and quantify differentiated pericytes in the stroma of the regenerating gingival tissue. This will allow for determination of the role of pericytes in contributing to myofibroblast populations in gingival tissue and the role of bFGF on these populations.

3.4 Limitations

As with any scientific study, there are several limitations to this work. Working with a three dimensional scaffold material poses challenges for reliable quantification of certain parameters. One such consideration is the quantification of cell number from a three dimensional culture (Ng, Leong et al. 2005). This was accounted for and the CyQUANT assay was used to give a measure of DNA content on the scaffolds, thus giving the most accurate measure of cell number. Another concern is the need for a homogenous cell suspension from which the quantifications are made, which was taken into consideration and vigorous vortexing was employed to account for cells within the scaffold interior. In this study we used immunofluorescence as a qualitative measure of assessing ECM deposition on the surface of the scaffolds, and although Western blot analysis could give a quantitative assessment of ECM secretion, this technique may be impractical for use with the three dimensional scaffolds. Although decorin and biglycan are small (36 kDa and 38 kDa, respectively) (Fisher, Termine et al. 1989, Hering, Kollar et al. 1996),

fibronectin is secreted as a dimer composed of two monomers of molecular weight 220-250 kDa (Potts and Campbell 1994). The large molecular weight of fibronectin may impede its removal from the fibrous scaffold making it difficult to obtain complete protein removal from the scaffolds to ensure accurate quantification.

The studies completed herein assumed that the bFGF released from the microspheres was at a sufficient concentration for *in vivo* experiments based on results from our *in vitro* and *ex-vivo* studies. However *in vivo*, the effects were non-significant which could be due to a sub-optimal concentration of bFGF. Although our laboratory has previously demonstrated that the scaffolds stimulate angiogenesis in a mouse subcutaneous model, *in vivo* fibrogenic response was not investigated (Guo, Elliott et al. 2012). Further studies using scaffolds loaded with a wider range of bFGF concentrations could confirm this.

3.5 Final Summary

The results presented in this thesis demonstrate that PCL electrospun scaffolds loaded with bFGF support the attachment, matrix deposition and proliferation of hGFs with bFGF increasing cell number in a temporal manner. The scaffolds are selectively cell permeable in that they support the infiltration of mesenchymal cells from gingival tissue while simultaneously excluding the infiltration of oral epithelial cells. The scaffolds exhibit biocompatibility in the early stages of gingival wound healing in the rat. This research suggests that PCL electrospun scaffolds, with or without bFGF microspheres, represent an alternative to the current cell-occlusive membranes used for GTR.

3.6 References

- Akita, S., K. Akino, T. Imaizumi and A. Hirano (2008). "Basic fibroblast growth factor accelerates and improves second-degree burn wound healing." Wound Repair Regen **16**(5): 635-641.
- Berrier, A. L. and K. M. Yamada (2007). "Cell-matrix adhesion." J Cell Physiol **213**(3): 565-573.
- Buckley-Sturrock, A., S. C. Woodward, R. M. Senior, G. L. Griffin, M. Klagsbrun and J. M. Davidson (1989). "Differential stimulation of collagenase and chemotactic activity in fibroblasts derived from rat wound repair tissue and human skin by growth factors." J Cell Physiol **138**: 70-78.
- Burridge, K., L. Molony and T. Kelly (1987). "Adhesion plaques: sites of transmembrane interaction between the extracellular matrix and the actin cytoskeleton." J Cell Sci Suppl **8**: 211-219.
- Chen, F.-A. and Y. Jin (2010). "Periodontal Tissue Engineering and Regeneration: Current Approaches and Expanding Opportunities." Tissue Eng Part B Rev **16**(2): 219-255.
- Choi, W., H. Kawanabe, Y. Sawa, K. Taniguchi and H. Ishikawa (2008). "Effects of bFGF on suppression of collagen type I accumulation and scar tissue formation during wound healing after mucoperiosteal denudation of rat palate." Acta Odontol Scand **66**(1): 31-37.
- Darby, I., O. Skalli and G. Gabbiani (1990). "Alpha-smooth muscle actin is transiently expressed by myofibroblasts during experimental wound healing." Lab Invest **63**(1): 21-29.
- Destal, T., J. Li, T. Chino and D. T. Graves (2010). "Altered fibroblast proliferation and apoptosis in diabetic gingival wounds." J Dent Res **89**(6): 609-614.
- Dulauroy, S., S. E. Di Carlo, F. Langa, G. Eberl and L. Peduto (2012). "Lineage tracing and genetic ablation of ADAM12(+) perivascular cells identify a major source of profibrotic cells during acute tissue injury." Nat Med **18**(8): 1262-1270.
- Fisher, L. W., J. D. Termine and M. F. Young (1989). "Deduced protein sequence of bone small proteoglycan I (biglycan) shows homology with proteoglycan II (decorin) and several nonconnective tissue proteins in a variety of species." J Biol Chem **264**(8): 4571-4576.
- Fournier, B. P., H. Larjava and L. Hakkinen (2013). "Gingiva as a source of stem cells with therapeutic potential." Stem Cells Dev **22**(24): 3157-3177.
- Friedl, P. and E.-B. Brocker (2000). "The biology of cell locomotion within three-dimensional extracellular matrix." Cell Mol Life Sci **57**: 41-64.

- Friedl, P., K. S. Zanker and E.-B. Brocker (1998). "Cell migration strategies in 3-D extracellular matrix: differences in morphology, cell matrix interactions, and integrin function." Microsc Res Tech **43**: 369-378.
- Fujisawa, K., Y. Miyamoto and M. Nagayama (2003). "Basic fibroblast growth factor and epidermal growth factor reverse impaired ulcer healing of the rabbit oral mucosa." J Oral Pathol Med **32**: 358-366.
- Funato, N., K. Moriyama, Y. Baba and T. Kuroda (1999). "Evidence for apoptosis induction in myofibroblasts during palatal mucoperiosteal repair." J Dent Res **78**(9): 1511-1517.
- Funato, N., K. Moriyama, H. Shimokawa and T. Kuroda (1997). "Basic fibroblast growth factor induces apoptosis in myofibroblastic cells isolated from rat palatal mucosa." Biochem Biophys Res Commun **240**: 21-26.
- Gospodarowicz, D. (1974). "Localisation of a fibroblast growth factor and its effect alone and with hydrocortisone on 3T3 cell growth." Nature **249**: 123-127.
- Greenhalgh, S. N., J. P. Iredale and N. C. Henderson (2013). "Origins of fibrosis: pericytes take centre stage." F1000Prime Rep **5**: 37.
- Guo, X., C. G. Elliott, Z. Li, Y. Xu, D. W. Hamilton and J. Guan (2012). "Creating 3D angiogenic growth factor gradients in fibrous constructs to guide fast angiogenesis." Biomacromolecules **13**(10): 3262-3271.
- Hakkinen, K. M., J. S. Harunaga, A. D. Doyle and K. M. Yamada (2011). "Direct comparisons of the morphology, migration, cell adhesions, and actin cytoskeleton of fibroblasts in four different three-dimensional extracellular matrices." Tissue Eng Part A **17**(5-6): 713-724.
- Hamilton, D. W., B. Chehroudi and D. M. Brunette (2007). "Comparative response of epithelial cells and osteoblasts to microfabricated tapered pit topographies in vitro and in vivo." Biomaterials **28**(14): 2281-2293.
- Hering, T. M., J. Kollar, T. D. Huynh and J. B. Varelas (1996). "Purification and characterization of decorin core protein expressed in Escherichia coli as a maltose-binding protein fusion." Anal Biochem **240**: 98-108.
- Hill, S. J. and J. L. Ebersole (1996). "The effect of lipopolysaccharide on growth factor-induced mitogenesis in human gingival fibroblasts." J Periodontol **67**: 1274-1280.
- Hinz, B. and G. Gabbiani (2010). "Fibrosis: recent advances in myofibroblast biology and new therapeutic perspectives." F1000 Biol Rep **2**: 78.
- Humphreys, B. D., S. L. Lin, A. Kobayashi, T. E. Hudson, B. T. Nowlin, J. V. Bonventre, M. T. Valerius, A. P. McMahon and J. S. Duffield (2010). "Fate tracing reveals the

- pericyte and not epithelial origin of myofibroblasts in kidney fibrosis." Am J Pathol **176**(1): 85-97.
- Hwang, C. M., Y. Park, J. Y. Park, K. Lee, K. Sun, A. Khademhosseini and S. H. Lee (2009). "Controlled cellular orientation on PLGA microfibers with defined diameters." Biomed Microdevices **11**(4): 739-746.
- Kanda, T., N. Funato, Y. Baba and T. Kuroda (2003). "Evidence for fibroblast growth factor receptors in myofibroblasts during palatal mucoperiosteal repair." Archives of Oral Biology **48**(3): 213-221.
- Karring, T., S. Nyman, J. Gottlow and L. Laurell (2000). "Development of the biological concept of guided tissue regeneration - animal and human studies." Periodontology 2000 **1**: 26-35.
- Kocgozlu, L., R. Elkaim, H. Tenenbaum and S. Werner (2009). "Variable cell responses to *P. gingivalis* lipopolysaccharide." J Dent Res **88**(8): 741-745.
- Liu, Y., Y. Ji, K. Ghosh, R. A. Clark, L. Huang and M. H. Rafailovich (2009). "Effects of fiber orientation and diameter on the behavior of human dermal fibroblasts on electrospun PMMA scaffolds." J Biomed Mater Res A **90**(4): 1092-1106.
- Lowery, J. L., N. Datta and G. C. Rutledge (2010). "Effect of fiber diameter, pore size and seeding method on growth of human dermal fibroblasts in electrospun poly(epsilon-caprolactone) fibrous mats." Biomaterials **31**(3): 491-504.
- Mann, B. K., A. T. Tsai, T. Scott-Burden and J. L. West (1999). "Modification of surfaces with cell adhesion peptides alters extracellular matrix deposition." Biomaterials **20**: 2281-2286.
- Moore, W. E. C. and L. H. Moore (1994). "The bacteria of periodontal diseases." Periodontology 2000 **5**: 66-77.
- Ng, K. W., D. T. W. Leong and D. W. Hutmacher (2005). "The challenge to measure cell proliferation in two and three dimensions." Tissue Eng **11**(1-2): 182-191.
- Oda, Y., H. Kagami and M. Ueda (2004). "Accelerating effects of basic fibroblast growth factor on wound healing of rat palatal mucosa." J Oral Maxofac Surg **62**: 73-80.
- Polimeni, G., A. V. Xiropaidis and U. M. E. Wikesjo (2006). "Biology and principles of periodontal wound healing/regeneration." Periodontology 2000 **41**: 30-47.
- Potts, J. R. and I. D. Campbell (1994). "Fibronectin structure and assembly." Curr Opin Cell Biol **6**: 648-655.
- Rampichova, M., J. Chvojka, M. Buzgo, E. Prosecka, P. Mikes, L. Vyslouzilova, D. Tvrdik, P. Kochova, T. Gregor, D. Lukas and E. Amler (2013). "Elastic three-dimensional poly (epsilon-caprolactone) nanofibre scaffold enhances migration,

proliferation and osteogenic differentiation of mesenchymal stem cells." Cell Prolif **46**(1): 23-37.

Reddy, G. K. and C. S. Enwemeka (1996). "A simplified method for the analysis of hydroxyproline in biological tissues." Clinical Biochemistry **29**(3): 225-229.

Schroeder, H. E. and M. A. Listgarten (1997). "The gingival tissues: the architecture of periodontal protection." Periodontology 2000 **13**: 91-120.

Shang, S., F. Yang, X. Cheng, X. F. Walboomers and J. A. Jansen (2010). "The effect of electrospun fibre alignment on the behaviour of rat periodontal ligament cells." Eur Cell Mater **19**: 180-192.

Shi, H. X., C. Lin, B. B. Lin, Z. G. Wang, H. Y. Zhang, F. Z. Wu, Y. Cheng, L. J. Xiang, D. J. Guo, X. Luo, G. Y. Zhang, X. B. Fu, S. Bellusci, X. K. Li and J. Xiao (2013). "The anti-scar effects of basic fibroblast growth factor on the wound repair in vitro and in vivo." PLoS One **8**(4): e59966.

Streuli, C. (1999). "Extracellular matrix remodelling and cellular differentiation." Curr Opin Cell Biol **11**: 634-640.

Sun, H. H., T. J. Qu, X. H. Zhang, Q. Yu and F. M. Chen (2012). "Designing biomaterials for in situ periodontal tissue regeneration." Biotechnol Prog **28**(1): 3-20.

Takahashi, N. (2005). "Microbial ecosystem in the oral cavity: Metabolic diversity in an ecological niche and its relationship with oral diseases." International Congress Series **1284**: 103-112.

Tan, Y., J. Xiao, Z. Huang, Y. Xiao, S. Lin, L. Jin, W. Feng, L. Cai and X. Li (2008). "Comparison of the therapeutic effects recombinant human acidic and basic fibroblast growth factors in wound healing in diabetic patients." Journal of Health Science **54**(4): 432-440.

Wang, P. L. and K. Ohura (2002). "Porphyromonas gingivalis lipopolysaccharide signaling in gingival fibroblasts-CD14 and Toll-like receptors." Crit Rev Oral Biol Med **13**(2): 132-142.

Wikesjo, U. M. E., W. H. Lim, R. C. Thomson and W. R. Hardwick (2003). "Periodontal repair in dogs: gingival tissue occlusion, a critical requirement for GTR?" J Clin Periodontol **30**: 655-664.

Appendix and Curriculum Vitae

Appendix A: Animal protocol approval.

AUP Number: 2012-011

AUP Title: Development of biomaterials for the regeneration of periodontal tissues.

Yearly Renewal Date: 08/01/2014

The YEARLY RENEWAL to Animal Use Protocol (AUP) 2012-011 has been approved, and will be approved for one year following the above review date.

1. This AUP number must be indicated when ordering animals for this project.
2. Animals for other projects may not be ordered under this AUP number.
3. Purchases of animals other than through this system must be cleared through the ACVS office.
Health certificates will be required.

REQUIREMENTS/COMMENTS

Please ensure that individual(s) performing procedures on live animals, as described in this protocol, are familiar with the contents of this document.

The holder of this Animal Use Protocol is responsible to ensure that all associated safety components (biosafety, radiation safety, general laboratory safety) comply with institutional safety standards and have received all necessary approvals. Please consult directly with your institutional safety officers.

Submitted by: Kinchlea, Will D

on behalf of the Animal Use Subcommittee

Appendix B: Human ethics approval.



Office of Research Ethics

Use of Human Subjects - Ethics Approval Notice

Principal Investigator: Dr. D. W. Hamilton

Review Number: 13937E

Review Date: February 14, 2008

Revision Number: 1

Review Level: Expedited

Protocol Title: Influence of substratum topography on human gingival cell physiology in vitro

Department and Institution: Dentistry, University of Western Ontario

Sponsor:

Ethics Approval Date: February 14, 2008

Expiry Date: December 31, 2012

Documents Reviewed and Approved: Letter of Information and Consent

Documents Received for Information:

This is to notify you that The University of Western Ontario Research Ethics Board for Health Sciences Research Involving Human Subjects (HSREB) which is organized and operates according to the Tri-Council Policy Statement: Ethical Conduct of Research Involving Humans and the Health Canada/ICH Good Clinical Practice Practices: Consolidated Guidelines; and the applicable laws and regulations of Ontario has reviewed and granted approval to the above referenced revision(s) or amendment(s) on the approval date noted above. The membership of this REB also complies with the membership requirements for REB's as defined in Division 5 of the Food and Drug Regulations.

The ethics approval for this study shall remain valid until the expiry date noted above assuming timely and acceptable responses to the HSREB's periodic requests for surveillance and monitoring information. If you require an updated approval notice prior to that time you must request it using the UWO Updated Approval Request Form.

During the course of the research, no deviations from, or changes to, the protocol or consent form may be initiated without prior written approval from the HSREB except when necessary to eliminate immediate hazards to the subject or when the change(s) involve only logistical or administrative aspects of the study (e.g. change of monitor, telephone number). Expedited review of minor change(s) in ongoing studies will be considered. Subjects must receive a copy of the signed information/consent documentation.

Investigators must promptly also report to the HSREB:

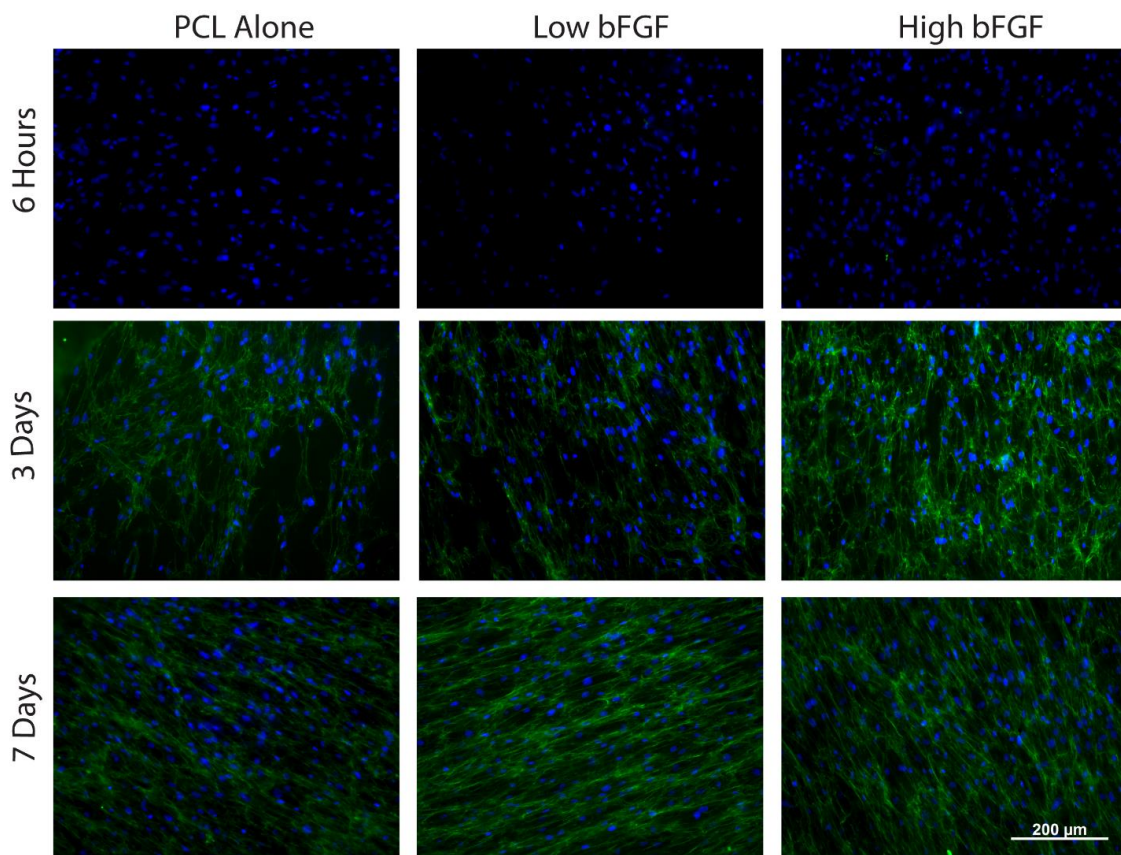
- a) changes increasing the risk to the participant(s) and/or affecting significantly the conduct of the study;
- b) all adverse and unexpected experiences or events that are both serious and unexpected;
- c) new information that may adversely affect the safety of the subjects or the conduct of the study.

If these changes/adverse events require a change to the information/consent documentation, and/or recruitment advertisement, the newly revised information/consent documentation, and/or advertisement, must be submitted to this office for approval.

Members of the HSREB who are named as investigators in research studies, or declare a conflict of interest, do not participate in discussion related to, nor vote on, such studies when they are presented to the HSREB.

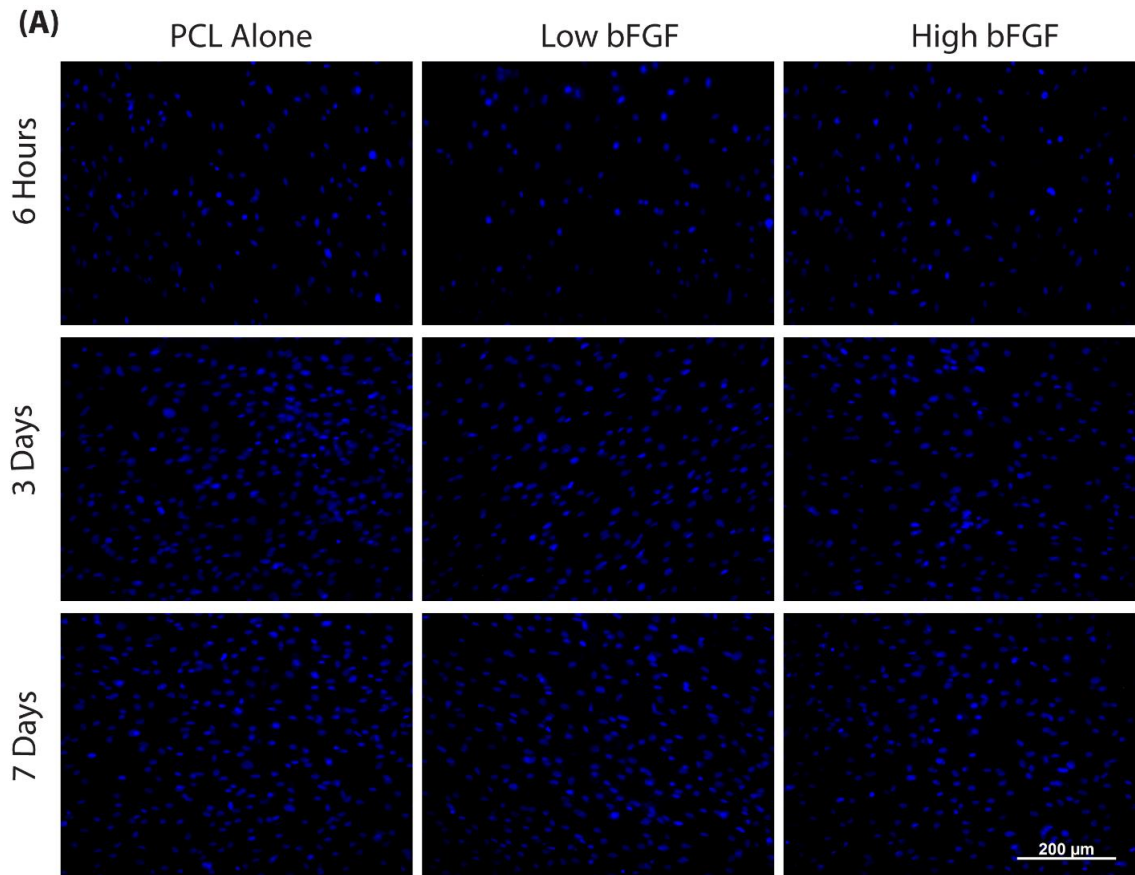
Appendix C: Fibronectin immunoreactivity on the scaffold surface at low magnification.

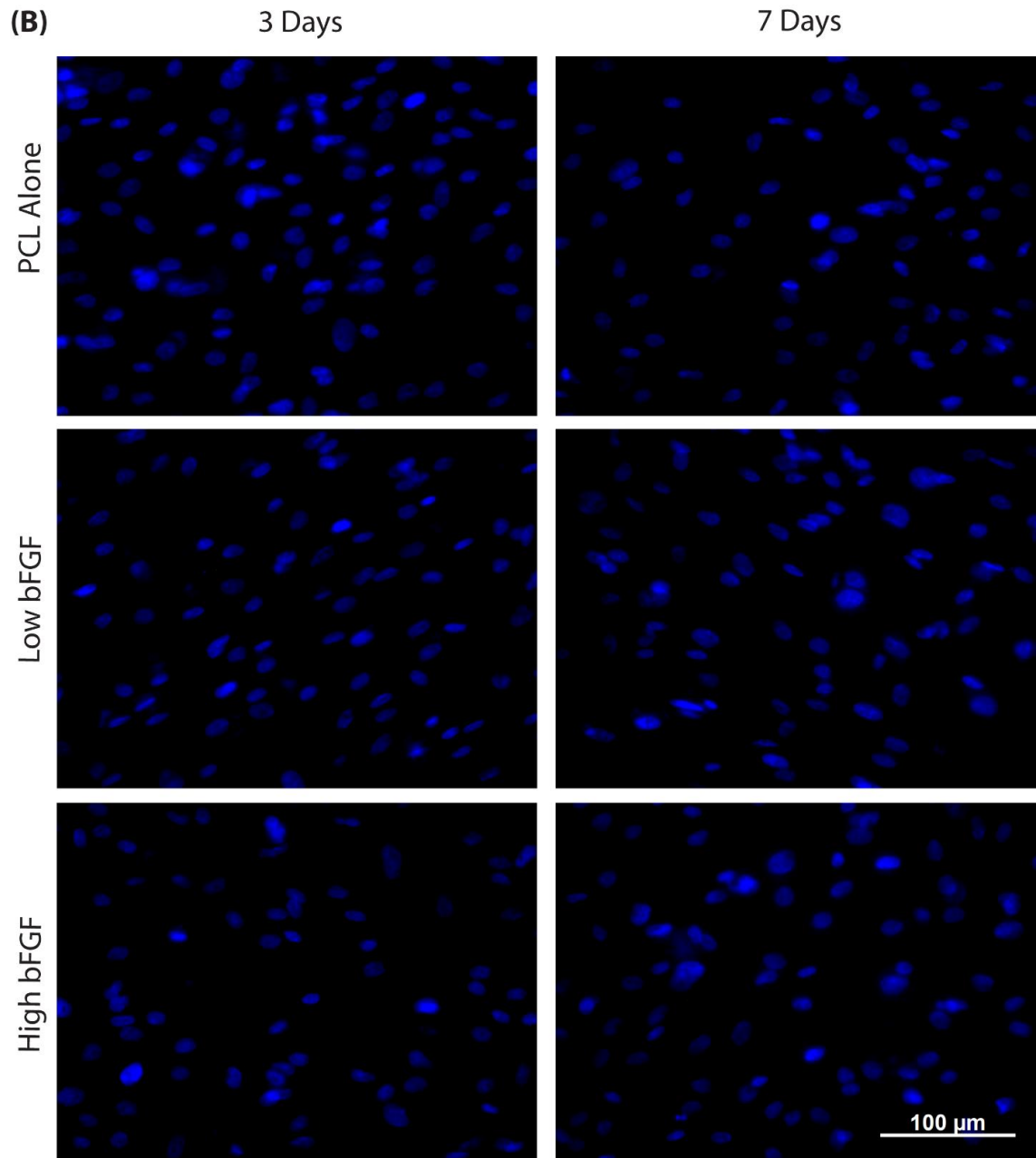
The secretion and deposition of the structural ECM protein fibronectin was visualized with immunocytochemistry; fibronectin (green), nuclei (blue). No fibronectin deposition is evident at 6 hours of culture for all three scaffold types. Fibronectin deposition becomes evident after 3 days of culture and remains visible after 7 days of culture.



Appendix D: No primary antibody negative control fibronectin immunofluorescence.

The secretion and deposition of the structural ECM protein fibronectin was visualized with immunocytochemistry; fibronectin (green), nuclei (blue). Negative control images in which no primary antibody was added were used to set the threshold value for fibronectin fluorescence. A) Low magnification negative control images. B) High magnification negative control images.

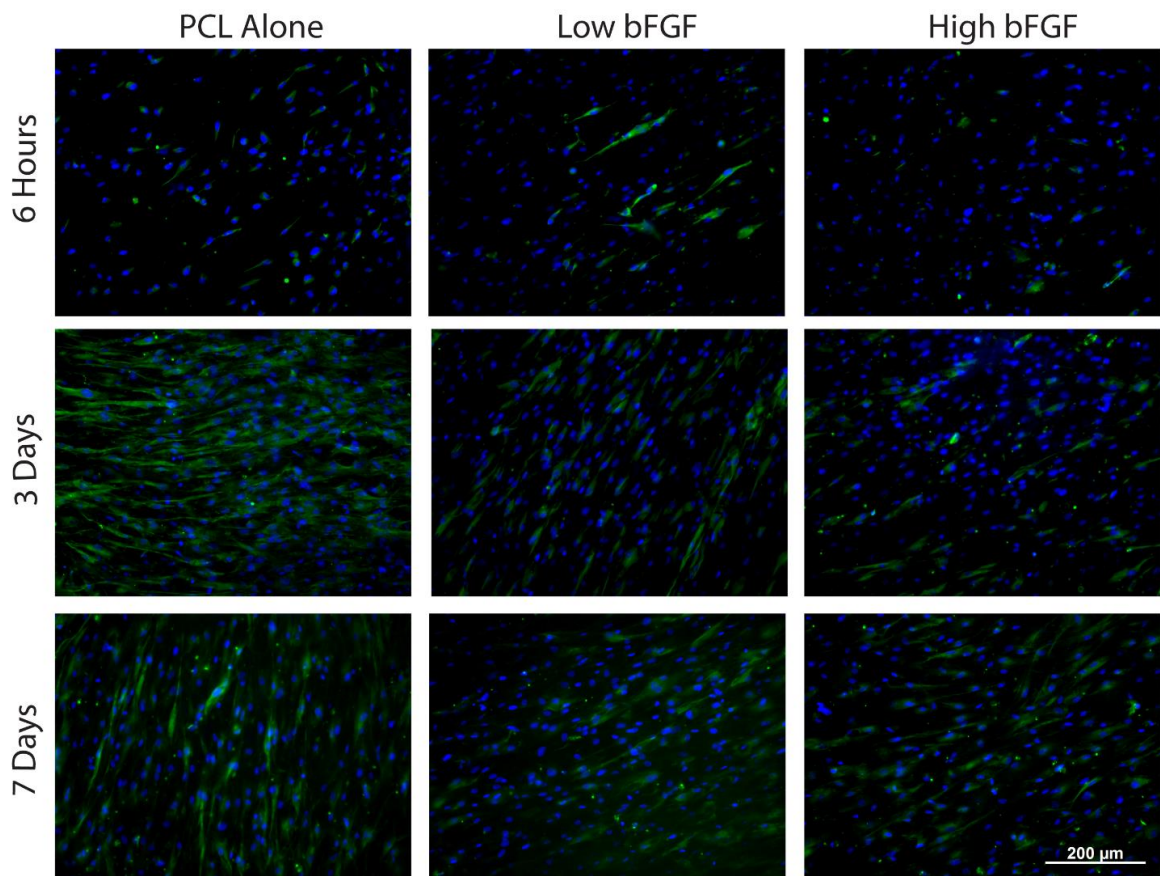




Appendix E: Biglycan immunoreactivity on the scaffold surface at low magnification.

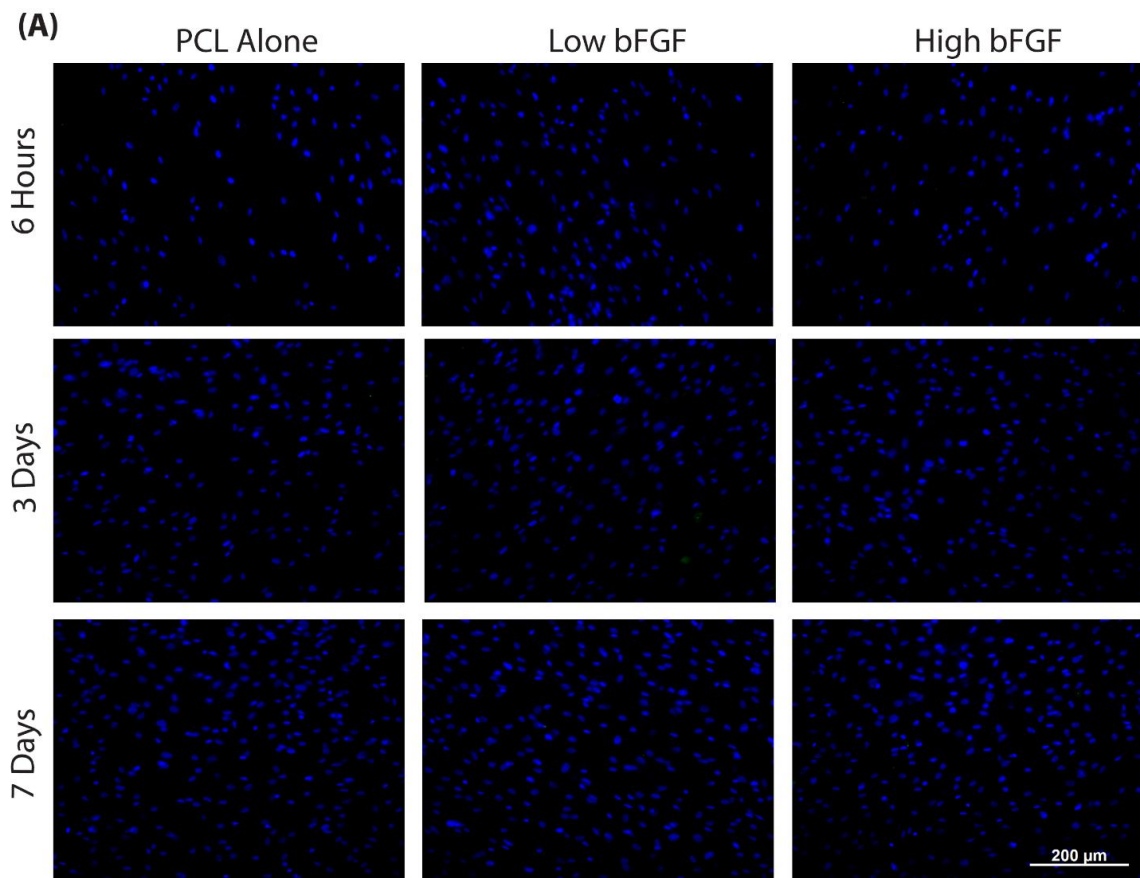
The production of the ECM proteoglycan biglycan was visualized with immunocytochemistry; biglycan (green), nuclei (blue). Minimal biglycan immunoreactivity is detected at 6 hours of culture for all three scaffold types.

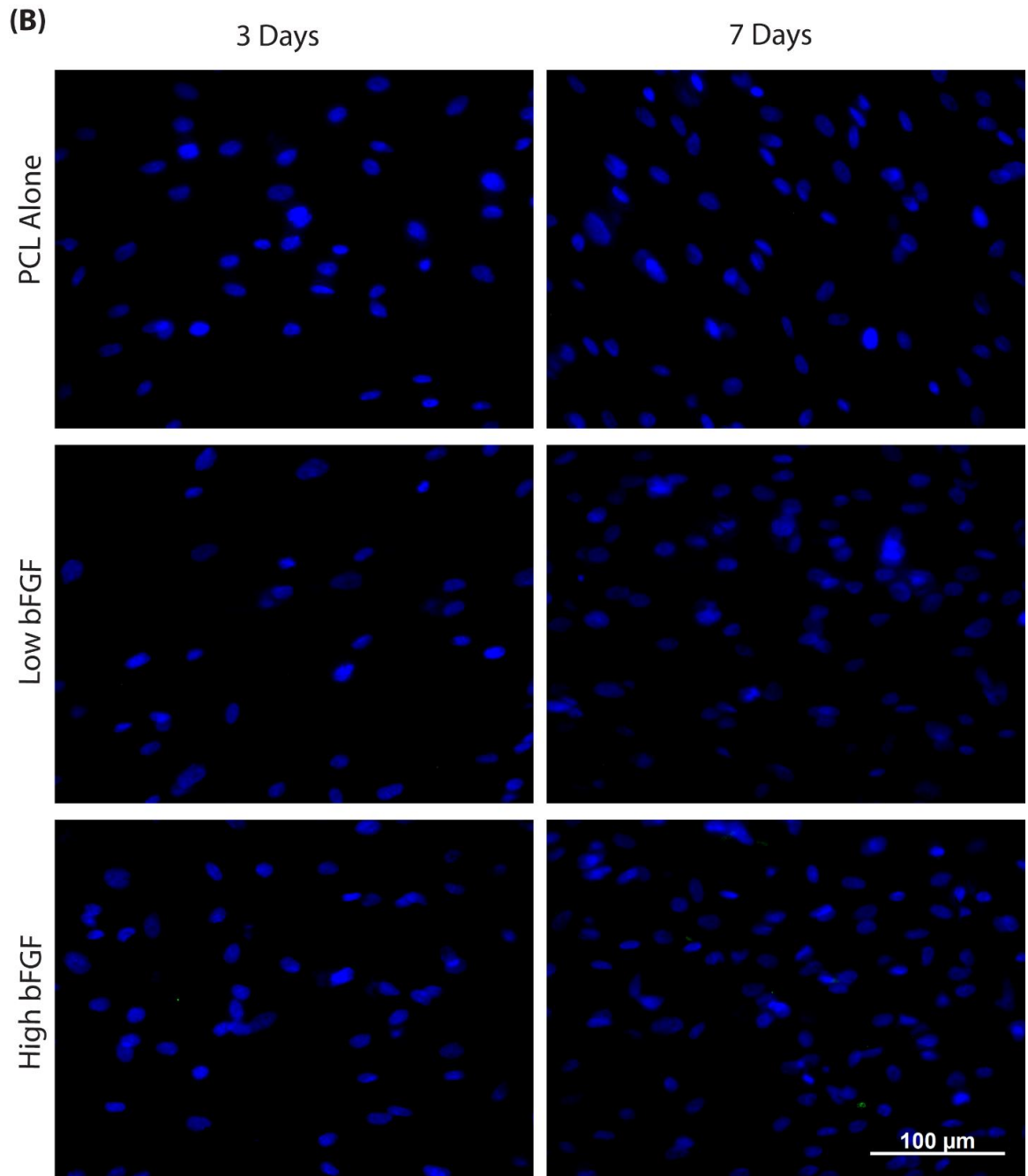
Intracellular biglycan becomes evident by 3 days on all three scaffold types and appears diminished in the presence of bFGF release. Intracellular biglycan immunoreactivity is also observed at 7 days.



Appendix F: No primary antibody negative control biglycan immunofluorescence.

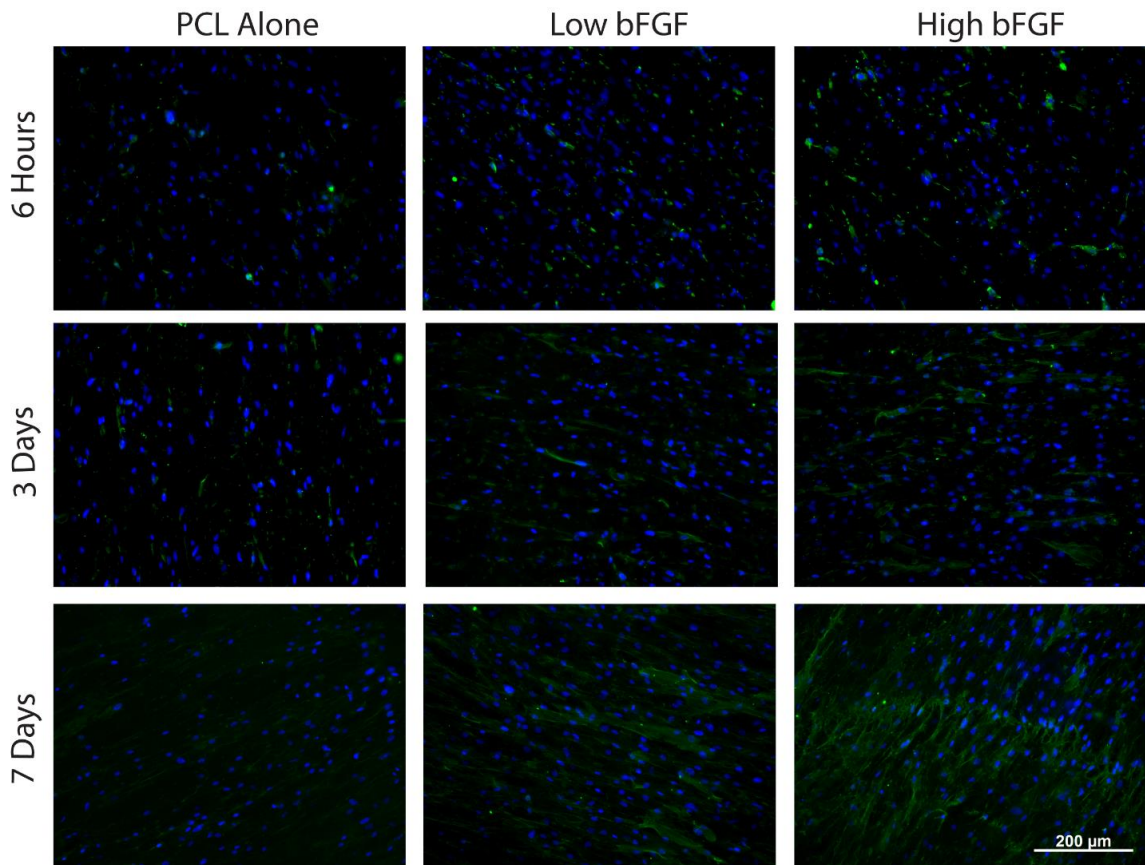
The production of the ECM proteoglycan biglycan was visualized with immunocytochemistry; biglycan (green), nuclei (blue). Negative control images in which no primary antibody was added were used to set the threshold value for biglycan fluorescence. A) Low magnification negative control images. B) High magnification negative control images.





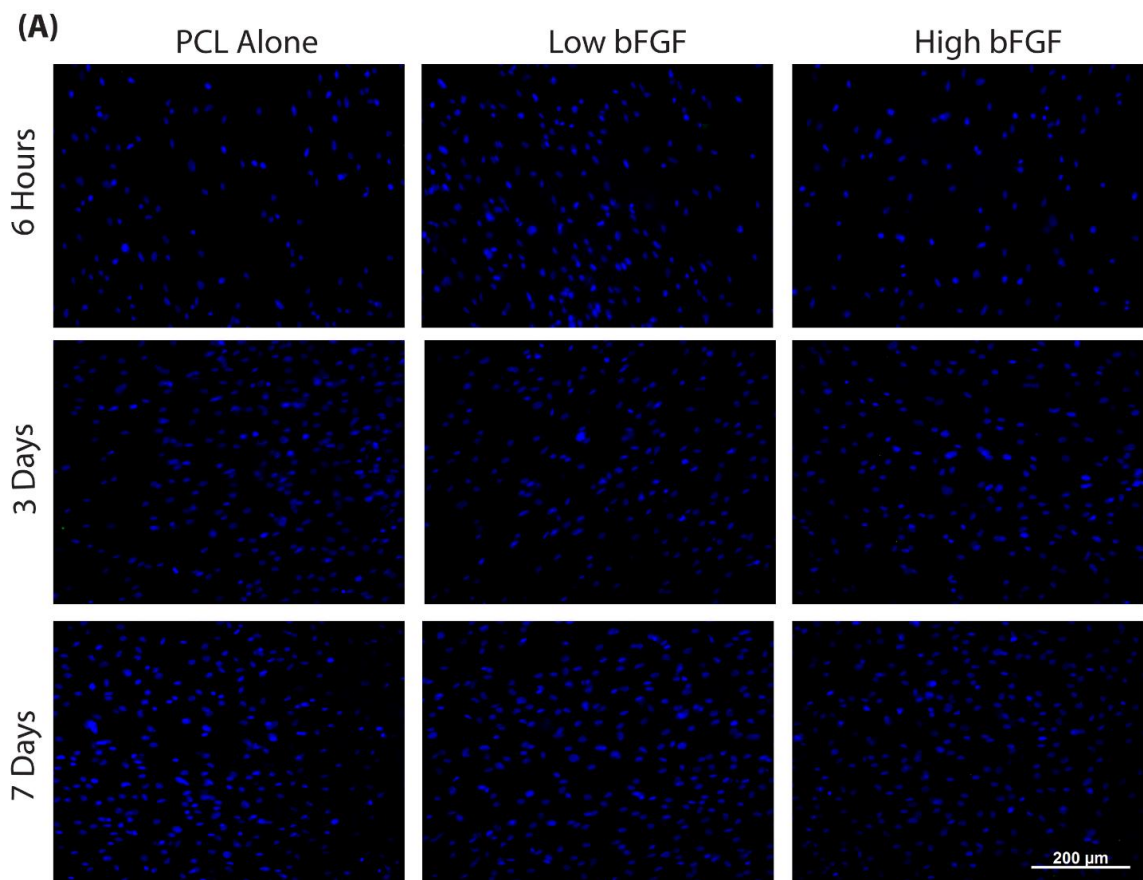
Appendix G: Decorin immunoreactivity on the scaffold surface at low magnification.

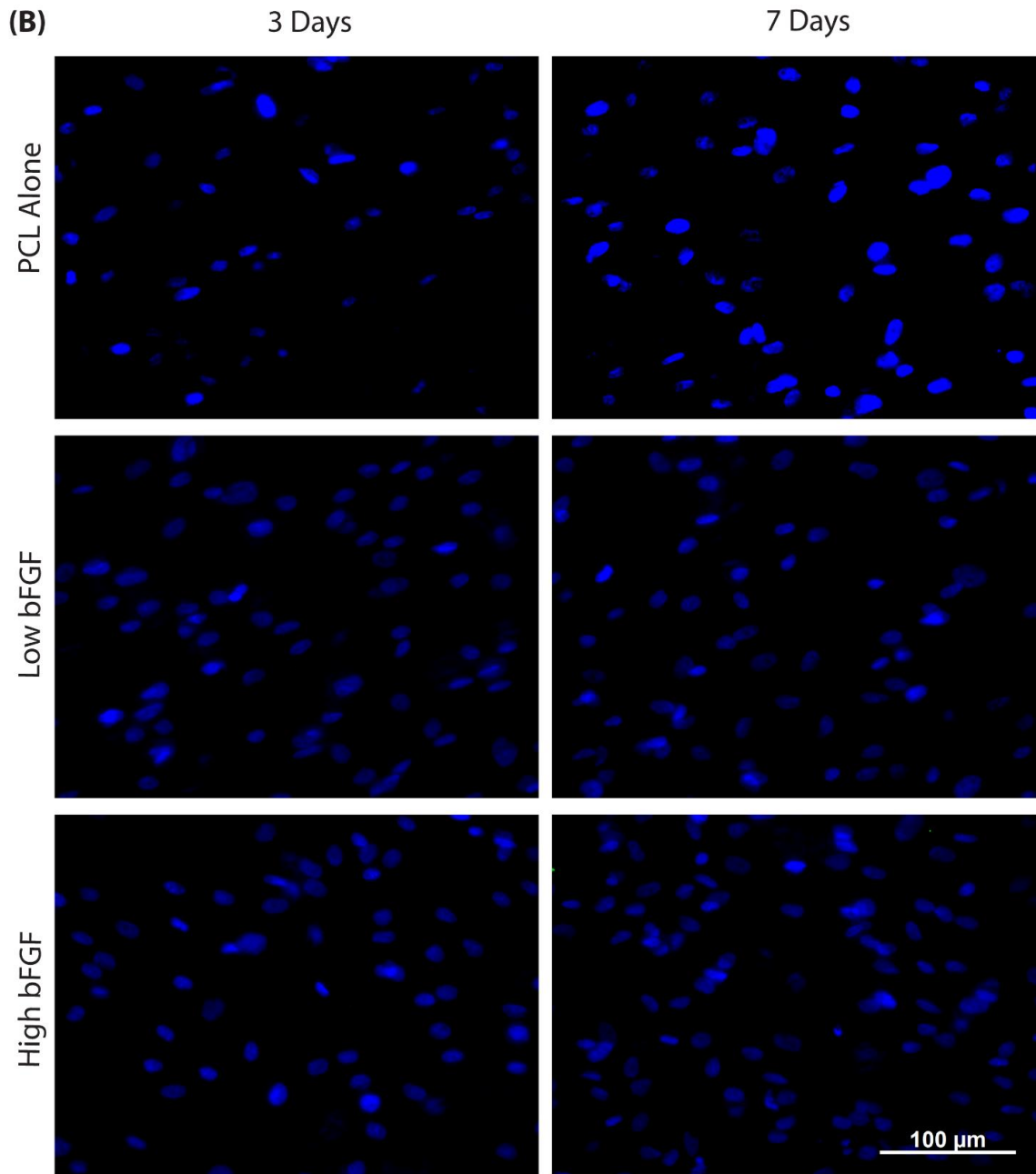
The production of the small ECM proteoglycan decorin was visualized with immunocytochemistry; decorin (green), nuclei (blue). Decorin immunoreactivity is observed on all three scaffold types at 6 hours. Decorin is observed on all three scaffold types at day 3 however appears less prominent on the PCL alone scaffold. Decorin appears localized to the cells after 7 days of culture.



Appendix H: No primary antibody negative control decorin immunofluorescence.

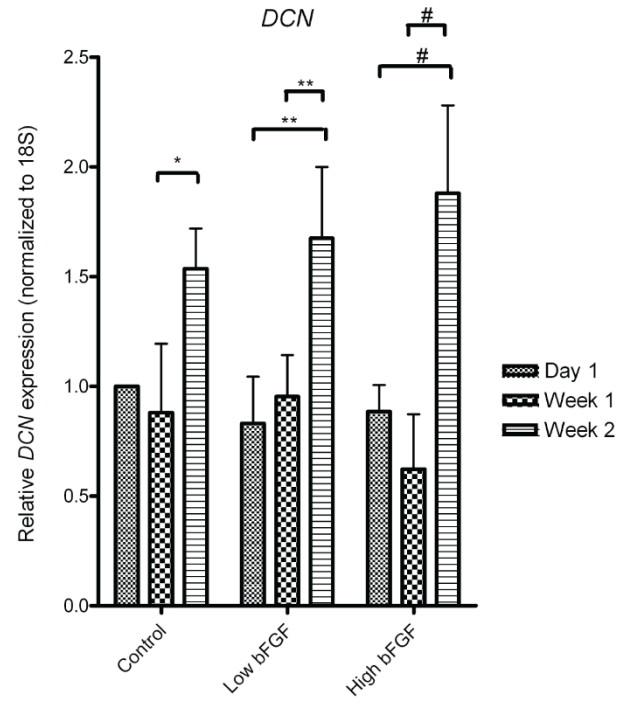
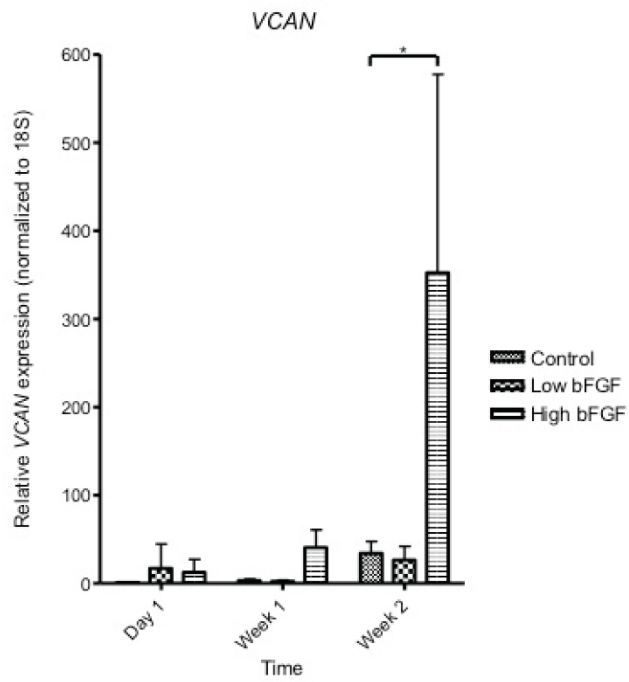
The production of the ECM proteoglycan decorin was visualized with immunocytochemistry; decorin (green), nuclei (blue). Negative control images in which no primary antibody was added were used to set the threshold value for decorin fluorescence. A) Low magnification negative control images. B) High magnification negative control images.





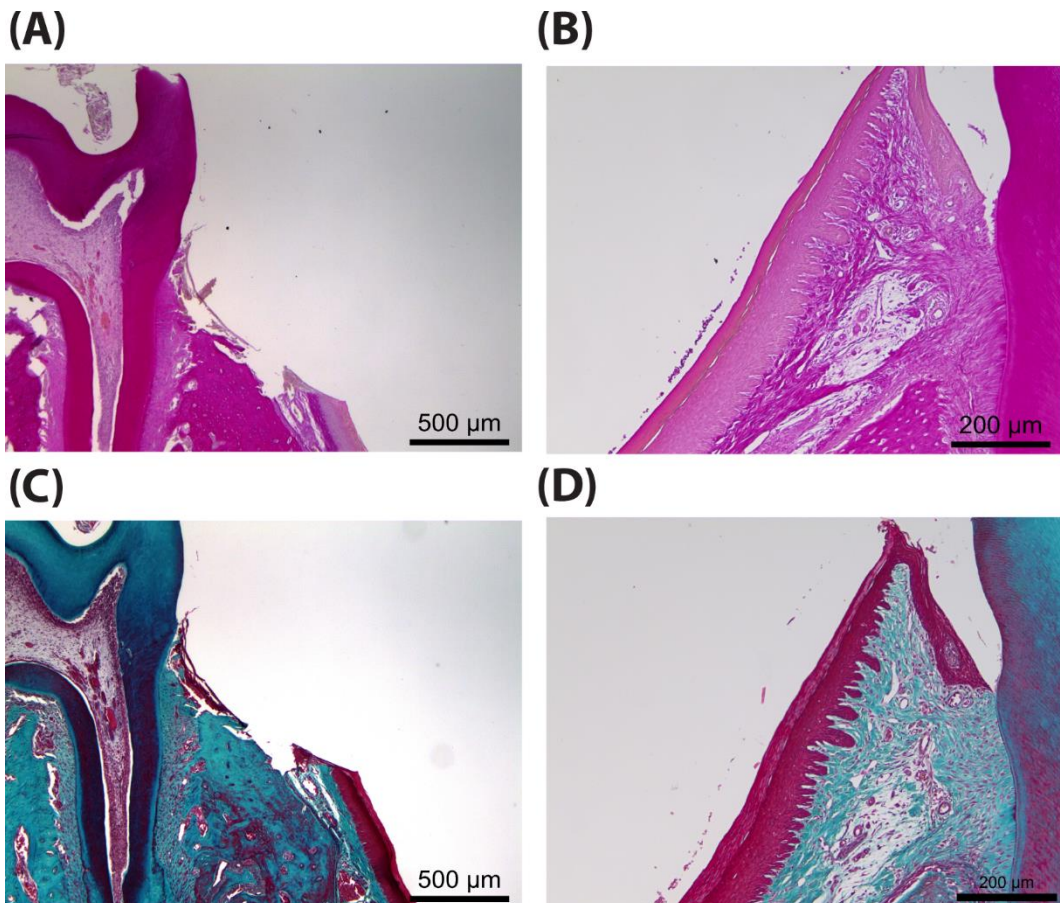
Appendix I: Influence of PCL electrospun scaffolds loaded with bFGF on decorin and versican mRNA levels.

hGFs were seeded and cultured on PCL electrospun fibrous scaffolds with and without bFGF microspheres for 1, 7 or 14 days. RNA was isolated and qRT-PCR was performed using primers specific for decorin (DCN, Hs00754870_s1) and versican (VCAN, HS00171642_m1). mRNA levels were normalized to endogenous 18S ribosomal RNA levels. A) Release of bFGF from the microspheres did not significantly alter the levels of decorin mRNA from that of the PCL alone scaffold. Decorin mRNA expression levels showed a significant increase at 14 days on all scaffolds suggesting that decorin mRNA expression is time dependent rather than bFGF dependent. B) Release of bFGF from the microspheres significantly increased the level of versican mRNA expression at 14 days of culture. Data are presented as mean \pm SD of three independent experiments. Two-way ANOVA with Bonferroni's post-test was used to compare means. * $p < 0.05$, ** $p < 0.01$, # $p < 0.001$.

(A)**(B)**

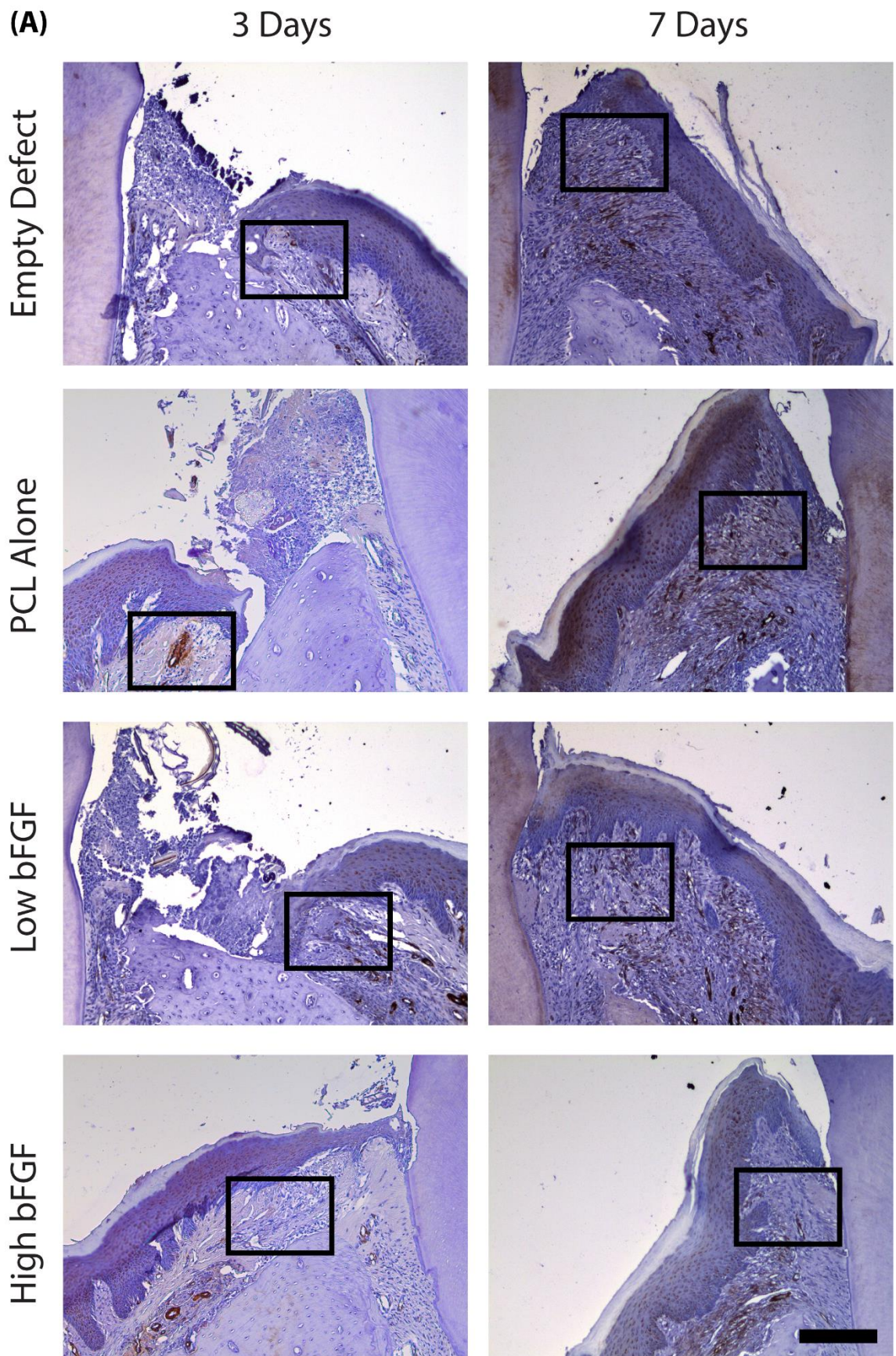
Appendix J: Collagen deposition in uninjured rat gingiva and immediately following gingivectomy.

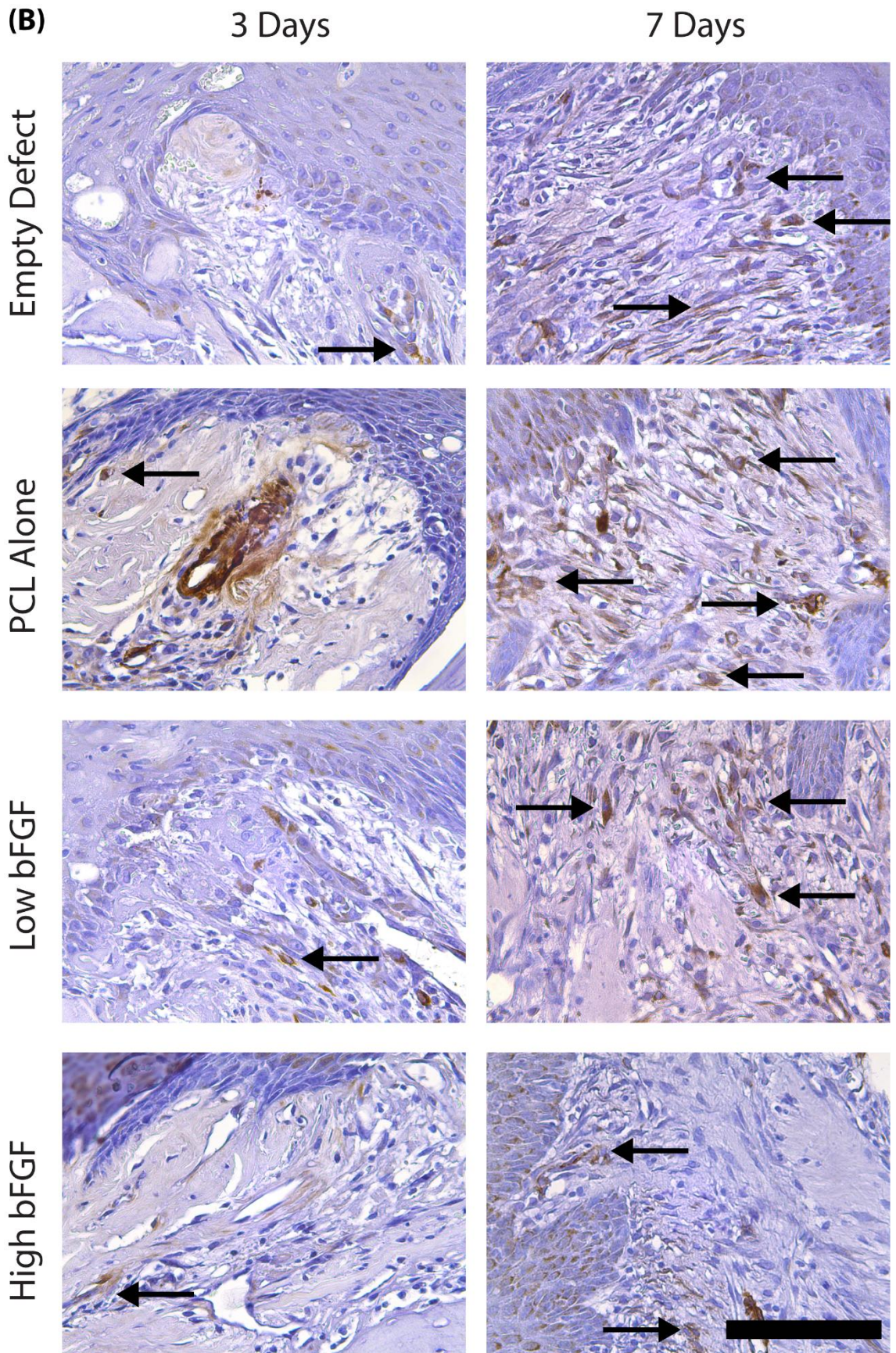
A) Van Gieson's stain showing collagen (bright pink) in rat gingival tissue immediately after gingivectomy. B) Van Gieson's stain showing collagen (bright pink) in unwounded, healthy rat gingival tissue. C) Masson's trichrome stain showing collagen (blue) in rat gingival tissue immediately after gingivectomy. D) Masson's trichrome stain showing collagen (blue) in unwounded, healthy rat gingival tissue.



Appendix K: Myofibroblast population following *in vivo* gingivectomy.

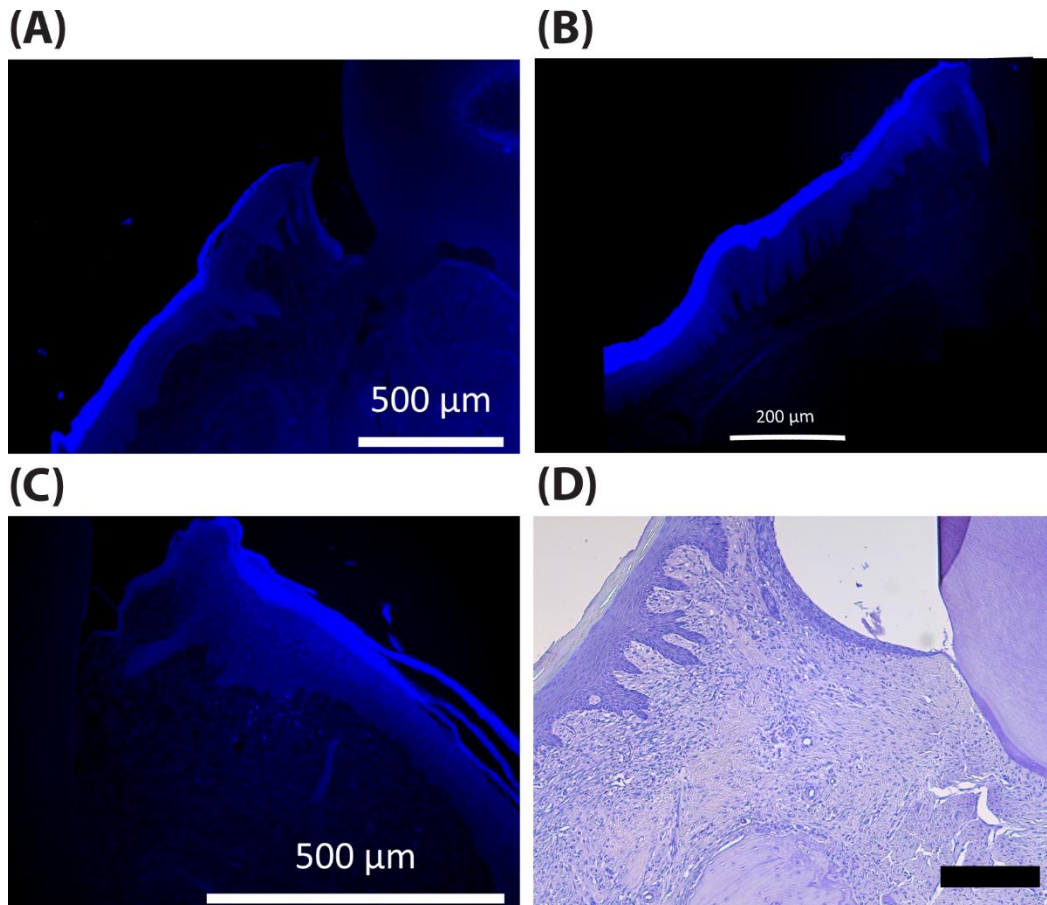
Gingivectomy was performed in a rat model and defects were treated with scaffold membranes of PCL alone, low bFGF loaded, high bFGF loaded or no treatment (empty defect). Sections were labelled with a primary antibody for α -SMA and visualized with DAB staining. A) Low magnification images. Scale bar = 200 μ m. B) High magnification images of the areas indicated by black boxes in A). Scale bar = 100 μ m.





Appendix L: No primary antibody negative control immunohistochemistry.

Negative control images in which no primary antibody was added were used to set the threshold value for fluorescence in rat gingival wound sections. A) Negative control image for arginase I immunofluorescence (cyan). B) Negative control image for α -SMA immunofluorescence (red). C) Negative control image for PCNA immunofluorescence (red). D) Negative control image for α -SMA immunohistochemistry. Scale bar = 200 μ m.



Curriculum Vitae

Name: Sarah Elizabeth Michelsons

Post-secondary Education and Degrees: Western University
London, Ontario, Canada
2008-2012 B.M.Sc.

Western University
London, Ontario, Canada
2012-2014 M.Sc.

Honours and Awards: NSERC CGS-M Graduate Scholarship
2013-2014

Anatomy & Cell Biology Graduate Entrance Scholarship
2012-2013

Related Work Experience: Teaching Assistant
Western University
2012-2014

Conferences Attended: 43rd Annual Meeting and Exhibition of the AADR
28th Annual Meeting of the CADR
Charlotte, N.C., USA
March 19-22, 2014